# FRICTION STIR WELDING OF 5083-H131 ALUMINUM ALLOY USING A2 AND H13 TOOL STEELS OR 420 STAINLESS STEEL TOOLING

by

Justin Michael Evans

A thesis submitted to the Graduate Faculty of
Auburn University
in partial fulfillment of the
requirements for the Degree of
Master of Science

Auburn, Alabama
December 13, 2014



Approved by

Lewis N. Payton, Associate Research Professor, Mechanical Engineering
Robert E. Thomas, Professor Emeritus, Industrial and Systems Engineering
Robert L. Jackson, Associate Professor, Mechanical Engineering

## Abstract

Friction Stir Welding (FSW) is a solid state welding method developed by The Welding Institute. The process is environmentally friendly, highly repetitive and easily adapted to manufacturing geometries. New welding schedules are being continuously developed for materials that are traditionally difficult to join by fusion welding methods (e.g. TIG/MIG/Stick).

This experiment develops the welding schedule and process parameters for acceptable welds in 5083-H131 aluminum using three different tool materials (A2 and H13 tool steel along with 420 Stainless Steel). The mechanical properties of all friction stir welds were compared against standard MIG welds (from a qualified industrial facility) and the as-delivered parent material.

All of the friction stir welds greatly outperformed the MIG welds. The welds produced by the H13 tool were statistically identical in bending to the original parent material. None of the friction stir welds performed more poorly than the MIG during ultimate tensile testing. The friction stir weld produced by the 420 SS tool was by far the best weld in terms of tensile strength. Equipment limitations (motor horsepower) may have prevented achieving a friction stir weld equal to or better than the parent material. All friction stir welds exhibited uniform hardness results across the weld that was much higher than the MIG welds hardness. None of the friction stir welds exhibited the porosity of the MIG welds when cross-sectioned.

The FSW machine used was actually a CNC mill that lacked the horsepower to extend the test to higher RPM/Feeds. Technical guidelines were developed (as an Appendix) from the lessons learned for the university research technician attempting to develop a welding schedule with a three-axis CNC machine not intended for friction stir welding.

Acknowledgments

I would like to dedicate this thesis to my family and friends who have supported me throughout my college career. Foremost, I would like to thank my beautiful wife, Stephanie, for your unconditional love and support as I complete my Master's. I cannot imagine my college years without you and look forward to many more years together.

I want to thank my parents, Mike and Tana, for always being there for me and supporting me in all the decisions I have made in my life. To my little brother, Austin, I am happy to have experienced college with you and proud of you for your accomplishments in life.

Next, I want to thank the many professionals outside the University (Brian Thompson, Don Hendry, Cale McGraw, Michael Peterson, Phillip Howell, and Kyle Williams) who provided services and technical support in completing my thesis research.

Finally, I would like to thank Dr. Payton for giving me the opportunity to work in the Design and Manufacturing Laboratory (DML) and providing guidance to complete my graduate degree. I would also like to thank my colleagues, Vishnu Chandrasekaran, Chase Wortman, Wesley Hunko, Drew Sherer, Michael Carter, and Jordan Roberts for all your help completing this thesis. I most especially would like to thank Wesley Hunko for giving me a place to stay and helping me on long nights of research.

Table of Contents

List of Tables

List of Figures

List of Abbreviations and Symbols

ANOVA – Analysis of Variance

CNC – Computer Numerical Control

FSW – Friction Stir Welding

ipm – inch per minute

ksi – 1000 pounds per square inch

lbs –pounds

MIG – Metal Inert Gas

rpm – revolutions per minute

SS – stainless steel

tpi – threads per inch

UNC – Unified National Course

UTS – Ultimate Tensile Strength

μm – $1x10^{-6}$ meters

# I. Introduction

Friction stir welding is a solid state welding process developed by Wayne Thomas at The Welding Institute (TWI) in 1991. The research was funded in part by the National Aeronautics and Space Administration (NASA) in an effort to find a welding method that would not add weight to orbital spacecraft. A major advantage of friction stir welding is that it is a solid state weld where the base material does not reach the melting point. Therefore, it does not exhibit the same deficiencies as fusion welding, which is associated with cooling from the liquid phase. Other benefits of friction stir welding include the ability to make welds in "hard-to-weld" materials and in dissimilar metals. It also eliminates toxic fumes which makes it much more environmentally friendly than fusion welds[1].

Friction stir welding is extensively used by NASA to join large portions of aluminum for their space shuttle external fuel tank at the Michoud research facility. It is the preferred NASA welding technique for their moon rocket. As friction stir welding advances and is used in more applications, tool materials will need to be selected for optimal weld efficiency. This thesis will determine the significance a tool material has on the mechanical properties of a friction stir weld in 5083-H131 aluminum.

The difference in the friction stir welds will be compared directly to both MIG welds and the parent material.

A fixture was developed which allowed welds to be performed in a vertical CNC machine. Test samples were cut from the workpiece for visual evaluation, tensile, bend, and hardness testing. Welds produced by three different tool materials were compared: H13 tool steel, 420 stainless steel, and A2 tool steel. The system developed at Auburn University, with support from Anniston Army Depot and NASA's Marshal Space Flight Center, uses a threaded pin and scrolled shouldered tool to perform welds as detailed in Figure 1 below.

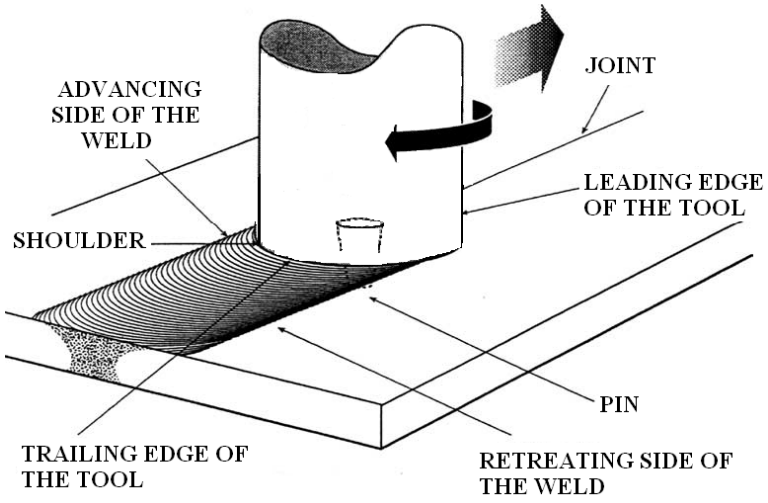


*Figure 1: Friction Stir Welding Process[1]*

Lastly, a conventional Computer Numerical Control (CNC) machine was used to produce welds. Although this machine is not ideal for production research, it is more available than a Friction Stir Machine and provides the data needed for this experiment. A procedural set of guidelines for use in university settings is provided in the Appendix.

## II. Scope and Objectives

The primary objective of this experiment was to show the effects that varying tool material has on the mechanical properties of a friction stir weld. Tool materials that were evaluated are: 420 stainless steel, H13 tool steel, and A2 tool steel. A common tool geometry, consisting of a scrolled shoulder and threaded pin, was used on all the tools. The tool is designed to flow material in towards the pin along the shoulder and down to the tip of the pin. The performance of the tool material was tested using welds in 5083-H131 aluminum. Friction stir welds' mechanical properties were statistically tested against that of production MIG welds from Anniston Army Depot and the parent material provided by Anniston Army Depot.

Summarizing all the objectives of this experiment includes:

1. Develop a better understanding of the friction stir welding process.
2. Compile a comprehensive review of the previous FSW literature that includes:
    a. Basic review of the Friction Stir Welding Process
    b. Single shoulder tool geometry
    c. Tool materials
    d. Visual and mechanical defects
    e. Process parameters
3. Develop tooling for rapid exchange and setup of samples.

4. Perform welds and identify acceptable weld parameters using 420 stainless steel, H13 tool steel, and A2 tool steel tools in 5083-H131 alloy aluminum.
5. Develop a FSW schedule that produces welds stronger than production MIG welds in 5083-H131 aluminum.
6. Determine mechanical properties of the friction stir welds, MIG welds, and parent material by subjecting the samples to the following tests:
    a. 3-point bend test
    b. Tensile test
    c. Hardness test
    d. Visual evaluation
7. Perform a statistical analysis to establish:
    a. The effects of type of weld on the mechanical properties of the weld joint in comparison with parent material.
    b. The effects of different tool materials on the mechanical properties of the friction stir weld joint.
8. Summarize lessons learned friction stir welding with the CNC machine for university researchers/technicians. Provide an initial procedure for researchers/technicians to use.

# III. Literature Review

This chapter provides an overview of the basic Friction Stir Welding (FSW) Process. Nomenclature associated with friction stir welding will be illustrated and reviewed along with tool geometries and tool materials. Previously reported studies of friction stir welding in 5083 aluminum will then be presented. The chapter closes with an extensive review of weld defects and process parameters in friction stir welding.

## Basic Review of the Friction Stir Welding Process

Friction stir welding may be performed as a lap joint or a butt joint. The lap joint is one in which overlapping materials are welded together. The butt joint is one where two pieces of material are pushed up against each other and welded along the seam.

The basic FSW process uses a pin tool with a shoulder (as illustrated in Figure 2). The tool is rotated and the pin is plunged into the work piece until the shoulder comes in contact. Once the shoulder is in contact with the workpiece, force is applied causing heat to build due to friction until the heat from the shoulder is great enough to bring the workpiece to an extrusion temperature. The tool is then traversed along the weld line. While the tool is traversing, material is being transported/extruded around the pin leaving a stirred zone in its wake. The material does not melt during this process, but rather, extrudes.

An anvil must be used to support the downward forces exerted by the tool or else the material would greatly deform away from the applied force[1]. The general process is illustrated in Figure 1 and the anvil is demonstrated in Figure 2.

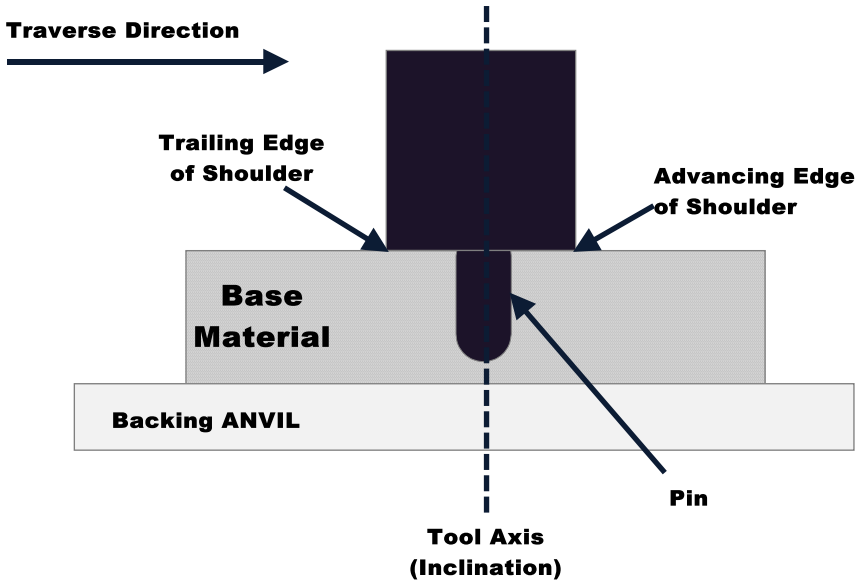


*Figure 2: Side view of the tool[1]*

Tool Geometry

Tool geometry plays an important role in friction stir weld joints. Cantin, David, Thomas, Curzio, and Babu studied the effects of a new tool geometry on lap joints in 5083-O[2]. They used a new type of tool called the A-Skew probe (Figure 3: Skew stir tool). This tool is best suited for wide weld areas such as lap joints; where the weld interface is perpendicular to the machine axis. They studied the mechanical properties and microstructures of welds using a conventional pin type tool as compared to the joints made using the Skew stir technique. Results showed that the Skew stir technique

produced joints with higher tensile strength and longer fatigue lives as compared to welds using the conventional pin type tool.

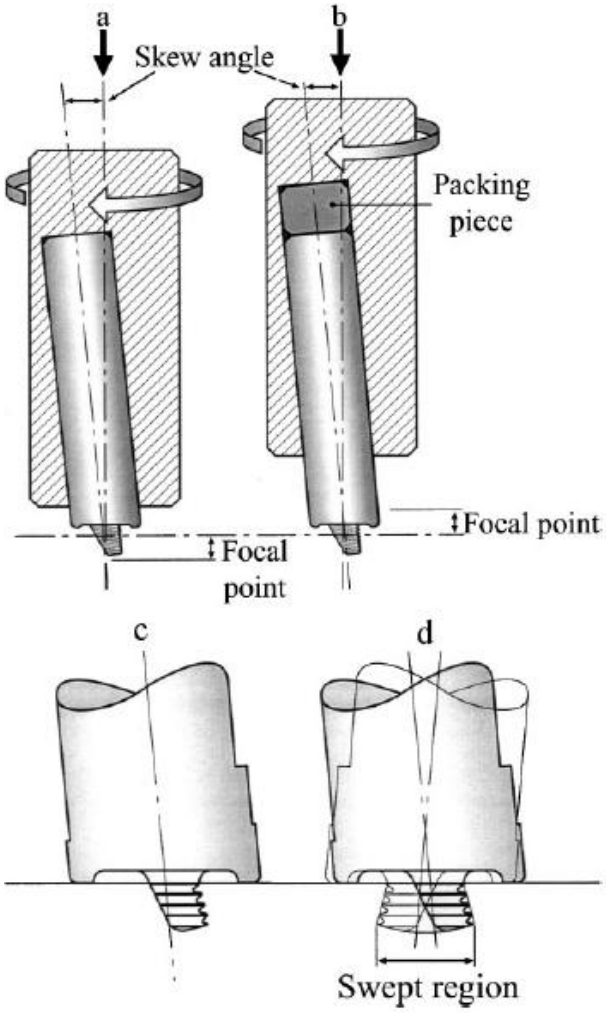


*Figure 3: Skew stir tool*

Another study regarding the effects of tool shape on the mechanical properties and microstructure of friction stir welded aluminum was done by Fujii, Cui, Maeda, and Nogi[3]. In an effort to find optimum tool geometry for welding aluminum, they used three different styles of pin geometries—a smooth pin, threaded pin, and triangular prism pin (Figure 4). These pins were used to run butt welds in three different types of aluminum. The aluminum used was 1050-H24, 6061-T6, and 5083-O (welding

parameters given in Table 1). These aluminum plates were 300 mm long, 70 mm wide, and 5 mm thick. Each tool had a pin length of 4.7 mm, a diameter of 6 mm, and a shoulder diameter of 15 mm with a $10^{o}$ concavity. Concave shoulders are sloped from the outer diameter of the shoulder to the base of the pin in the opposite direction of the pin. The results for 1050-H24 aluminum showed that the smooth pin tool produced a weld with the best mechanical properties. This was attributed to this tool's ability to create a weld with lesser defects than that of the other tool geometries. Using the 6061-T6 aluminum, the tool geometry did not significantly affect the weld joints mechanical properties or microstructure. However, although the 5083-O aluminum did have the highest deformation resistance its weldability was found to be greatly affected by the rotational speed of the tool. The triangular prism tool worked best at the high rotational speed (1500 rpm). The threaded pin tool worked best at the middle rotational speed (800 rpm). At the lowest speed (600 rpm), the tool geometry did not significantly affect the microstructure or the mechanical properties of the weld.

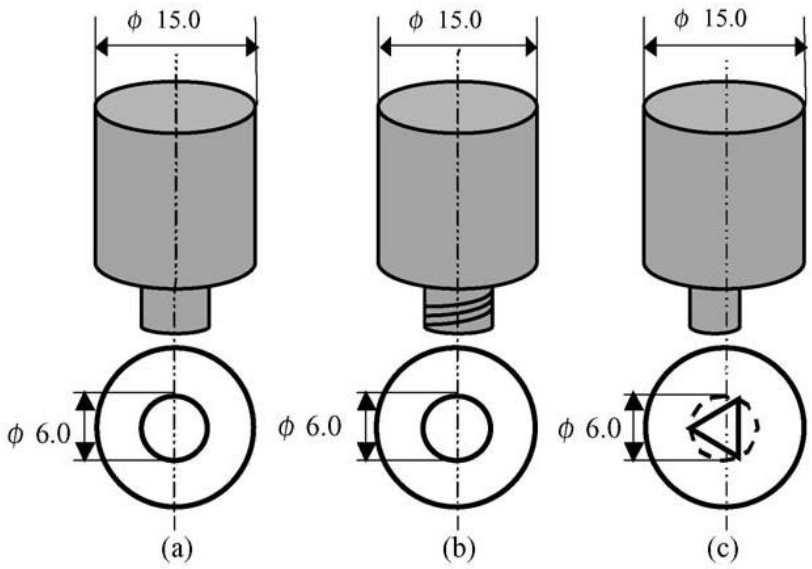


*Figure 4: Tool Geometry: (a) smooth pin, (b) threaded pin, (c) triangular prism*

*Table 1: Welding Parameters*

Welding parameters

| Type of material | Rotation speed (rpm) | Welding speed (mm/min) | Revolutionary pitch (mm/r) |
|---|---|---|---|
| 1050-H24 | 1500 | 100–700 | 0.07–0.47 |
| 6061-T6 | 1500 | 100–1000 | 0.07–0.67 |
| 5083-O | 600–1500 | 25–200 | 0.02–0.27 |

Tool Material

Many friction stir tools have been used in short run experimental environments, but when they are used for production in a manufacturing environment, the tool wear becomes a concern. Prado, Murr, Shindo and Soto performed a study of tool wear in 6061 aluminum[4]. The butt welds were done in commercial 6061-T6 that was 0.6 cm thick and extruded MMC 6061-T6 that was 0.5 cm thick. The tool was made of 01 tool steel heat treated to a Rockwell C hardness of 62. The pin was threaded to ¼-20 UNC, slightly upset using a press, and rounded. Rotational speeds were 500, 1000, 1500, and 2000 for MMC and 1000 for the commercial 6061-T6. All welds had a traverse speed of 1 mm/s. The tool wear was calculated by finding the percent change in the tool volume over the distance the tool traveled in a weld. The tools were photographed after each run of a certain distance (seen in Figure 5). The results showed that the tool wear in the MMC 6061 was maximum at 1000 rpm with an effective wear rate of 0.64% per cm. Furthermore, the MMC 6061 wear rate declined once the tool reached a speed above 1000 rpm. At 1500 rpm, the wear rate was noted at 0.42% per cm, but rose to 0.56% per cm at 2000 rpm. There was no measurable wear on the tool used to weld the commercial 6061.

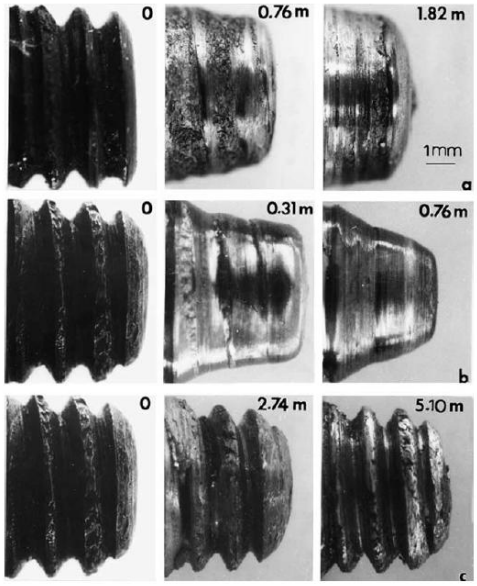


*Figure 5: Tool wear with corresponding locations. (a) MMC FSW at 500 rpm, (b) MMC FSW at 1000 rpm, (c) Commercial 6061 FSW at 1000 rpm*

Microstructure and Mechanical Properties

Shigematsu, Kwon, Suzuki, Imai and Saito looked at the joining of 5083 and 6061 aluminum alloys[5]. These welds consisted of butt welds in combinations of 5083-5083, 6061-6061, and 5083-6061 in 3 mm thick plates. They studied the hardness and the tensile strength of the welds and the parent materials. The hardness across the weld between two plates of 5083 was slightly higher in the weld compared to the parent material. The tensile specimens had a cross sectional area of 30 $mm^2$ and produced strength and elongation values (shown in Table 2). Using tensile testing techniques, the results showed that the weld between 6061-6061 was 63% as strong as the original material. The weld between 5083-5083 was 97% as strong as the original material in the sheet metal welds. The tool in this case had a pin with a diameter of 3.0 mm and a

shoulder diameter of 10 mm. Tool rotational speeds were 890 rpm and 1540 rpm. The traverse speeds were 118 mm/min and 155 mm/min.

*Table 2: Tensile strength of parent and joint material*

| | Strength (MPa) | Elongation (%) |
|---|---|---|
| Alloy | | |
| 5083 | $328 \pm 2$ | $24 \pm 1$ |
| 6061 | $320 \pm 2$ | $16 \pm 1$ |
| Joint | | |
| 5083-5083 | $318 \pm 2$ | $21 \pm 3$ |
| 6061-6061 | $199 \pm 6$ | $11 \pm 1$ |
| 6061-5083 | $202 \pm 3$ | $7 \pm 1$ |

Microstructure, mechanical properties, and residual stresses all change with the process parameters. Peel, Steuwer, Preuss and Withers studied the effects of changing process parameters on those properties within the welds in AA5083[6]. The weld parameters used for their experiment consisted of a fixed rotational speed and various traverse speeds. The tool they used had a pin with an M5 thread and a shoulder diameter of 18 mm; but they also ran one set of welds with an M6 thread pin to investigate the effects of tool geometry. The tool was tilted $2^{o}$ with the rear of the tool lower than the front and the front of the tool plunged to 0.55 mm below the plate surface. Table 3 outlines the welding parameters as well as the results from testing. The study also found that increasing traverse speed reduces heat input. Recrystallization in the weld zone had considerably lower hardness and yield strength than the parent material. During tensile testing, almost all of the plastic deformation observed was in the recrystallized weld zone. An analysis of residual stresses was performed using the electronic speckle pattern

interferometry technique, which exploits the properties of multiple defocused lasers directed at rough surfaces to track displacements of samples during deformation. These displacements are converted to strains for stress analysis. The data indicated that the weld zone is in tension—both in the longitudinal and transverse directions of the weld. Longitudinal stresses increased as the traverse speed increased. This direct proportion is most likely a result of the steeper thermal gradients because the welds do not have enough time for stresses to resolve.

*Table 3: Summery of the mechanical testing experiments*

| Designation | Tool | Traverse speed (mm/min) | Average 0.2% yield stress (MPa) | UTS (MPa) | Weld efficiency (%) | Failure location |
|---|---|---|---|---|---|---|
| Parent material | – | – | 392 ± 4.3 | 457 ± 2.3 | – | – |
| 81 | M5 | 100 | 154 ± 7.5 | 304 ± 13 | 67 | Retreating side (~10 mm from weld line) |
| 82 | M5 | 150 | 149 ± 9.9 | 216 ± 15 | 47 | Weld line |
| 83 | M5 | 200 | 147 ± 8.0 | 186 ± 20 | 41 | Weld line |
| 84 | M6 | 200 | 145 ± 6.5 | 259 ± 17 | 57 | Retreating side (~10 mm from weld line) |

Defects in Friction Stir Welding

While testing the mechanical properties of welds, defects are discovered. The root cause of defect formation is linked to the parameters in which the weld was performed. William Arbegast created a flow-partitioned deformation zone model for defect formation[7]. The model divides material flow into different deformation zones around the pin probe beneath the shoulder. Ultimately, the model (Figure 6) relates defects to insufficient process parameters, such as feed and speed of the tool. The model also associates defects with excessive cold or hot welding states.

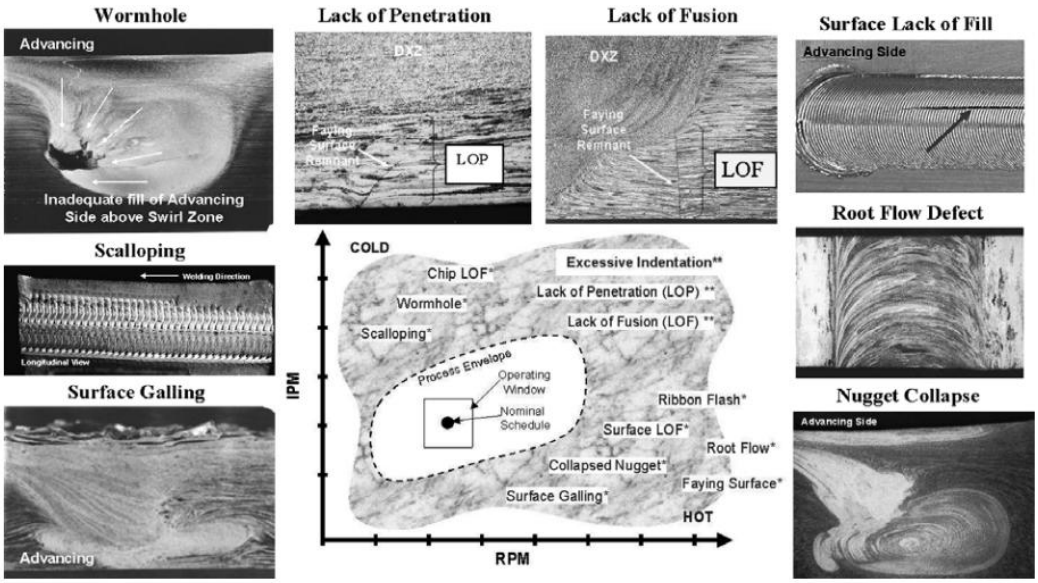


*Figure 6: Flow-partitioned Deformation Zone Model[7]*

In 2001, Zucchi, Trabanelli and Grassi studied the pitting and stress corrosion cracking resistance of friction stir welded AA 5083 [8]. They compared a friction stir weld between two 5083 plates to a MIG weld using 5183 as a filler metal on the 5083 plates. They found that the FSW did not show a decrease in pitting and surface crack corrosion resistance with respect to the AA5083 alloy. In fact, FSW was more corrosion resistant than the base alloy. The MIG welded specimens showed signs of pitting in the heat affected zone as well as being more likely to have surface crack corrosion than the base alloy. It was determined that the FSW produced welds that showed high fatigue resistance in addition to a good resistance to pitting corrosion and surface crack corrosion.

Dickerson and Przydatek studied root flaws or "kissing bonds" in friction stir welds done in 5083 aluminum[9]. Kissing bonds occur when the root of a single-sided weld has not fully bonded to the parent material or it has bonded but with poor strength.

They compared the fatigue behavior of butt welds with and without root flaws in order to find the significance of the presence of root flaws. One set of welds were done at optimum welding parameters to get a weld with no root flaws. Then, another set of welds were done with a change in the parameters to get a flawed weld. They tested both the flawed and un-flawed welds with X-ray radiographs and dye penetrate, along with visual inspection of welds. They reported no difference between the two welds. Bend tests showed cracking or fracture of the flawed welds, where as tensile tests proved to be of little use in determining a flawed weld from a flaw free weld since the tensile strength did not show a significant difference. Fatigue endurance testing was performed, but it did not give any insight into the root flaws of a weld; therefore, the testing was abandoned. They concluded that root flaws up to 0.35 mm deep do not degrade the mechanical performance when compared to the flaw free welds.

Another study on kissing bonds was done by Zhou, Yang and Luan[10]. They studied the fatigue behavior of friction stir welds in 5083-H321 Al with and without kissing bond defects. Fatigue tests were performed in a high frequency fatigue test machine with a 100 KN load capacity, sinusoidal load-time function, stress ratio R= 0.1, and an oscillation frequency of 85-90 Hz. Results showed the fatigue life of welds with kissing bonds was 21-43 times shorter than that of sound welds. The fatigue values of each weld decreased from 100.24 MPa for sound welds to 65.57 MPa for bonded welds at $2x10^6$ cycles. Fatigue fractures were found to be cracks initiated from the root tip of a kissing bond.

Process Parameters

Han, Lee, Park, Ko, Woo and Kim evaluated the mechanical properties of friction stir welds while varying process parameters in 5083-O aluminum alloy[11]. Their tool had a shoulder diameter of 20 mm, a threaded pin with a length, diameter, and thread pitch of 4.5, 5.0, and 2.0 mm respectively. The tool was made from SK tool steel, tilted at $2^{o}$, and had a plunging depth of 4.5-4.7 mm. Welds were done at 500, 800, 1800 rpm and 124, 267, 342 mm/min. Tensile tests were performed on all welds. The welds performed at 500 rpm and 800 rpm showed a reduction in quality as the traverse feed increased. At 1800 rpm, all weld speeds produced defects. In turn, these welds exhibited very low quality mechanical properties. All fractures during tensile testing occurred in the stir zone. The optimum FSW parameters for this experiment were 800 rpm and 124 mm/min which had an ultimate tensile strength around 350 MPa.

The influence of friction stir welding parameters upon grain size in 5083 aluminum alloy was studied by Hirata, Oguri, Hagino, Tanaka, Chung, Takigawa, and Higashi[12]. They performed single-pass butt welds with a friction stir tool set to an angle of $3^{o}$ with a pin and shoulder diameter of 12 and 14 mm respectively. They performed hardness, tensile, and bulge tests in addition to looking at the microstructure from different welding parameters (shown in Table 4). The study found that the microstructure of the stir zones (Figure 7) consisted of a fine grain structure at the various process parameters shown in Table 4. The hardness of the stir zone increased with a decrease in frictional heat flow. This was a result of the reduction in grain size due to the change in heat flow. The tensile strength for each welding condition was nearly the same.

*Table 4: Process Parameters*

FSW parameters used in the present study

| Sample | Rotational speed, Rt (rpm) | Welding speed, *V* (mm/min) |
|---|---|---|
| Sample A | 500 | 100 |
| Sample B | 800 | 100 |
| Sample C | 800 | 200 |
| Sample D | 1000 | 100 |

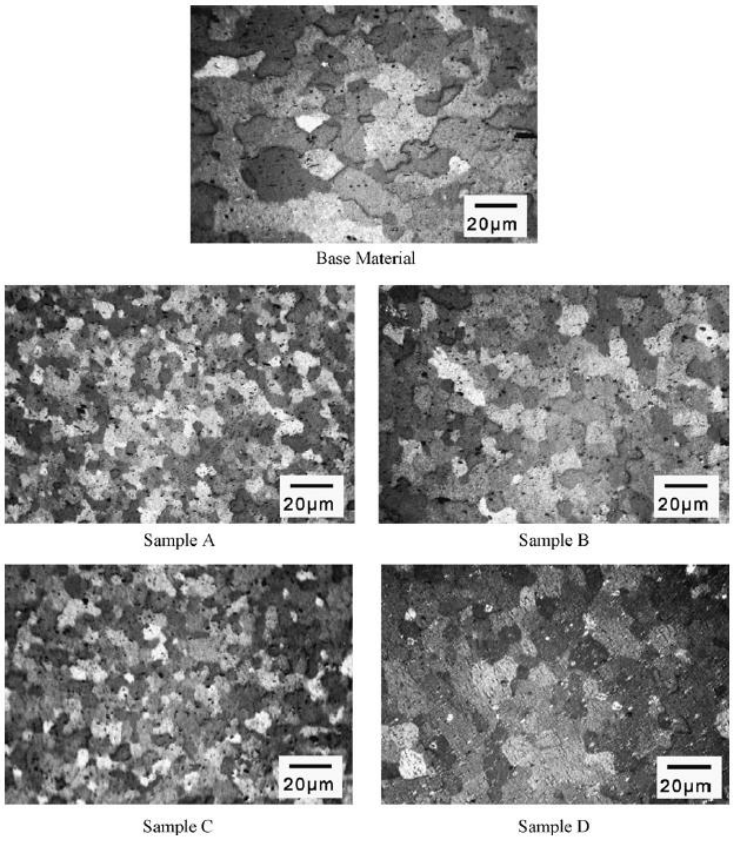


*Figure 7: Microstructure of the stir zones*

James, Hattingh and Bradley examined the relationship between weld tool travel speeds and fatigue life of friction stir welds in 5083-H321 aluminum[13]. The theory is that larger 'onion rings' on the surface will increase the risk of crack initiation (Figure 8) therefore affecting the endurance limit and fatigue life of the weld. They found that the

lower welding speeds give a higher endurance limit and the smallest reduction in fatigue strength. They also polished some test specimens and got an eight percent increase in the endurance limit. The 'onion skin' defects were never associated with fatigue crack initiation, but data indicates they will affect overall fatigue life by providing easily linking paths between initiated cracks.

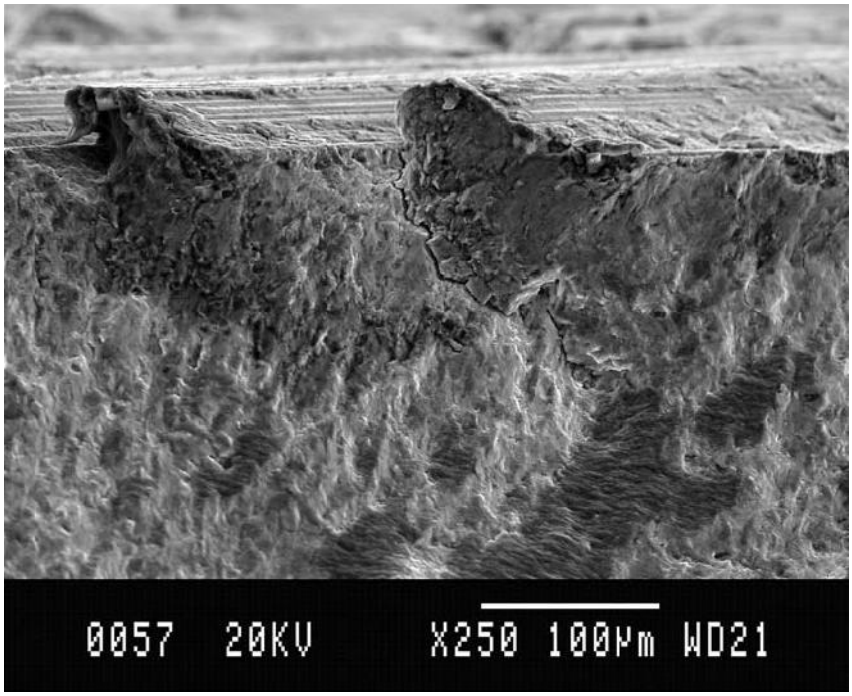


*Figure 8: Surface notches (onion rings) association with crack initiation*

Sato, Urata, Kokawa and Ikeda studied the effect of grain size on hardness in the stir zones[14]. They examined the grain structure and hardness of 5083-O aluminum alloy before and after the FSW. They discovered that the combination of frictional heating and intense plastic deformation during the weld always results in a fine recrystallized microstructure in Al alloys. The results showed that the hardness of the stir zone decreases and the grain size increases with an increase in rotational speed.

Comparing Figures 9 and 10, one can see that an increase in rotational speed leads to the lower hardness values of the stir zone and produces a larger grain size.

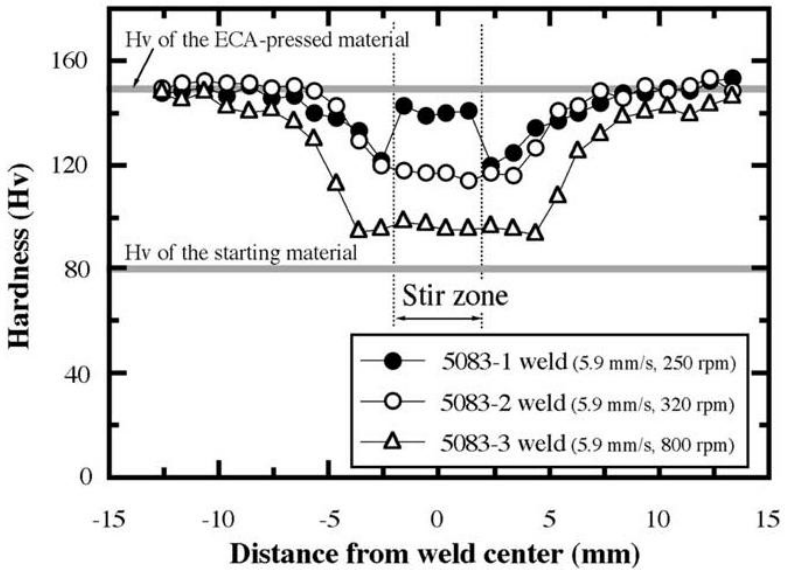


*Figure 9: Hardness of stir zone in 5083-O*

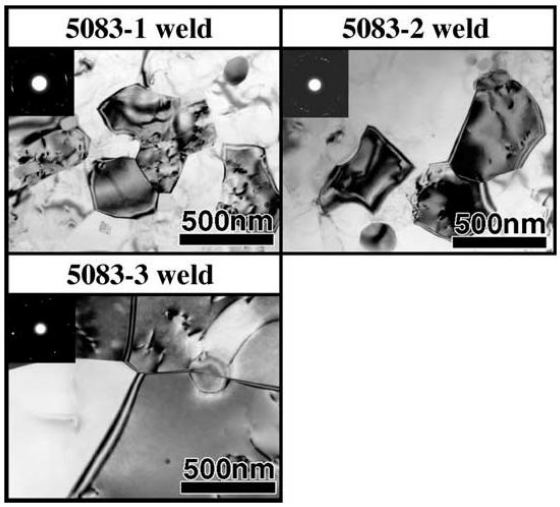


*Figure 10: Grain size of stir zone in 5083-O FSW's*

In 2011, Bisadi, Tour and Tavakoli investigated the effect of process parameters on microstructure and mechanical properties of friction stir welded 5083 Al lap

joints[15]. They performed a number of welds at different feeds and speeds, and gathered data from tensile tests as well as Vickers hardness tests. The speeds, feeds, and maximum tensile load can be seen in Table 5 below. Their studies showed that lower rotational speeds and feeds produce better properties of the weld joint, but changing the welding speed at higher rotational speeds has an inverse effect on the joint properties. Also, they found the weld nugget had the finest grain size and highest hardness of the other weld areas. The heat affected zone had the largest grain size and the lowest hardness. They observed that most all fractures during tensile testing took place in the heat affected zone of the advancing side of the weld.

*Table 5: Bisadi Testing results*

| Samples | Rotational speed (rev/min) | Welding speed (mm/min) | Maximum load(N) |
|---|---|---|---|
| 1 | 600 | 32 | 10617 |
| 2 | 600 | 60 | 8872 |
| 3 | 825 | 32 | 14217 |
| 4 | 825 | 60 | 13647 |
| 5 | 1115 | 32 | 13309 |
| 6 | 1115 | 60 | 13615 |
| 7 | 1550 | 32 | 7701 |
| 8 | 1550 | 60 | 8225 |

A study on optimizing friction stir welding process parameters to minimize defects and maximize fatigue life in 5083-H321 aluminum was done by Lombard, Hattingh, Steuwer and James[16]. They used a tool with a 50 mm shoulder diameter and a threaded/fluted pin 10 mm in diameter and 5.7 mm long. The tool was tilted at an angle of $2.5^{o}$ and the process parameter combinations can be seen in Table 6. Tensile testing

was performed and compared to the parent material which can be seen in Table 7. Fatigue life of the samples are given in Table 8. Their research shows that tool rotational speed was a big factor in governing tool torque, temperature, frictional power, fatigue performance, and tensile strength.

*Table 6: Process Parameter Combinations*

Tool rotational speed, feed and pitch values used in this work

| 85 mm/min | | | 135 mm/min | | | 185 mm/min | | |
|---|---|---|---|---|---|---|---|---|
| RPM[a] | Pitch[b] (mm/rev) | Weld no.[c] | RPM | Pitch (mm/rev) | Weld no. | RPM | Pitch (mm/rev) | Weld no. |
| 400 | 0.21 | 8 | 635 | 0.21 | 11 | 870 | 0.21 | 4 |
| 266 | 0.32 | 6 | 423 | 0.32 | 2 | 617 | 0.3 | 10 |
| 201 | 0.42 | 3 | 318 | 0.42 | 9 | 436 | 0.42 | 1 |
| | | | 254 | 0.51 | 5 | 348 | 0.53 | 7 |

[a] RPM, tool rotational speed in revolutions per minute.
[b] Pitch, distance moved forwards along the weld by the tool during one revolution.
[c] Weld no., identification number of a particular specimen.

*Table 7: Parent Material Comparison*

Tensile (UTS) and 0.2% proof strength data for 5083-H321 parent plate and the FS welds

| Weld No. | Average UTS[a] (MPa) | UTS/PP[b] | Average 0.2% Proof Strength[c] (MPa) | Proof/PP[d] |
|---|---|---|---|---|
| 1 | 289 | 0.78 | 171 | 0.67 |
| 2 | 241 | 0.65 | 153 | 0.60 |
| 3 | 313 | 0.84 | 161 | 0.63 |
| 4 | 254 | 0.68 | 144 | 0.57 |
| 5 | 308 | 0.83 | 165 | 0.65 |
| 6 | 315 | 0.85 | 164 | 0.65 |
| 7 | 294 | 0.79 | 150 | 0.59 |
| 8 | 308 | 0.83 | 145 | 0.57 |
| 9 | 273 | 0.74 | 145 | 0.57 |
| 10 | 310 | 0.84 | 148 | 0.58 |
| 11 | 306 | 0.82 | 141 | 0.56 |
| Parent plate | 371 | | 254 | |

[a] Average UTS value across the weld obtained from 3 tests in each welded plate.
[b] UTS/PP = ratio of average tensile strength of welded specimen to the parent plate value (average of 3 tests).
[c] Average 0.2% proof strength value from 3 tests in each welded plate.
[d] Proof/PP = ratio of average 0.2% proof strength for each welded plate to the parent plate value (average) for the 0.2% proof strength.

*Table 8: Fatigue Life*

Fatigue life for each combination of process parameters

| | | | | |
|---|---|---|---|---|
| RPM | 400 | 266 | 201 | |
| Pitch (mm/rev) | 0.21 | 0.32 | 0.42 | |
| Feed[a] (mm/min) | 85 | 85 | 85 | |
| Fatigue life[b] (cycles) | 21521 | 68798 | 50000 | |
| RPM | 635 | 423 | 318 | 254 |
| Pitch (mm/rev) | 0.21 | 0.32 | 0.42 | 0.51 |
| Feed (mm/min) | 135 | 135 | 135 | 135 |
| Fatigue life (cycles) | 74616 | 12746 | 14818 | 28624 |
| RPM | 870 | 617 | 436 | 348 |
| Pitch (mm/rev) | 0.21 | 0.30 | 0.42 | 0.53 |
| Feed (mm/min) | 185 | 185 | 185 | 185 |
| Fatigue life (cycles) | 32694 | 85897 | 16792 | 45021 |

[a] Tool feed rate during weld manufacture.
[b] Average of five tests for each welded plate.

## Conclusions of the Literature Review

Studies on defects and mechanical properties of friction stir welds in 5083 aluminum are extensive. Studies showing optimum process parameters to reduce defects are limited to a few common tool materials. Furthermore, few studies show a direct comparison of friction stir welds performed using different tool materials in 5083 aluminum. Additionally, few studies introduce new tool materials and compare its effectiveness with a common tool material or conventional fusion welds. Therefore, a study will be performed showing the effects of varying tool material on mechanical properties of the weld, as well as, the performance of each tool compared to conventional MIG welds and the parent material in 5083-H131 aluminum.

# IV. Materials and Equipment

This chapter provides a detailed listing of materials used (Table 9), as well as all the equipment used for processing and testing. Accuracy of the equipment is also provided.

*Table 9: Materials used in Experiments*

| **Tool Material** | **Thermal Conductivity** | **Specific Heat** | **Heat Treated Hardness** |
|---|---|---|---|
| H13 Tool Steel | 169 BTU-in/hr-ft²-°F | 0.110 BTU/lb-°F | 54 HRC |
| 420 Stainless Steel | 173 BTU-in/hr-ft²-°F | 0.110 BTU/lb-°F | 56 HRC |
| A2 Tool Steel | 198 BTU-in/hr-ft²-°F | 0.110 BTU/lb-°F | 59 HRC |
| **Welded Material** | **Comments** | | |
| 5083-H131 Alloy | Armored Aluminum Certified by Alcoa Inc. | | |
| **Etching Solution** | **Comments** | | |
| Sodium Hydroxide | Sodium Hydroxide reagent (20g of Sodium hydroxide in 100 mL of distilled water) | | |

A Cincinnati Computer Numerical Controlled (CNC) 3 axis milling machine was used to make the workpiece holder, tools, perform welds, and cut test specimens (Figure 11). It was programmed by using hand written g-code, canned cycles, Mastercam, and HSM Express. It has a positional accuracy of +/-0.0005", +/-0.05 ipm, and rotational accuracy under load of +/- 5 rpm.


*Figure 11: Cincinnati CNC Vertical Milling Machine*

A Southbend engine lathe was used to manually create the friction stir tool geometry from the 1" round stock (Figure 12). It has an accuracy of +/-0.0005".


*Figure 12: Southbend Lathe*

The friction stir tooling was designed in Solidworks. Three tool materials were used to make three sets of identical tools: H13 tool steel, 420 stainless steel, and A2 steel (pictured in Figure 13). Scrolled shoulder operations were performed on the Cincinnati CNC mill. Pin and shoulder tolerances are +/-0.0005" while other tolerances are +/-0.005. The tools were heat treated and tempered to produce a hardness above 50 HRC.

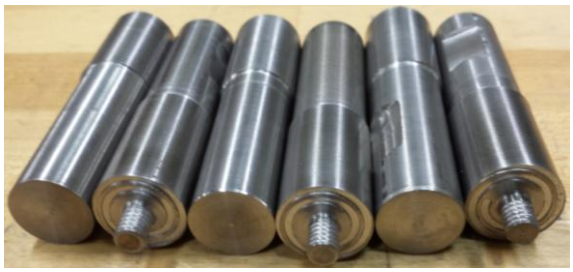

*Figure 13: Friction Stir Tooling*

The friction stir tools were designed with a ¾ inch shank to fit the available CAT-40 tool holder (Figure 14).

*Figure 14: CAT-40 ¾" shank tool holder with pin tool*

A Bridgeport mill, with an accuracy of +/-0.001", was used for drilling operations on the workpiece holder, friction stir tooling, and weld sample preparation (Figure 15).

*Figure 15: Bridgeport Vertical Milling Machine*

The workpiece holder was made from 1020 steel, designed in Solidworks, and cut using the Cincinnati CNC Vertical Milling machine (Figure 16). Manual operations were performed on the Bridgeport mill. All tolerances are within +/-0.002". It features six finger clamps and four set screws to fully constrain all axes of the workpieces. Figure 16 also shows the material to be welded after a one inch channel has been milled by the Cincinnati CNC to provide a consistently flat weld surface.

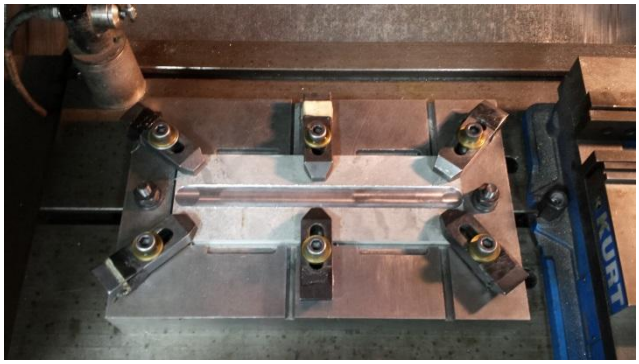

*Figure 16: Workpiece Holder*

A belt sander was used to deburr weld coupons and test specimens (Figure 17).

*Figure 17: Wilton Belt Sander*

A Tinius Olsen 1000 tensile tester was fitted with a 3-point bend test setup in the DML (Figure 18). It was set to 0.5 ipm speed with a peak hold of loads measured in pounds. The load cell has an accuracy of +/-5 lbs.

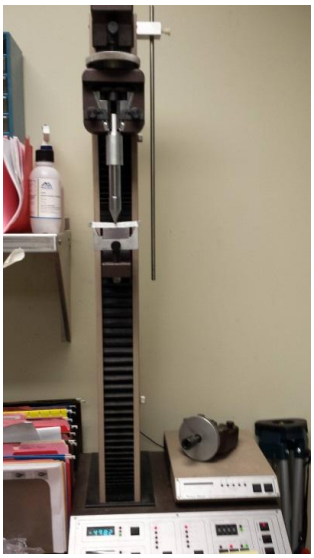

*Figure 18: Tinius Olsen 1000*

The Instron 5569 Universal Tester was used for tensile tests (Figure 19). The calibration of the Instron Model 5569, used by the Southern Nuclear Operating Company Dedication Lab, is performed annually under Instron's NVLAP accredited QA Program. For the load cell portion of this calibration, these forces are verified to be within +/-1% accuracy, 1% repeatability and zero return tolerance. The verification and equipment used in this service conform to a quality assurance program which meets the specifications outlined in ANSI/NCSL Z540-1, ISO 10012, ISO 9001:2008 and ISO/IEC 17025:2005.

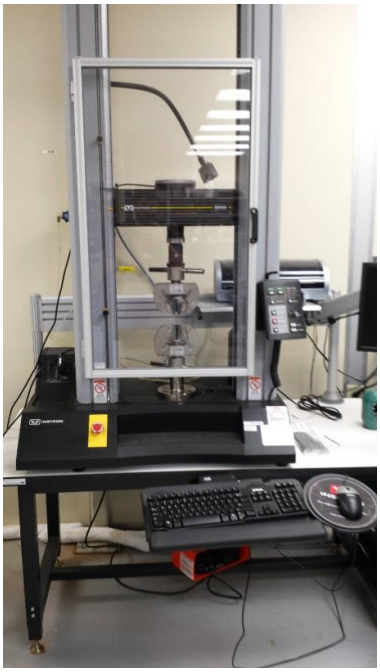

*Figure 19: Instron 5569 tensile tester*

The Keyence microscopes, located in the Auburn University Physics Lab, were used for precision void and micro crack measurements (Figure 20). They are capable of 5000x magnification.

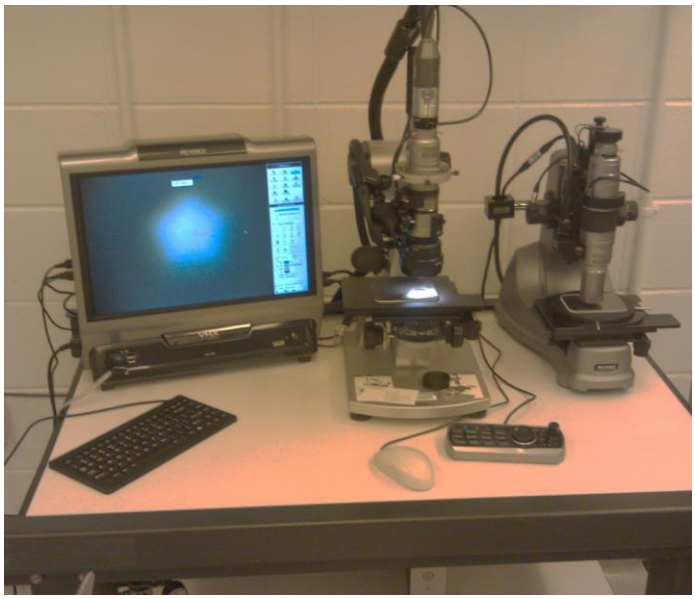

*Figure 20: Keyence Microscope*

The Aven Mighty Scope was used to obtain initial macroscopic images with magnification capabilities from 10x-200x (Figure 21).

*Figure 21: Aven Mighty Scope*

The Newage Indentron hardness tester was used to measure Rockwell B hardness across the weld profile (Figure 22). Hardness tester is maintained by Southern Nuclear Dedication Facility with an accuracy of +/- 1 Rockwell B.


*Figure 22: Newage Indentron Rockwell B hardness tester*

A MTM scale was used to measure 20g of sodium hydroxide for the etchant solution (Figure 23). The scale has an accuracy of +/- 0.1 grams.


*Figure 23: MTM Scale*

# V. Methodology

## Tool Selection and Preparation

H13 tool steel was selected because it was commonly used by others in the literature review. The 420 stainless steel was chosen for its very similar thermal characteristics to H13 (see Table 9). A2 tool steel was chosen for its higher thermal conductivity as well as ease of fabrication.

Figures 24 and 25 show the tool geometry used in this experiment. This geometry was based on findings during trial runs, literature reviews, and discussions with other friction stir welding research institutions. Tools were cut from one inch round stock using manual machining techniques on the Southbend lathe. The ¼" pin is slightly oversized at 0.254" on the diameter and the left hand 20 tpi threads were cut 0.008" deep with a 5/64" radius lathe insert. The lathe insert is triangular at 60 degrees and has relief angle of 15 degrees. The scrolled shoulder was cut 0.010" deep using a 1/8" flat end mill on the Cincinnati CNC vertical milling machine. The H13 and 420 stainless tools were heat treated to approximately 56 HRC at Pinson Valley Heat Treating located in Pinson, AL. The A2 steel tools were heat treated to approximately 59 HRC in the Auburn University Design and Manufacturing Laboratory (DML). The tools were designed for use in the Cincinnati CNC vertical mill and were loaded/seated into an available CAT-40 style ¾" shank tool holder.

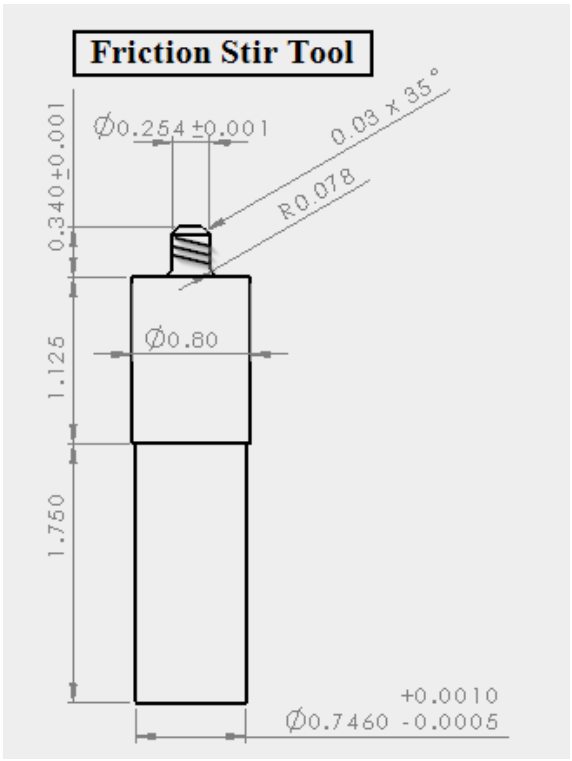


*Figure 24: Friction Stir Tool Geometry*

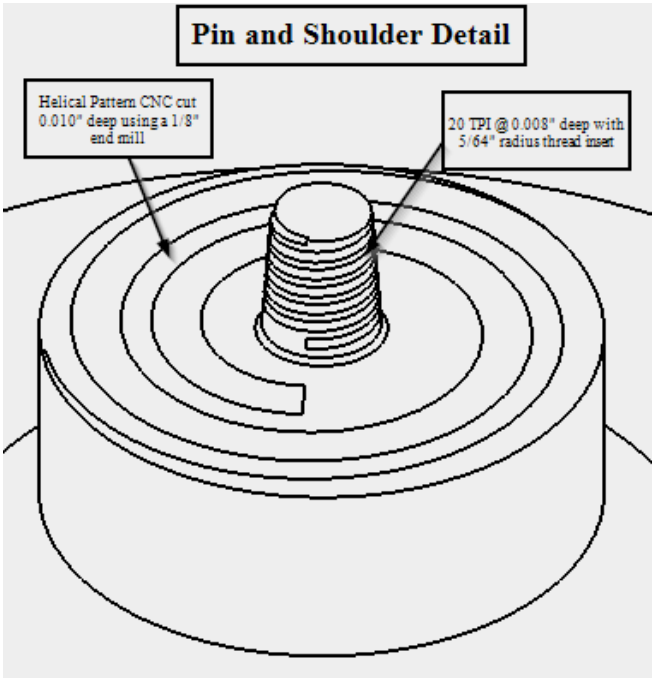


*Figure 25: Pin and Shoulder Detail*

Workpiece Holder

A workpiece holder was designed for use in the Cincinnati CNC vertical milling machine (see Figure 26). It was manufactured out of 1020 steel to accommodate two weld coupons in a butt weld configuration. Holes were drilled and tapped to allow using standard finger clamps. Set screws were used to ensure the coupons were held together tightly. The workpiece holder is designed to provide rigid support with a solid anvil surface to withstand the downforce during welds. Additionally, 18 gauge galvanized sheet metal was used as backing to protect the holder from damage during trial weld runs.

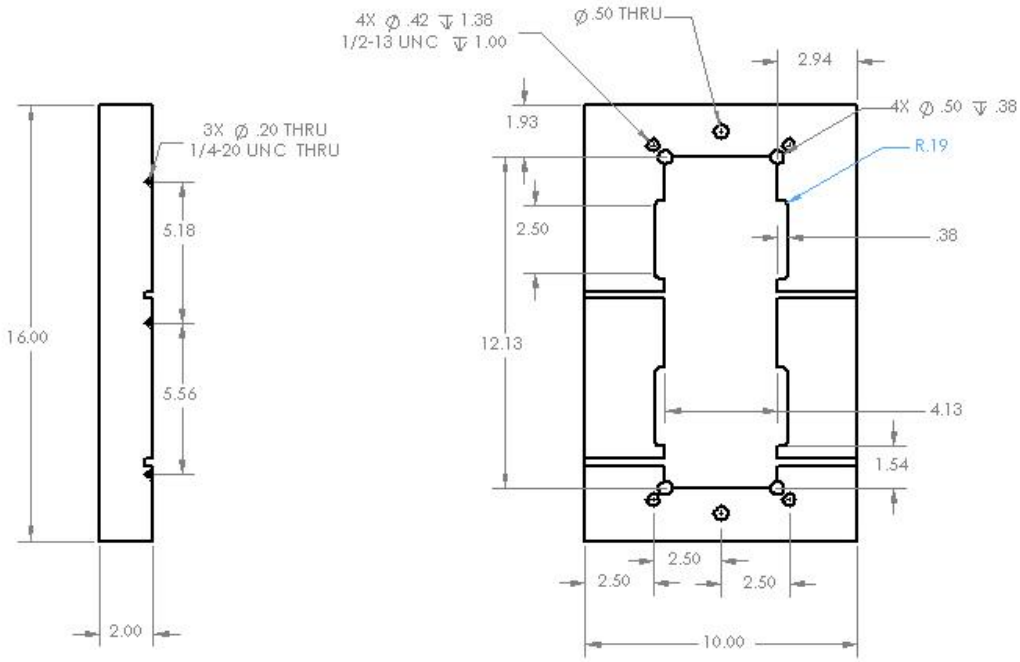


*Figure 26: Workpiece Holder Detail*

Material Preparation

The workpiece material was certified Aluminum 5083-H131, supplied by Anniston Army Depot as 2 inch wide, 12 inch long, 3/8 inch thick coupons. The edges

were water jet cut, requiring additional local operations to ensure they mate up with one another in a butt weld. The weld coupon's 3/8 inch x 12 inch edges were face milled on a Bridgeport vertical milling machine and deburred on the Wilton belt sander.

## Welding Program Schedules

The workpiece holder is mounted and aligned in the Cincinnati CNC vertical mill. A g-code program was written to prepare the workpiece for welding. Before butt welding two coupons together, a one inch flat end mill was used to make a 0.020" depth of cut pass along the butt seam to ensure a surface for uniform shoulder contact and forces during tool transits. The next portion of the g-code drills and bottom mills a ¼" pilot hole at 0.0005" past the depth the pin will be inserted in order to prevent compressive stresses on the pin. Then the program lowered the rotating friction stir tool into the pilot hole slowly until the shoulder was approximately -0.010" to 0.018" into the workpiece. Once the plunge depth was reached the tool dwelled for three seconds before traversing. The tool is traversed at a given rate for 1" down the seam between the two weld coupons before it retracted.

## Welding Parameter Selection

Initial experiments were conducted with 420 stainless steel and H13 tool steel, using various feeds and speeds to methodically narrow down a process window for welds with minimum defects. The process parameters were optimized for the respective tool material in the Cincinnati CNC by varying one parameter while keeping the others constant. Cross-sections of the welds were macroetched for visual examination of defects and their size noted with each variation in parameters until welds were obtained

free from visual defects in the cross-section of the weld. Samples were placed under a bend load to identify whether kissing bonds were present in the weld. Figure 27 shows how visual inspection of defects is used to verify optimal process parameters. Figure 28 shows how bend loads are used to reveal kissing bonds in plunge depth variation samples as described by Dickerson and Przydatek[9].

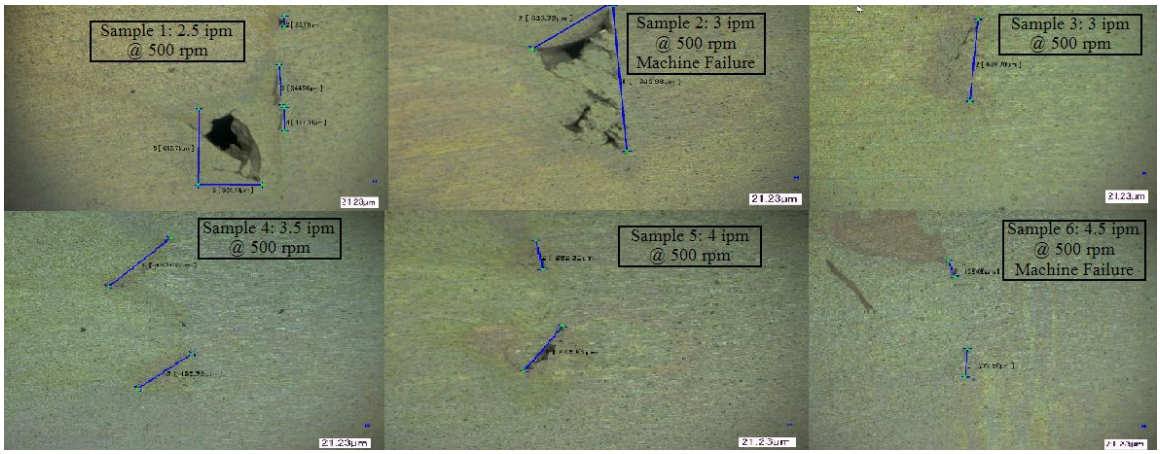


*Figure 27: Process Parameter Selection Using A2 Tools*


*Figure 28: Bend Tests for Kissing Bonds*

A procedure was developed based on the methods and lessons learned from optimizing parameters during initial weld runs with H13 tool steel and 420 stainless steel

tools for future university researchers to obtain similar weld results (see Appendix 1). The procedure was utilized to obtain the acceptable process parameters with A2 tool steel. Optimum weld parameters used in this experiment are shown in Table 10.

*Table 10: Optimal Process Parameters*

| **Tool material** | **Feed (ipm)** | **Speed (rpm)** |
|---|---|---|
| H13 Tool Steel | 3.5 | 500 |
| 420 Stainless Steel | 4 | 675 |
| A2 Tool Steel | 3.5 | 500 |

Statistical Comparison

Having produced welds that were visually free of weld defects, the experiment was designed to test the weld properties of three tool materials and compare the results with those from the parent material and MIG welds. Table 11 tabulates the number of replicates that were required for each test with a confidence level of 95%. Data was then compared for significance using t-tests and ANOVA.

*Table 11: Experimental Factors*

| **Factors: 3** | Parent Material | MIG Weld | FSW |
|---|---|---|---|
| **Levels** | 1 | 1 | 3 |
| **Responses: 3** | Bend Load | Tensile Strength | Hardness |
| Note: FSW @ 3 Levels: 3 different tool materials H13, 420, A2<br># of Replicates: 10 per factor level<br>Total Samples: 150 | | | |

Macroscopic and Microscopic Evaluation

Once a weld was complete, a test specimen was cut out from the cross section of the weld. The examinations used in this experiment include: visual inspection after

milling/sanding the cross-section of a weld to identify large defects, macroetching to see smaller defects, and microscopy measurements for microcracks. Samples are cut from the midpoint of the welds between the entrance and exit of the friction stir tool. Macroscopic samples were inspected on the cross-sectional face and viewed in the direction of the weld. Samples were cut using the DoAll vertical band saw and the cross-section milled with the Bridgeport mill. The milled surface was sanded to 4,000 grit and etched using Sodium Hydroxide reagent for one minute[17]. Macroscopic examination was performed with an Aven Mighty Scope for overall view up to 200x. The Keyence microscope was used for detailed measurements of defects. Visual examination samples of welds for each of the tool materials at the selected process parameters used in this experiment can be seen in Figure 29.

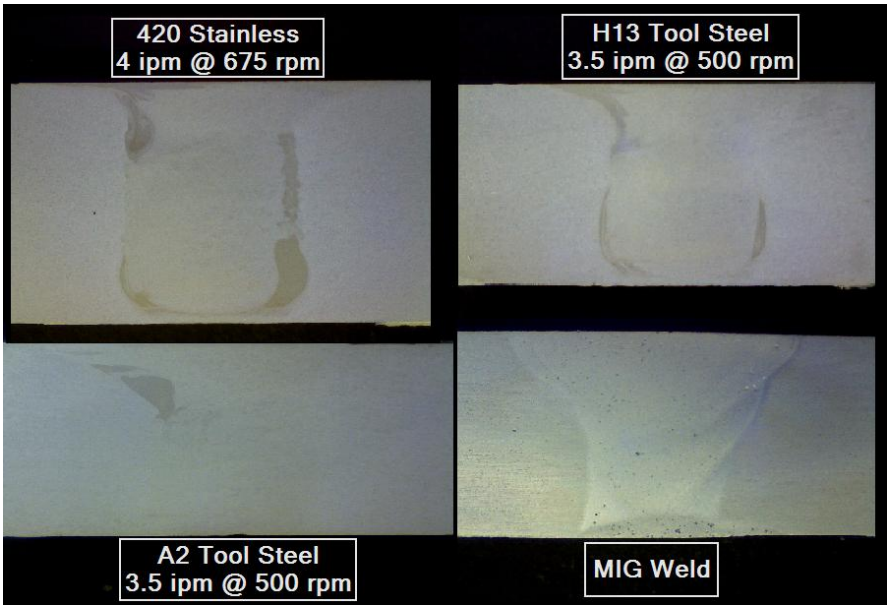


*Figure 29: Visual Examination of Final Welds*

Hardness Testing

Once the images were taken for visual examination, the samples were subsequently tested for hardness across the weld section (see Figure 30) using the Indentron hardness tester. This tester is set up for Rockwell B using a 1/16" ball indenter as per ASM guidelines for hardness testing in aluminum[18]. A total of 5 hardness tests were performed across the weld.

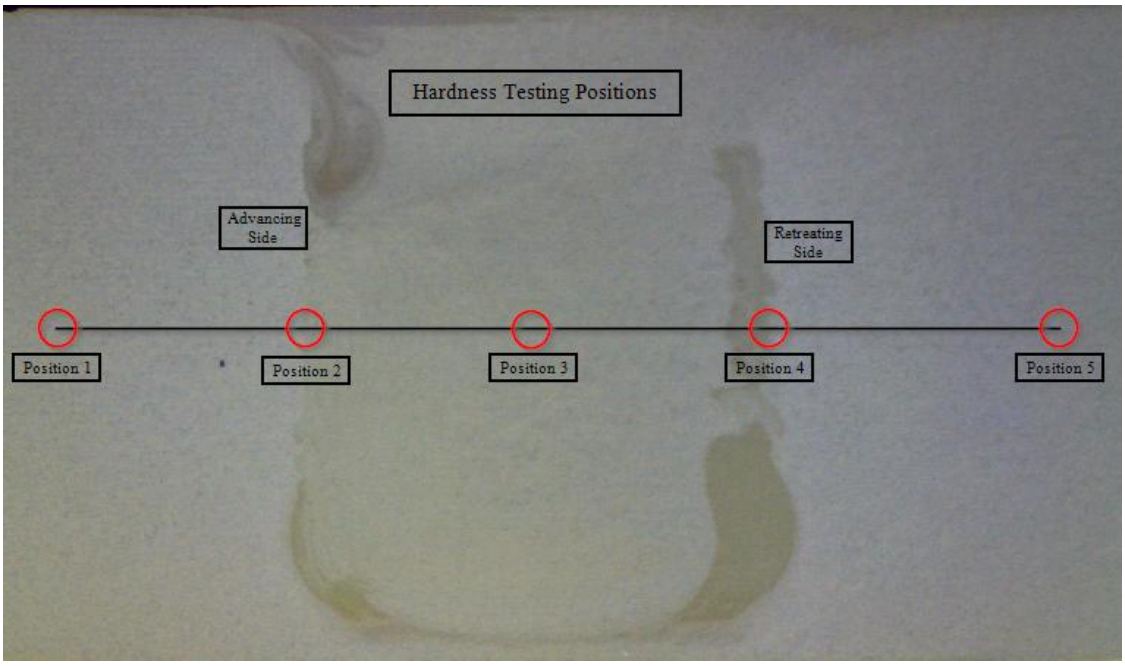


*Figure 30: Hardness Testing Locations*

Bend Testing

Bend testing was set up and performed to meet the specific needs of this experiment using guidance from the ASM "Mechanical Testing" handbook[18]. Bend test samples were cut using the DoAll vertical band saw and milled on the Bridgeport mill to the specification in Figure 31, with a tolerance of +/-0.003". Samples were placed on the Tinius Olsen for bend testing and set to run tests at 0.5 ipm. Bend testing was set up as illustrated in Figure 32.

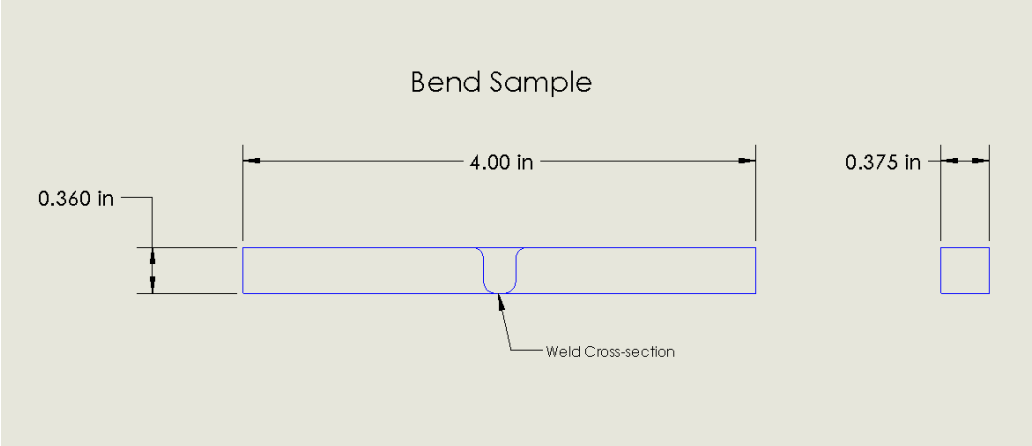


*Figure 31: Bend Sample*

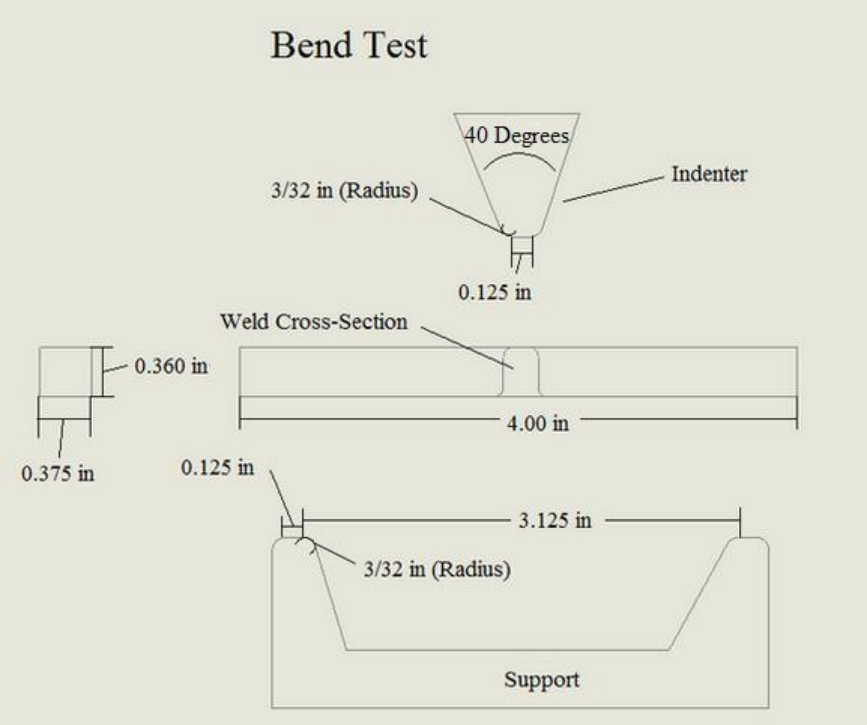


*Figure 32: Bend Testing Configuration*

Tensile Testing

For tensile tests, a g-code program was created for the Cincinnati CNC vertical mill which cut tensile specimens to dimensions consistent with ASTM guidelines[19]. Tensile specimens were manually milled on the Bridgeport milling machine to a specific

thickness in order to obtain test specimens from the centroid of the weld (see Figure 33). The tensile tests were performed at Southern Company's Nuclear Dedication Facility at Farley Nuclear plant using an Instron 5569 tensile tester with 0.5 ipm rate of pull.

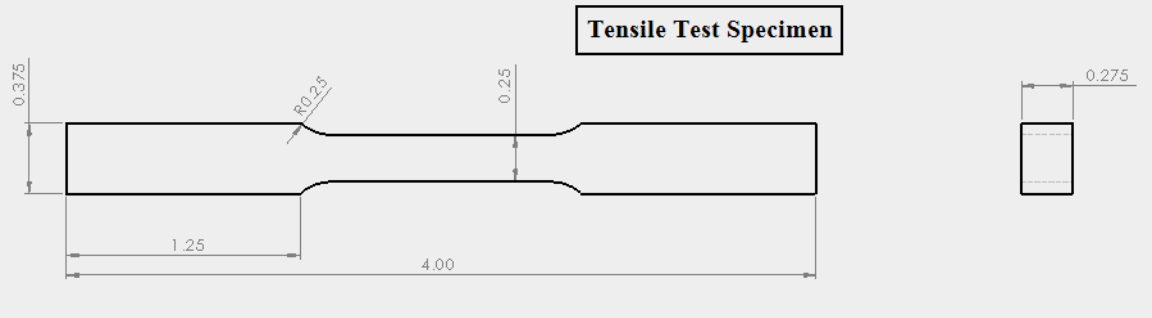


*Figure 33: Tensile Test Specimens*

# VI. Results of the Experiment

In this section, the results are shown in mean values for each of the mechanical tests and evaluated for significance. The raw data for each of the tests may be viewed in Appendices 3, 4, and 5. The test results for the mechanical properties of the sample groups are evaluated using an ANOVA analysis to show whether the group means are different. A p-value $< 0.05$ indicates that data results are significantly different, with greater than 95% confidence. If the ANOVA indicates the group data has significantly different means, then one or more of the sets of means in the data are different. Thus, t-tests are performed to show whether a significant difference in means exist between two groups of data. This will be used to identify the weld samples which are significantly different.

## Bend Testing

Results are shown in Figure 34 comparing mean bend strength of friction stir welds, MIG welds, and parent material. A subsequent ANOVA is performed to verify whether the means between all the sets of data are significantly different.

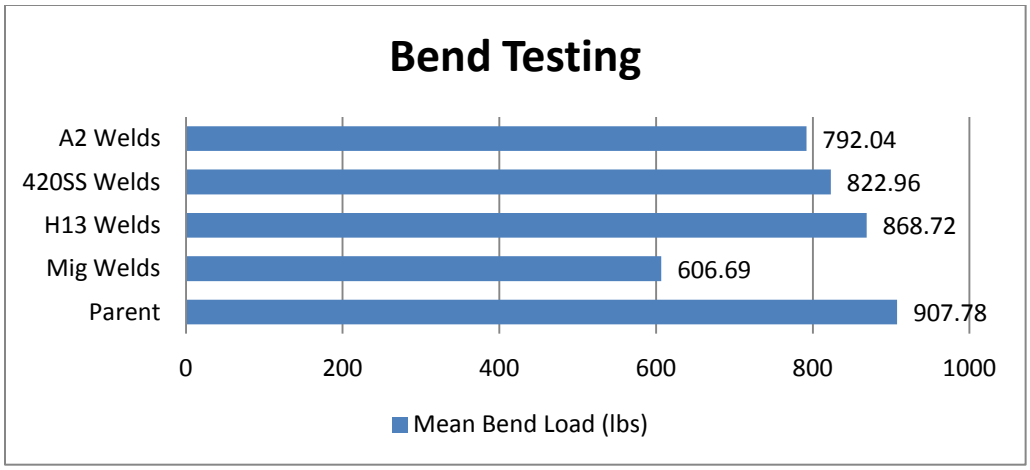


*Figure 34:Mean Bend Results*

The ANOVA of the bend tests in Table 12 shows the P-value is less than 0.05 which proves there is a significant difference (with 95% confidence) in the means for each set of results. Therefore, a two sample t-test was performed to determine if each set of test results were significantly different from each other.

*Table 12: Bend Test ANOVA*

**Anova: Single Factor**

SUMMARY

| *Groups* | *Count* | *Sum* | *Average* | *Variance* |
|---|---|---|---|---|
| Parent | 10 | 9077.8 | 907.78 | 3296.6 |
| MIG Welds | 10 | 6066.9 | 606.69 | 1466.5 |
| H13 Welds | 10 | 8687.2 | 868.72 | 2288.1 |
| 420SS Welds | 10 | 8229.6 | 822.96 | 1625.6 |
| A2 Welds | 10 | 7920.4 | 792.04 | 70.294 |

ANOVA

| *Source of Variation* | *SS* | *df* | *MS* | *F* | *P-value* | *F crit* |
|---|---|---|---|---|---|---|
| Between Groups | 542975.91 | 4 | 135743.98 | 77.594 | 1.323E-19 | 2.579 |
| Within Groups | 78723.129 | 45 | 1749.4029 | | | |
| Total | 621699.04 | 49 | | | | |

Data from t-tests which compare means between each factor level are shown in Table 13. As one can see from Figure 34, the t-tests document that there is a significant difference in bend loads for the mean loads between friction stir welds and MIG welds. The only comparison that did not show a significant difference in mean was H13 tool steel welds versus the parent material. However, there was a significant difference in the bend loads between the other two friction stir welds and the parent material. The H13 friction stir welds are statistically identical to the parent material in bending.

*Table 13: Individual Bend Test Comparison*

| Mean Comparison | T-test Results | | Significant if P < 0.05 (95% Confidence) |
|---|---|---|---|
| H13 vs 420 | t Stat | 2.313102292 | |
| | P(T<=t) two-tail | 0.03274729 | Significant |
| | t Critical two-tail | 2.100922037 | |
| A2 vs H13 | t Stat | 4.993173361 | |
| | P(T<=t) two-tail | 0.000542769 | Significant |
| | t Critical two-tail | 2.228138842 | |
| A2 vs 420 | t Stat | 2.374337115 | |
| | P(T<=t) two-tail | 0.038987529 | Significant |
| | t Critical two-tail | 2.228138842 | |
| H13 vs MIG | t Stat | 13.52295056 | |
| | P(T<=t) two-tail | 7.20709E-11 | Significant |
| | t Critical two-tail | 2.100922037 | |
| H13 vs Parent | t Stat | 1.652853404 | |
| | P(T<=t) two-tail | 0.115695916 | Not Significant |
| | t Critical two-tail | 2.100922037 | |
| A2 vs MIG | t Stat | -14.95155017 | |
| | P(T<=t) two-tail | 3.60668E-08 | Significant |
| | t Critical two-tail | 2.228138842 | |
| A2 vs Parent | t Stat | 6.30768842 | |
| | P(T<=t) two-tail | 0.000139703 | Significant |
| | t Critical two-tail | 2.262157158 | |
| 420 vs MIG | t Stat | 12.29904646 | |
| | P(T<=t) two-tail | 3.39196E-10 | Significant |
| | t Critical two-tail | 2.100922037 | |
| 420 vs Parent | t Stat | 3.823141786 | |
| | P(T<=t) two-tail | 0.001245474 | Significant |
| | t Critical two-tail | 2.100922037 | |

Tensile Testing

Results are shown in Figure 35 comparing mean tensile strength of friction stir welds, MIG welds, and parent material. An ANOVA is performed to verify the means between all the sets of data are significantly different.

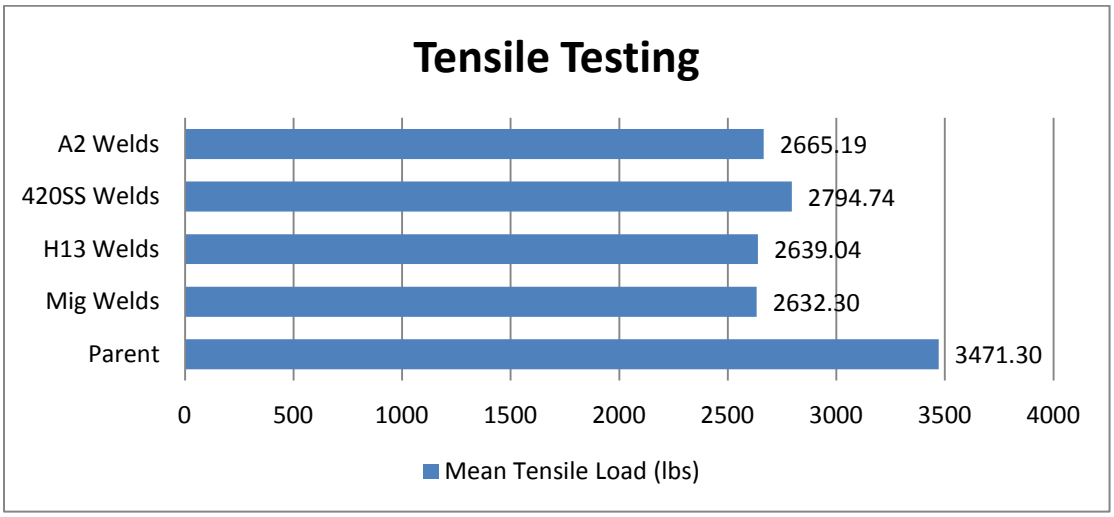


*Figure 35: Mean Tensile Results*

The ANOVA of the tensile tests in Table 14 shows the P-value is less than 0.05 which proves there is a significant difference (with 95% confidence) in means for each set of results. Further analysis is required using two sample t-tests to determine if means between the test results are significantly different.

*Table 14: Tensile Test ANOVA*

**Anova: Single Factor**

SUMMARY

| *Groups* | *Count* | *Sum* | *Average* | *Variance* |
|---|---|---|---|---|
| Parent | 10 | 34712.95 | 3471.295 | 4285.3 |
| MIG Welds | 10 | 26323.01 | 2632.301 | 7181.3 |
| H13 Welds | 10 | 26390.35 | 2639.035 | 9568.9 |
| 420SS Welds | 10 | 27947.39 | 2794.739 | 25233 |
| A2 Welds | 10 | 26651.9 | 2665.19 | 46729 |

ANOVA

| *Source of Variation* | *SS* | *df* | *MS* | *F* | *P-value* | *F crit* |
|---|---|---|---|---|---|---|
| Between Groups | 5146649.66 | 4 | 1286662.42 | 69.177 | 1.225E-18 | 2.579 |
| Within Groups | 836977.287 | 45 | 18599.4953 | | | |
| Total | 5983626.95 | 49 | | | | |

Data from t-tests comparing mean tensile loads between each factor level are shown in Table 15. As it is apparent in Figure 35, the parent material has a significantly higher tensile strength than the welded samples. There is no significant difference in tensile strength between MIG welds, A2, and H13 tool welds. The 420 tool welds are significantly stronger than MIG and H13 welds in tension.

*Table 15: Individual Tensile Testing Comparison*

| Between Groups | T-test Results | | Significant if P < 0.05 (95% Confidence) |
|---|---|---|---|
| H13 vs 420 | t Stat | -2.6393596 | |
| | P(T<=t) two-tail | 0.0166591 | Significant |
| | t Critical two-tail | 2.100922 | |
| A2 vs H13 | t Stat | 0.3485848 | |
| | P(T<=t) two-tail | 0.7329817 | Not Significant |
| | t Critical two-tail | 2.1603687 | |
| A2 vs 420 | t Stat | -1.5271525 | |
| | P(T<=t) two-tail | 0.1441041 | Not Significant |
| | t Critical two-tail | 2.100922 | |
| H13 vs MIG | t Stat | 0.1645368 | |
| | P(T<=t) two-tail | 0.8711422 | Not Significant |
| | t Critical two-tail | 2.100922 | |
| H13 vs Parent | t Stat | -22.359862 | |
| | P(T<=t) two-tail | 1.393E-14 | Significant |
| | t Critical two-tail | 2.100922 | |
| A2 vs MIG | t Stat | 0.4479345 | |
| | P(T<=t) two-tail | 0.6621801 | Not Significant |
| | t Critical two-tail | 2.1788128 | |
| A2 vs Parent | t Stat | -11.286145 | |
| | P(T<=t) two-tail | 2.179E-07 | Significant |
| | t Critical two-tail | 2.2009852 | |
| 420 vs MIG | t Stat | 2.8531163 | |
| | P(T<=t) two-tail | 0.0127712 | Significant |
| | t Critical two-tail | 2.1447867 | |
| 420 vs Parent | t Stat | -12.452562 | |
| | P(T<=t) two-tail | 3.198E-08 | Significant |
| | t Critical two-tail | 2.1788128 | |

Hardness Testing

Results are shown in Figure 36 comparing mean hardness across the welds (refer to Figure 30) of friction stir welds, MIG welds, and average hardness of the parent material. An ANOVA is performed to verify whether the means between all the sets of data are significantly different.

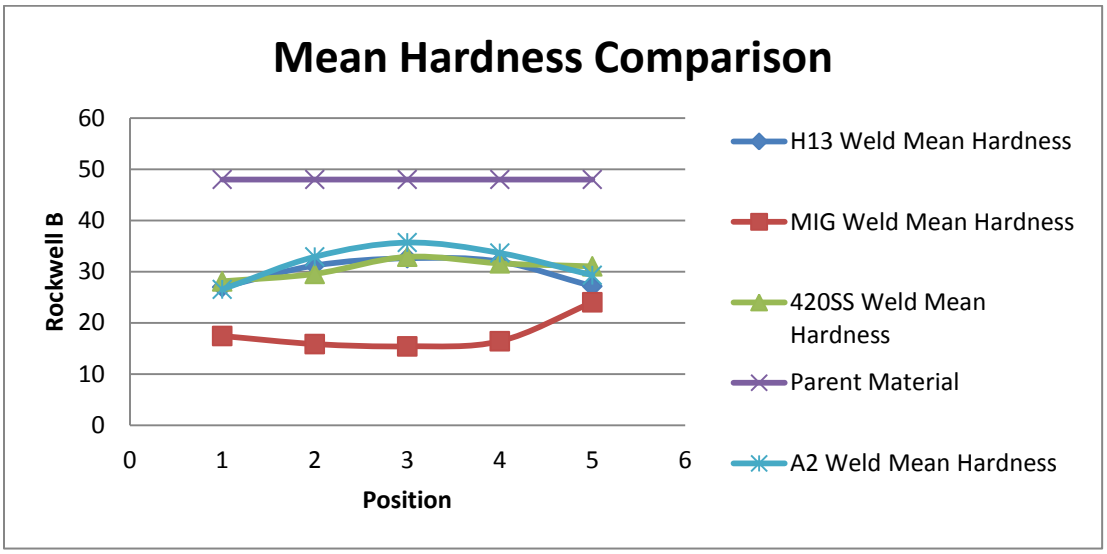


*Figure 36: Mean Hardness Results*

The ANOVA of the hardness tests in Table 16 shows the P-value for the material variation is less than 0.05 which indicates the average hardness is significantly different (with 95% confidence) between the welds and parent material, which requires further analysis.

*Table 16: Hardness Tests ANOVA*

Anova: Two-Factor Without Replication

| *SUMMARY* | *Count* | *Sum* | *Average* | *Variance* |
|---|---|---|---|---|
| Parent | 5 | 240 | 48 | 0 |
| MIG | 5 | 89.06 | 17.812 | 12.57937 |
| H13 TS | 5 | 149.89 | 29.978 | 7.40347 |
| 420 SS | 5 | 153.19 | 30.638 | 3.50177 |
| A2 TS | 5 | 158.04 | 31.608 | 13.38467 |

ANOVA

| *Source of Variation* | *SS* | *df* | *MS* | *F* | *P-value* | *F crit* |
|---|---|---|---|---|---|---|
| Material | 2313.125 | 4 | 578.2813 | 83.02618 | 1.72E-10 | 3.006917 |
| Error | 111.4408 | 16 | 6.965048 | | | |
| Total | 2460.603 | 24 | | | | |

Table 17 shows results from multiple ANOVA analysis comparing interactions between the three friction stir tool welds, the tool welds versus MIG, and tool welds versus the parent material. As seen in Figure 36, the ANOVA tests for mean hardness across the welds show that interactions between friction stir welds are the same and significantly different than MIG weld samples. Furthermore, the parent material is significantly different than the friction stir welds.

*Table 17: Hardness Testing Comparison*

| Interactions | ANOVA Results | | Significant if P < 0.05 (95% Confidence) |
|---|---|---|---|
| A2, H13, 420 | F-value | 1.6992897 | |
| | P-value | 0.242637 | Not Significant |
| | F crit | 4.4589701 | |
| A2, H13, 420, MIG | F-value | 24.742384 | |
| | P-value | 1.999E-05 | Significant |
| | F crit | 3.4902948 | |
| A2, H13, 420, Parent | F-value | 124.31098 | |
| | P-value | 2.656E-09 | Significant |
| | F crit | 3.4902948 | |

# VII. Discussion

This chapter discusses the findings from the experiment and the collected data. First, the results from the bend test are presented along with the analysis of statistical data comparing the means of the group and each pair. Then the results from the tensile tests and statistical analysis are discussed, as well as, the factors affecting the results. Next, the hardness tests and visual examinations are discussed along with the statistical determinations which compared the means for the samples. The discussion chapter will close with the findings using the initial weld results to find the process parameters for A2 tool steel.

## Bend Tests

Bend testing was a valuable tool in determining the strength of a weld compared to the parent material. When finding the initial process parameters the bend tests were used to detect kissing bonds in the welds. When a weld containing a kissing bond was bent, the loads would be extremely low compared to the parent material. Data was collected for comparison purposes which assisted in the development of welds with fewer defects. The bend samples were cut using the CNC machine and were dimensionally correct but variations in the parent material bend loads were higher than the welded samples. It can be seen in Table 18 that the parent material had the highest standard deviation. The welds lower standard deviation may be due to the processing of the material during welding which lowers the hardness. The H13 tool weld samples also had

a high standard deviation, but is considered statistically equivalent in bending to the parent material.

*Table 18: Bend Testing Data*

| Material | Parent | MIG Welds | H13 Welds | 420SS Welds | A2 Welds |
|---|---|---|---|---|---|
| Sample # | Bend Testing (lbs) | | | | |
| 1 | 821.2 | 547.3 | 812.7 | 775.8 | 770.5 |
| 2 | 839.3 | 562.4 | 824.7 | 779.8 | 788.7 |
| 3 | 842.2 | 576 | 824.8 | 782.3 | 789.7 |
| 4 | 901.2 | 580 | 826.4 | 787.1 | 792.1 |
| 5 | 903.4 | 598.8 | 851.6 | 804.4 | 793 |
| 6 | 922.9 | 632.5 | 870 | 847.8 | 794.5 |
| 7 | 942.9 | 635.2 | 898 | 851.7 | 796.4 |
| 8 | 946.8 | 636.1 | 911.8 | 863.3 | 797.9 |
| 9 | 977.3 | 646.3 | 920 | 867.1 | 798.4 |
| 10 | 980.6 | 652.3 | 947.2 | 870.3 | 799.2 |
| Mean: | 907.78 | 606.69 | 868.72 | 822.96 | 792.04 |
| Std Dev: | 57.41583 | 38.2947763 | 47.8337816 | 40.31851518 | 8.3841385 |

Tensile Tests

The tensile tests were an excellent tool to understand the strength of the weld as compared to that of the parent material and other welds. Initial tensile tests showed defects, such as micro cracks and kissing bonds which produced low tensile strengths. Adjustments to the down force, while running optimal process parameters of the tool, helped mitigate these defects. The results in Table 19 show the mean loads for each set of samples. It is apparent that the MIG welds and parent material have large differences in strength, which is consistent with the ANOVA in Table 14. The MIG welds were equivalent to the A2 and H13 tool welds in tension. However, tensile testing of the A2 and H13 tool welds revealed underlying defects which resulted a low mean tensile

strength (Table 19). Since the tensile specimens did not show any visible defects prior to testing, it is likely that welds had microcracks due to a lack of downforce, that were not visible in the cross-section of the welds. Weld efficiency was calculated as a percentage of the parent material tensile strength. The 420 tool welds had the highest weld efficiency at 80.5%. This may be a result of the fact that the lowest hardness across the weld profile is higher than any of the other welds lowest hardness. This results in a stronger weak point to yield first, since hardness is directly related to tensile strength.

*Table 19: Cumulative Tensile Testing Data*

| Material | Parent | MIG Welds | H13 Welds | 420SS Welds | A2 Welds |
|---|---|---|---|---|---|
| Sample # | Tensile Testing (lbs) | | | | |
| 1 | 3391.6 | 2450.9 | 2535.72 | 2544.52 | 2401.22 |
| 2 | 3407.46 | 2557.19 | 2551.44 | 2641.06 | 2513.5 |
| 3 | 3433.27 | 2572.84 | 2569.61 | 2687.92 | 2524.67 |
| 4 | 3439.75 | 2623 | 2589.83 | 2696.27 | 2538.69 |
| 5 | 3444.94 | 2628.8 | 2610.83 | 2788.09 | 2540.88 |
| 6 | 3461.7 | 2683.28 | 2613.05 | 2794.4 | 2604.72 |
| 7 | 3470.07 | 2690.1 | 2631.7 | 2821.6 | 2711.19 |
| 8 | 3516.58 | 2690.38 | 2684.77 | 2945.62 | 2797.26 |
| 9 | 3543.37 | 2709.52 | 2757 | 3006.17 | 2920.93 |
| 10 | 3604.21 | 2717 | 2846.4 | 3021.74 | 3098.84 |
| Mean: | 3471.30 | 2632.30 | 2639.04 | 2794.74 | 2665.19 |
| Std Dev: | 65.46184 | 84.74262268 | 97.82072892 | 158.8488664 | 216.1690412 |
| UTS (ksi) | 50.49 | 38.29 | 38.39 | 40.65 | 38.77 |
| Weld Efficiency | 100.0% | 75.8% | 76.0% | 80.5% | 76.8% |

Hardness Tests

The friction stir tool material did not have an effect on the hardness of the welds. It was noted that the hardness of the MIG welds was significantly lower than the rest of the samples and may be attributed to the high temperatures during the fusion process. The hardness profile of the friction stir welds were lower than the parent material but

were not as low as the MIG welds because they do not melt the material or add filler material.

Procedural Weld Results

The procedure in Appendix 1 was created as a guide for finding acceptable weld parameters for 5083 aluminum, using steel tools with similar geometries, in a vertical CNC mill. Subsequent researchers following this procedure can eliminate common mistakes which could lead to weld defects. The procedure was compiled from experiences in obtaining acceptable weld parameters using H13 tool steel and 420 stainless steel. The use of the procedure for determining operating parameters with A2 tools is described below.

The procedure began with the proper set up for repeatable welds. The tool was seated properly and all coordinates obtained in the CNC machine. Test welds were ran to establish plunge depth and to assist in seating the tool. Feed selection runs were performed using various feed rates from 2.5-5 ipm and a fixed speed of 500 rpm. The 5 ipm weld run was discarded because the CNC machine could not handle the load. The visual examination of the feed selection runs did not reveal surface tears or extremely large tunnel voids. Most voids became apparent after etching and some not apparent until viewed under a microscope. The feed selected which produced the smallest defect was 3.5 ipm and can be seen in Figure 27.

The speed selection step in the procedure was run using the previously identified feed of 3.5 ipm and varying the speed from 300-800 rpm. The speed of 300 and 400 rpm were thrown out due to massive surface tears. The speed selected with the least defects was 500 rpm and produced a void free weld. Figure 37 shows the lack of voids or

microcracks in the area where defects normally occur on the advancing side of the weld. The black dots in the figure are microscopic cavities from over etching.

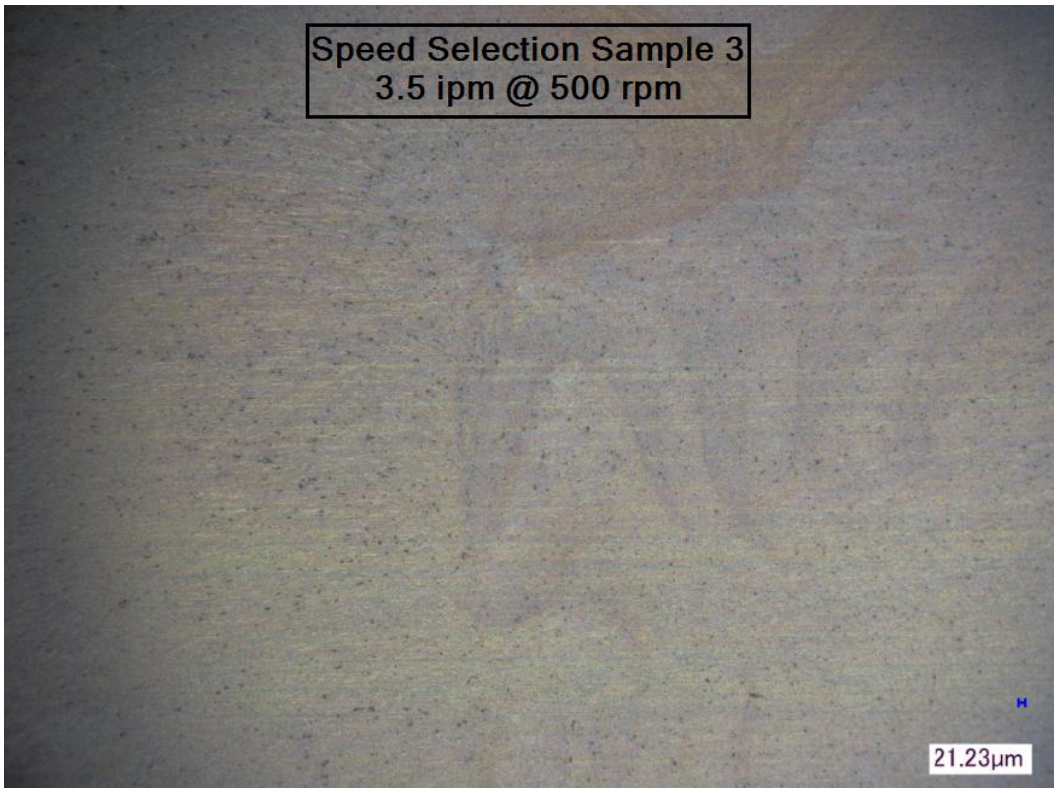


*Figure 37: Speed Selection Sample 3*

Speed verification used weld speeds above and below the previously selected speed (500 rpm) in order to identify weld parameters which produce less defects. Samples in Appendix 4 show a decrease in defects from samples 1-3 and an increase in defects in samples 4-6, indicating the previously selected speed of 500 rpm is correct. Feed verification used feeds above and below the previously selected feed of 3.5 ipm in order to identify weld parameters which produce an acceptable weld. Samples can be seen in Appendix 4 and show a decrease in defects from samples 1-3 and an increase in defects in samples 4-6, indicating the previously selected feed of 3.5 ipm is correct.

Repeatability tests were performed to verify that repeatable welds could be obtained. This was done by running six welds at the selected feed and speed of 3.5 ipm and 500 rpm. The welds were cut into bend samples and bent to verify consistency. Bend results were consistent with a standard deviation of 8.38 lbs (see Table 18) and indicated that the weld was stronger than the MIG welds. Therefore, the weld parameters are acceptable for experimental use. Final testing was completed for hardness and tensile strength. Mean values for tensile and hardness can be seen in Figures 34 and 35 or raw data can be seen in Appendix 4 and 5 respectively.

With the exception of the H13 tool steel weld bend tests, the friction stir welds did not exhibit mechanical strengths as great as the parent material. This is most likely a result of the thermal cycle during the welding process. Since the FSW does not get hot enough to melt the material, like MIG welds, the mechanical strengths of the weld fall between that of the MIG welds and parent material. The H131 designates the cold rolled process which gives the material higher hardness and tensile strengths[20]. Post weld work (strain) hardening, such as cold rolling, may return the material to the strength of the parent material. This would be possible with friction stir welds as they do not add a new material to the weld joint like MIG welds.

# VIII. Conclusions and Future Work

A comprehensive literature review was conducted covering topics such as general review of the friction stir welding process, tool geometry, tool materials, microstructure/mechanical properties, defects, and process parameters. Tooling was developed for experimental welds and a rapid exchange of the workpiece. Initial welds were performed to establish acceptable welding parameters in 5083 aluminum. Using the identified weld parameters, welds were performed to show the effects that various tool materials have on the mechanical properties of a friction stir weld. The experimental results compare data from mechanical testing between the various tool materials, MIG welds, and parent material for statistical significance. Additionally, a procedure was created from the initial findings to develop acceptable welds using new tool materials for researchers. The results from this experiment are listed below.

- 3-Point bend test results comparing MIG welds and friction stir welds are significantly different than one another. Friction stir welds with H13 tool steel tools produced the best bend results compared to MIG welds
- 3-Point bend test results were significantly different between the parent material and all welds except for friction stir welds using H13 tool steel tools. H13 tool steel welds produced bend tests identical to the parent material.

- Tensile testing results show that there is not a significant difference in tensile strength of friction stir welds using A2 tools as compared to 420 or H13 tools. However, there is a significant difference in tensile strength of friction stir welds using H13 tools as compared to 420 tools, in which 420 tool welds were better.
- Mig welds do not have a significantly different tensile strength than friction stir welds using H13 and A2 tools. Friction stir welds using 420 tools have a significantly stronger tensile strength than MIG welds.
- The parent material tensile strength is significantly different than the friction stir welds and MIG welds. It is better in all cases.
- The data obtained from the friction stir welds hardness profile of each group of friction stir welds was not significantly different, indicating the choice of tool material has no effect on the weld hardness.
- The friction stir welds had a significantly higher hardness profile than MIG welds but a lower hardness than the parent material.
- Procedural welds using A2 tools showed evidence of process parameter improvements to acceptable weld conditions in microscopy defect measurements, which are documented in the report. In general, A2 tools produced welds with no visual defects in visual and microscopic examinations.
- Procedural friction stir welds using A2 tools were stronger than MIG welds in bending and hardness, but not in tensile strength.
- The optimal weld of 5083 aluminum obtained locally by friction stir welding was done with 420 stainless steel tools at 4 ipm and 675 rpm.

Recommendations for Future Work

Friction stir welding using the vertical CNC machine is more accessible than a friction stir welding machine for researching the weld process. However, the methods for controlling certain parameters had to be improvised. The machine was underpowered for running low speed welds and would shut off after hitting overload limits. There was no way to control the downforce of a weld and constant adjustments had to be made utilizing the spindle load and assessments of visual defects. Additionally, there was no way to tilt the tool and downforce was lost in long welds due to the tool sinking into the workpiece.

It is recommended that the future experiments should:

- Compare weld results using a $2^{o}$ tilted tool and same weld parameters
- Add a load cell to measure down force during welds
- Add a dynamometer to measure the traversing loads while varying process parameters
- Gain access to radiography capabilities for non destructive analysis of welds
- Experiment with varying feeds and speeds in a single continuous weld and observe the change in void defects using radiographic examination
- Acquire a more powerful machine designed for continuous duty welding
- Compare results of the friction stir welds before and after work hardening the weld area to see if the hardness increases to that of the parent material
- Using different tool geometries such as triangular pin profiles
- Extend the procedure by welding other materials

# IX. References


1. Kandaswaamy, S.P., L. N., *Thermal Field Mapping Technique for Friction Stir Process,* in *Mechanical Engineering*. 2009, Auburn University.
2. Cantin, G.M.D., et al., *Friction Skew-stir Welding of Lap Joints in 5083-O Aluminium.* Science and Technology of Welding and Joining, 2005. 10(3): p. 268-280.
3. Fujii, H., et al., *Effect of Tool Shape on Mechanical Properties and Microstructure of Friction Stir Welded Aluminium Alloys.* Materials Science and Engineering, 2006(A419): p. 25-31.
4. R.A. Prado, L.E.M., D.J. Shindo, K.F. Soto, *Tool Wear in the Friction-stir Welding of Aluminium Alloy 6061 + 20% $Al_2O_3$: a Preliminary Study.* Scripta Materialia, 2001(45): p. 75-80.
5. Saito, N., et al., *Joining of 5083 and 6061 Aluminium Alloys by Friction Stir Welding.* Journal of Material Science Letters, 2003(22): p. 353-356.
6. Peel, M., et al., *Microstructure, Mechanical Properties and Residual Stresses as a Function of Welding Speed in Aluminium AA5083 Friction Stir Welds.* Acta Materialia, 2003.
7. Arbegast, W.J., *A Flow-partitioned Deformation Zone Model for Defect Formation During Friction Stir Welding.* Scripta Materialia, 2008.

8. Zucchi, F., G. Trabanelli, and V. Grassi, *Pitting and Stress Corrosion Cracking Resistance of Friction Stir Welded AA5083.* Materials and Corrosion, 2001(52): p. 853-859.

9. Dickerson, T.L. and J. Przydatek, *Fatigue of Friction Stir Welds in Aluminium Alloys that Contain Root Flaws.* International Journal of Fatigue, 2003(25): p. 1399-1409.

10. Zhou, C., X. Yang, and G. Luan, *Effect of Kissing Bond on Fatigue Behavior of Friction Stir Welds on Al 5083 Alloy.* J. Materials Science, 2006(21): p. 2771-2777.

11. Han, M.-S., et al., *Optimum Condition by Mechanical Characteristic Evaluation in Friction Stir Welding for 5083-O Al Alloy.* Transactions of Nonferrous Metals Society of China, 2009(19): p. 17-22.

12. Hirata, T., et al., *Influence of Friction Stir Welding Parameters on Grain Size and Formability in 5083 Aluminium Alloy.* Materials Science and Engineering, 2007(A 456): p. 344-349.

13. James, M.N., D.G. Hattingh, and G.R. Bradley, *Weld Tool Travel Speed Effects on Fatigue Life of Friction Stir Welds in 5083 Aluminium.* International Journal of Fatigue, 2003(25).

14. Sato, Y.S., et al., *Hall-Petch Relationsip in Friction Stir Welds of Equal Channel Angular-Pressed Aluminium Alloys.* Materials Science and Engineering, 2003(A354): p. 298-305.

15. Bisadi, H., M. Tour, and A. Tavakoli, *The Influence of Process Parameters on Microstructure and Mechanical Properties of Friction Stir Welded Al 5083 Alloy Lap Joint.* American Journal of Materials Science, 2011. 1(2): p. 93-97.

16. Lombard, H., et al., *Optimising FSW Process Parameters to Minimise Defects and Maximise Fatigue Llife in 5083-H321 Aluminium Alloy.* Engineering Fracture Mechanics, 2008(75): p. 341-354.

17. Society, A.W., *Structural Welding Code - Aluminum*, in *AWS D1.2/D1.2M:2014*. 2013.

18. Newby, J.R., *Volume 8: Mechanical Testing*, in *ASM Handbook*. 1992.

19. ASTM, *Standard Test Methods for Tension Testing of Metallic Materials*, in *ASTM E8 / E8M-09*. 2009, ASTM International: West Conshohocken, PA.

20. Davis, J.R., *Volume 2: Properties and Selection: Nonferrous Alloys and Special-Purpose Materials*. 1993.

# Appendix 1

## Weld Procedure for 5083-H131 Al using CNC Machine

Assumptions:

Welding will take place using a vertical CNC machine of adequate horsepower and an accuracy of at least +/- 0.001 in the z-axis. Weld material is certified in consistency and is cut with all edges square. Friction stir tools are made with a shoulder below the shank to prevent tool movement once the tool is seated against the holder. Tools are heat treated and tempered with hardness above 50 HRC. All pin and shoulder dimensions are within +/-0.0005" for consistency between tools. The work piece holder is designed to be rigid and fully constrain the work piece.

Preparation:

The set up for a friction stir weld consists of the work piece holder mounted/aligned in the CNC machine, all programs loaded, all cutting tools loaded, and the machine coordinate system set relative to the work piece holder. Two work pieces with machined flat edges butted together are placed into the work piece holder on top of a sheet metal layer to protect the holder. Set screws adjusted and the six large clamps are tightened to fully constrain the samples in the holder to prevent movement. A weld channel is cut down the seam between the two work pieces to eliminate down force

variations due to varying work piece thickness since only position control is available. Careful consideration is given to pin length in relation to work piece thickness after the weld channel is cut. The shoulder should be plunged between around 6-10 thousandths while the pin should be no less than 5 thousandths from the bottom. In cases where the shoulder is scrolled, the shoulder plunge depth should be taken from the bottom of the scroll. In order to reduce stresses on the tool and the machine a pilot hole should be drilled and milled flat at the bottom for the tool to enter the work piece. The pin diameter should be about 5 thousandths greater than the diameter of the pilot hole to aid in heat input. When adjusting for down force, always update the plunge depth of the pilot hole to be 0.5 thousandths of an inch greater than the plunge depth of the friction stir tool. This update is performed in order to prevent large stresses on the pin. The welding program should contain a dwell time for the tool after it has reached plunge depth and before it begins to traverse. Dwell time affects the initial heat input and can greatly affect the weld quality. A standard dwell time of 3 seconds should be used but can be modified depending on weld characteristics. Initial fixed weld parameters are selected based upon successful weld parameters for steel tools with a ¼" diameter pin and 0.8" diameter shoulder. Please see Appendix B before performing this procedure.

In order to make experimental welds repeatable, precautions must be taken to remove as many variables as possible.

- Tool seat – Following tool replacement in the CAT-40 tool holder, snug the set screw on the tool holder into the tool. Using a piece of brass/aluminum round stock with a hole drilled larger than the FSW tool pin, place in contact with the tool shoulder and tap with a hammer to seat

the tool. Then fully tighten the set screws. This step prevents tool creep and loss of down force in the first set of welds with the new tool.

- Material preparation – Work piece material should be clean and the surfaces to be welded should be milled flat and deburred in order for a positive mating surface. Before welding a weld channel must be milled in order to provide a consistently flat surface for the friction stir tool shoulder.
- Work holder – Ensure the work pieces are seated flat against the anvil surface and that the setscrews and clamps are tight.
- Temperature – Between welds the tool must be cooled with compressed air until it is warm to the touch (approx 115$^{o}$F). It is not about temperature but consistency. It is also possible to start each weld equal time apart.
- Tool geometry – Critical tool dimensions (shoulder/pin diameter, pin length) should be within +/-0.0005" for repeatability when replacing a broken tool.
- Dwell time – It is necessary for the tool to build heat before traversing and to ensure consistent heat is delivered each time. A dwell can be used in the welding program for consistency. A dwell time sensitivity analysis may be performed by varying dwell time from 0-5 seconds, but typically 0 to 3 seconds is sufficient.

Acceptance Criteria:

Welds must be cut along the cross-section perpendicular to the weld direction and inspected for voids. Welds may be bent using a press or bend tester to check for kissing bonds. Tensile testing should be used as a final determination for weld strength and should achieve at least 80% weld efficiency.

Establish Plunge Depth:

Initial down force assessment is performed when selecting the down force for the first time for a given feed and speed. A position control machine controls downforce by positioning the FSW tool shoulder below the surface of the workpiece. While the tool is rotating against the workpiece the deflection of the machine is maintaining the downforce. Testing should be performed varying the plunge depth, or position of the shoulder into the workpiece, to find a position that provides adequate downforce.

- Run 6 welds at different plunge depths in 0.001" increments
  - Starting point [0.005, 0.006, 0.007, 0.008, 0.009, 0.010]
  - Measured from the shoulder or depth of scroll. Depending on weld parameters the plunge depth may be less.
- Testing: Visual inspection of tunnel void and surface finish

Feed Selection:

- Perform welds with a fixed rpm and varying feed rate.
  - 500 rpm @ 2.5, 3, 3.5, 4, 4.5, 5 (ipm)
- Perform testing on each weld.

- Cut sample from the center of each weld and face mill the cross section surface to reveal voids.
- Measure voids, if present, and make note of the rpm with the smallest void or void free weld to be used in the next step.

Speed Selection:

- Perform welds with a fixed feed rate and varying rpm.
  - Use the best feed from last step @ 300, 400, 500, 600, 700, 800 (rpm)
- Perform testing on each weld.
  - Cut sample from the center of each weld and face mill the cross section surface to reveal voids.
  - Measure voids, if present, and make note of the rpm with the smallest void or void free weld to be used in the next step.

Speed Verification:

- Perform welds with a fixed feed rate and varying rpm.
  - Same feed rate from last step @ Six welds total. 3 above and below the best previous rpm in 10 rpm increments.
- Perform testing on each weld.
  - Cut sample from the center of each weld and face mill the cross section surface to reveal voids.

- Measure voids, if present, and make note of the rpm with the smallest void or void free weld to be used in the next step. At this point voids should be very small if any are present.

Feed Verification:

- Perform welds with a fixed rpm and varying feed rate.
  - Use the best rpm from last step @ Six welds total. 3 above and below the best previous feed rate in 0.1 ipm increments.
- Perform testing on each weld.
  - Cut sample from the center of each weld and face mill the cross section surface to reveal voids.
  - Measure voids, if present, and make note of the rpm with the smallest void or void free weld to be used in the next step. At this point voids should be very small if any are present.

Repeatability:

- With all things the same, perform six welds at the best Feed/Speed from the previous tests.
- Perform testing on each weld
  - Cut bend sample from the center of each weld and face mill the cross section surface to reveal defects.
  - If small defects are present a downforce sensitivity analysis should be performed by varying the shoulder plunge above and below the current setting by 0.001" at a time. Visual examination of samples

will indicate the optimal plunge depth for help reducing/eliminating the defects.

- Perform bend tests to verify repeatability of welds

Final Welds:

- Perform 12 welds each for bend, tensile, and hardness testing. Visual and Microscopic examination may be performed on the hardness testing samples prior to testing.

# Appendix 2

## Lessons Learned using the CNC Milling Machine

Typical Defects:

Surface galling – Insufficient down force and/or speed too high

Surface tear – Same as surface galling

Excessive Flashing – Down force too high, feed rate too low, or speed too high

Tunnel void – May be caused by a cold weld (feed rate too high), loss of material due to excess flashing, or insufficient down force.

Microcracks – May be caused by a cold weld (feed rate too high) or loss of material due to excess flashing, or insufficient down force. Microcracks are a good indication that the acceptable process parameters are very close.

Kissing weld – May be caused by a cold weld (feed rate too high) or loss of material due to excess flashing, or insufficient down force. Kissing welds with little to no visible voids are a good indication that the acceptable process parameters are very close.

Down Force:

Down force plays a large role in the quality of friction stir welds. Too much down force can cause excessive flashing, high machine loads, high tool stresses, and tool failures.

However, the lack of down force can result in tunnel voids, micro cracks, scalloping, surface galling, and kissing welds. Typically the down force needed using a position control machine for a quality weld would require a shoulder plunge of about 7-8 mils into the work piece. Tools with scrolled shoulders should be plunged the additional depth of the scroll. Once a sufficient down force/plunge depth is found, make note of the associated spindle loads. Spindle loads can be an important tool to monitor down force as it is associated with the amount the shoulder is engaged into the work piece.

It is important to understand that tool design and orientation also play a big role in maintaining down force when using position control machines (lacking force control). Tool designs such as threaded pins can effect down force at different rpm/ipm if the machine is not ridged. The threads rotating and stirring the metal create forces which must be countered by the machine. In a case where the threaded pin is running in reverse to push material away from the shoulder; the forces will be greater causing more deflection in a cold weld as opposed to a hot weld. The machine will not indicate deflection but it will be reflected in the weld quality. This must be taken into consideration when performing welds in a wide range of feeds and speeds. The most obvious sign of a lack of down force is when the shoulder doesn't make full contact or a noticeable change in surface finish.

Tool orientation largely contributes to maintaining down force. A tool that is tilted 2 degrees back from the weld direction is able to maintain a pressure gradient from the point the shoulder meets the work piece to the heal that is plunged to a given depth. A tool which is perpendicular to the work piece is subject to a loss of down force when the tool sinks below the work surface causing excessive flashing; thus the machine

deflection decreases as the tool plunges deeper into the work piece. Indicators include a void which may not be present in the beginning of the weld but increase in size as the tool sinks. Tool designs with chamfered shoulders may help decrease the loss of down force.

## Tool Design

A good tool design can significantly change weld characteristics and reduce the void size. For example, a smooth pin/shoulder tool producing welds with voids at the end of the pin while producing excess flashing can be improved by adding a reverse thread which pulls material down to fill the void. The result may be that with extra material being pulled down the pin, a surface tear becomes present. Adding a scrolled shoulder to pull material in to the pin can reduce flashing and prevent surface tears. Additionally it is thought that flats on the pin reduce tool stresses and provide even flow along the length of the pin to reduce/eliminate voids. A large pin diameter may make it difficult to have material carried around the pin and consolidated with the other side. Tool shoulder diameter also plays a role in adding heat. The machine capabilities should be taken into consideration when sizing the shoulder as it takes more power for a large diameter shoulder. Slow feed rates do not require a larger shoulder as the tool has time to build heat in the workpiece.

## Weld Parameters

Welding parameters differ greatly between tool materials, geometries, and the materials being welded. Welding parameters are mostly found using methods described in Appendix 1 and consist of feed (ipm) and speed (rpm). When narrowing the search for

acceptable weld parameters during trial runs, it is necessary to understand the effects each weld parameter has on the weld quality to reduce or increase defects. Together, feed and speed determine the amount of heat put into the workpiece. The rpm determines how fast the heat will build under the shoulder so if the speed is high then the heat will build quickly or if the speed is slow it will take longer to build heat. The feed rate controls the rate at which the building heat under the shoulder is distributed into the workpiece. For example, at a set speed the feed rate can be low which allows time for heat to build around the tool and when the tool is traversing there is a smaller heat differential between the leading edge of the shoulder to the leading edge of the pin resulting in a weld condition where the pin does not encounter material temperatures less than the workpiece hotwork temperature. If the feed rate is too high, then the heat added by the tool does not have enough time to bring the material up to hotwork temperature before the pin travels through. Examples of these welding parameters and the associated defects can be seen in the chart below.

| | Low Speed (rpm) | High Speed (rpm) |
|---|---|---|
| High Feed (ipm) | Tunnel Void, Scalloping, Excessive tool stresses | Kissing welds, Micro cracks |
| Low Feed (ipm) | Excessive tool stresses, Tunnel void, Surface Galling | Excess Flashing, Surface tear, Surface Galling |

Appendix 3

Bend Results Data

| Material | Parent | Mig Welds | H13 Welds | 420SS Welds | A2 Welds |
|---|---|---|---|---|---|
| Sample # | Bend Testing | | | | |
| 1 | 821.2 | 547.3 | 812.7 | 775.8 | 770.5 |
| 2 | 839.3 | 562.4 | 824.7 | 779.8 | 788.7 |
| 3 | 842.2 | 576 | 824.8 | 782.3 | 789.7 |
| 4 | 901.2 | 580 | 826.4 | 787.1 | 792.1 |
| 5 | 903.4 | 598.8 | 851.6 | 804.4 | 793 |
| 6 | 922.9 | 632.5 | 870 | 847.8 | 794.5 |
| 7 | 942.9 | 635.2 | 898 | 851.7 | 796.4 |
| 8 | 946.8 | 636.1 | 911.8 | 863.3 | 797.9 |
| 9 | 977.3 | 646.3 | 920 | 867.1 | 798.4 |
| 10 | 980.6 | 652.3 | 947.2 | 870.3 | 799.2 |
| Mean: | 907.78 | 606.69 | 868.72 | 822.96 | 792.04 |
| Std Dev: | 57.41583 | 38.2947763 | 47.8337816 | 40.31851518 | 8.3841385 |
| Kurtosis: | 1.714397 | 1.33272699 | 1.56423399 | 0.762834488 | 8.4340755 |
| Skewness: | -0.3113 | -0.3015645 | 0.37643006 | -0.0173949 | -2.149207 |

Statistical Analysis of Data

F-Test Two-Sample for Variances

| *Bend Tests* | *H13 Welds* | *420SS Welds* |
|---|---|---|
| Mean | 868.72 | 822.96 |
| Variance | 2288.070667 | 1625.582667 |
| Observations | 10 | 10 |
| df | 9 | 9 |
| F | 1.407538794 | |
| P(F<=f) one-tail | 0.309392335 | Equal Variance |
| F Critical one-tail | 3.178893105 | |

t-Test: Two-Sample Assuming Equal Variances

| *Bend Tests* | *H13 Welds* | *420SS Welds* |
|---|---|---|
| Mean | 868.72 | 822.96 |
| Variance | 2288.070667 | 1625.582667 |
| Observations | 10 | 10 |
| Pooled Variance | 1956.826667 | |
| Hypothesized Mean Difference | 0 | |
| df | 18 | |
| t Stat | 2.313102292 | |
| P(T<=t) one-tail | 0.016373645 | |
| t Critical one-tail | 1.734063592 | |
| P(T<=t) two-tail | 0.03274729 | Unequal Means |
| t Critical two-tail | 2.100922037 | |

F-Test Two-Sample for Variances

| *Bend Tests* | *H13 Welds* | *A2 Welds* |
|---|---|---|
| Mean | 868.72 | 792.04 |
| Variance | 2288.070667 | 70.29377778 |
| Observations | 10 | 10 |
| df | 9 | 9 |
| F | 32.55011665 | |
| P(F<=f) one-tail | 8.27768E-06 | Unequal Variance |
| F Critical one-tail | 3.178893105 | |

t-Test: Two-Sample Assuming Unequal Variances

| *Bend Tests* | *H13 Welds* | *A2 Welds* |
|---|---|---|
| Mean | 868.72 | 792.04 |
| Variance | 2288.070667 | 70.29377778 |
| Observations | 10 | 10 |
| Hypothesized Mean Difference | 0 | |
| df | 10 | |
| t Stat | 4.993173361 | |
| P(T<=t) one-tail | 0.000271385 | |
| t Critical one-tail | 1.812461102 | |
| P(T<=t) two-tail | 0.000542769 | Unequal Means |
| t Critical two-tail | 2.228138842 | |

F-Test Two-Sample for Variances

| *Bend Tests* | *420SS Welds* | *A2 Welds* |
|---|---|---|
| Mean | 822.96 | 792.04 |
| Variance | 1625.582667 | 70.29377778 |
| Observations | 10 | 10 |
| df | 9 | 9 |
| F | 23.1255556 | |
| P(F<=f) one-tail | 3.52783E-05 | Unequal Variance |
| F Critical one-tail | 3.178893105 | |

t-Test: Two-Sample Assuming Unequal Variances

| *Bend Tests* | *420SS Welds* | *A2 Welds* |
|---|---|---|
| Mean | 822.96 | 792.04 |
| Variance | 1625.582667 | 70.29377778 |
| Observations | 10 | 10 |
| Hypothesized Mean Difference | 0 | |
| df | 10 | |
| t Stat | 2.374337115 | |
| P(T<=t) one-tail | 0.019493765 | |
| t Critical one-tail | 1.812461102 | |
| P(T<=t) two-tail | 0.038987529 | Unequal Means |
| t Critical two-tail | 2.228138842 | |

F-Test Two-Sample for Variances

| *Bend Tests* | *H13 Welds* | *Mig Welds* |
|---|---|---|
| Mean | 868.72 | 606.69 |
| Variance | 2288.070667 | 1466.489889 |
| Observations | 10 | 10 |
| df | 9 | 9 |
| F | 1.560236238 | |
| P(F<=f) one-tail | 0.258996074 | Equal Variance |
| F Critical one-tail | 3.178893105 | |

t-Test: Two-Sample Assuming Equal Variances

| *Bend Tests* | *H13 Welds* | *Mig Welds* |
|---|---|---|
| Mean | 868.72 | 606.69 |
| Variance | 2288.070667 | 1466.489889 |
| Observations | 10 | 10 |
| Pooled Variance | 1877.280278 | |
| Hypothesized Mean Difference | 0 | |
| df | 18 | |
| t Stat | 13.52295056 | |
| P(T<=t) one-tail | 3.60355E-11 | |
| t Critical one-tail | 1.734063592 | |
| P(T<=t) two-tail | 7.20709E-11 | |
| t Critical two-tail | 2.100922037 | |

F-Test Two-Sample for Variances

| *Bend Tests* | *Parent* | *H13 Welds* |
|---|---|---|
| Mean | 907.78 | 868.72 |
| Variance | 3296.577333 | 2288.070667 |
| Observations | 10 | 10 |
| df | 9 | 9 |
| F | 1.440767272 | |
| P(F<=f) one-tail | 0.297584288 | Equal Variance |
| F Critical one-tail | 3.178893105 | |

t-Test: Two-Sample Assuming Equal Variances

| *Bend Tests* | *Parent* | *H13 Welds* |
|---|---|---|
| Mean | 907.78 | 868.72 |
| Variance | 3296.577333 | 2288.070667 |
| Observations | 10 | 10 |
| Pooled Variance | 2792.324 | |
| Hypothesized Mean Difference | 0 | |
| df | 18 | |
| t Stat | 1.652853404 | |
| P(T<=t) one-tail | 0.057847958 | |
| t Critical one-tail | 1.734063592 | |
| P(T<=t) two-tail | 0.115695916 | |
| t Critical two-tail | 2.100922037 | |

F-Test Two-Sample for Variances

| *Bend Tests* | *Mig Welds* | *A2 Welds* |
|---|---|---|
| Mean | 606.69 | 792.04 |
| Variance | 1466.489889 | 70.29377778 |
| Observations | 10 | 10 |
| df | 9 | 9 |
| F | 20.86230012 | |
| P(F<=f) one-tail | 5.42636E-05 | |
| F Critical one-tail | 3.178893105 | |

t-Test: Two-Sample Assuming Unequal Variances

| *Bend Tests* | *Mig Welds* | *A2 Welds* |
|---|---|---|
| Mean | 606.69 | 792.04 |
| Variance | 1466.489889 | 70.29377778 |
| Observations | 10 | 10 |
| Hypothesized Mean Difference | 0 | |
| df | 10 | |
| t Stat | -14.95155017 | |
| P(T<=t) one-tail | 1.80334E-08 | |
| t Critical one-tail | 1.812461102 | |
| P(T<=t) two-tail | 3.60668E-08 | |
| t Critical two-tail | 2.228138842 | |

F-Test Two-Sample for Variances

| *Bend Tests* | *Parent* | *A2 Welds* |
|---|---|---|
| Mean | 907.78 | 792.04 |
| Variance | 3296.577333 | 70.29377778 |
| Observations | 10 | 10 |
| df | 9 | 9 |
| F | 46.89714278 | |
| P(F<=f) one-tail | 1.71181E-06 | |
| F Critical one-tail | 3.178893105 | |

t-Test: Two-Sample Assuming Unequal Variances

| *Bend Tests* | *Parent* | *A2 Welds* |
|---|---|---|
| Mean | 907.78 | 792.04 |
| Variance | 3296.577333 | 70.29377778 |
| Observations | 10 | 10 |
| Hypothesized Mean Difference | 0 | |
| df | 9 | |
| t Stat | 6.30768842 | |
| P(T<=t) one-tail | 6.98515E-05 | |
| t Critical one-tail | 1.833112923 | |
| P(T<=t) two-tail | 0.000139703 | |
| t Critical two-tail | 2.262157158 | |

F-Test Two-Sample for Variances

| *Bend Tests* | *420SS Welds* | *Mig Welds* |
|---|---|---|
| Mean | 822.96 | 606.69 |
| Variance | 1625.582667 | 1466.489889 |
| Observations | 10 | 10 |
| df | 9 | 9 |
| F | 1.108485424 | |
| P(F<=f) one-tail | 0.440289307 | |
| F Critical one-tail | 3.178893105 | |

t-Test: Two-Sample Assuming Equal Variances

| *Bend Tests* | *420SS Welds* | *Mig Welds* |
|---|---|---|
| Mean | 822.96 | 606.69 |
| Variance | 1625.582667 | 1466.489889 |
| Observations | 10 | 10 |
| Pooled Variance | 1546.036278 | |
| Hypothesized Mean Difference | 0 | |
| df | 18 | |
| t Stat | 12.29904646 | |
| P(T<=t) one-tail | 1.69598E-10 | |
| t Critical one-tail | 1.734063592 | |
| P(T<=t) two-tail | 3.39196E-10 | |
| t Critical two-tail | 2.100922037 | |

F-Test Two-Sample for Variances

| *Bend Tests* | *Parent* | *420SS Welds* |
|---|---|---|
| Mean | 907.78 | 822.96 |
| Variance | 3296.577333 | 1625.582667 |
| Observations | 10 | 10 |
| df | 9 | 9 |
| F | 2.027935829 | |
| P(F<=f) one-tail | 0.153535933 | |
| F Critical one-tail | 3.178893105 | |

t-Test: Two-Sample Assuming Equal Variances

| *Bend Tests* | *Parent* | *420SS Welds* |
|---|---|---|
| Mean | 907.78 | 822.96 |
| Variance | 3296.577333 | 1625.582667 |
| Observations | 10 | 10 |
| Pooled Variance | 2461.08 | |
| Hypothesized Mean Difference | 0 | |
| df | 18 | |
| t Stat | 3.823141786 | |
| P(T<=t) one-tail | 0.000622737 | |
| t Critical one-tail | 1.734063592 | |
| P(T<=t) two-tail | 0.001245474 | |
| t Critical two-tail | 2.100922037 | |

# Appendix 4

## Tensile Test Results

| Material | Parent | Mig Welds | H13 Welds | 420SS Welds | A2 Welds |
|---|---|---|---|---|---|
| Sample # | Tensile Testing (lbsF) | | | | |
| 1 | 3391.6 | 2450.9 | 2535.72 | 2544.52 | 2401.22 |
| 2 | 3407.46 | 2557.19 | 2551.44 | 2641.06 | 2513.5 |
| 3 | 3433.27 | 2572.84 | 2569.61 | 2687.92 | 2524.67 |
| 4 | 3439.75 | 2623 | 2589.83 | 2696.27 | 2538.69 |
| 5 | 3444.94 | 2628.8 | 2610.83 | 2788.09 | 2540.88 |
| 6 | 3461.7 | 2683.28 | 2613.05 | 2794.4 | 2604.72 |
| 7 | 3470.07 | 2690.1 | 2631.7 | 2821.6 | 2711.19 |
| 8 | 3516.58 | 2690.38 | 2684.77 | 2945.62 | 2797.26 |
| 9 | 3543.37 | 2709.52 | 2757 | 3006.17 | 2920.93 |
| 10 | 3604.21 | 2717 | 2846.4 | 3021.74 | 3098.84 |
| Mean: | 3471.30 | 2632.30 | 2639.04 | 2794.74 | 2665.19 |
| Std Dev: | 65.46184 | 84.7426227 | 97.8207289 | 158.8488664 | 216.16904 |
| Kurtosis: | 3.460092 | 3.92320902 | 4.02396293 | 2.045526706 | 3.2817452 |
| Skewness: | 0.96228 | -1.1444346 | 1.24415929 | 0.108581458 | 0.9879172 |
| UTS (ksi) (Area = 0.25 x 0.275 in) | 50.49 | 38.29 | 38.39 | 40.65 | 38.77 |
| Weld Efficiency | 100.0% | 75.8% | 76.0% | 80.5% | 76.8% |

Tensile Data

Specimen numbers are labeled in the top right hand corner of each image.

Parent Material

9/5/2013 2:27:22 PM PARENT 2.ls_tens

**Southern Nuclear**
**Dedication and Test Facility**

Graph 1

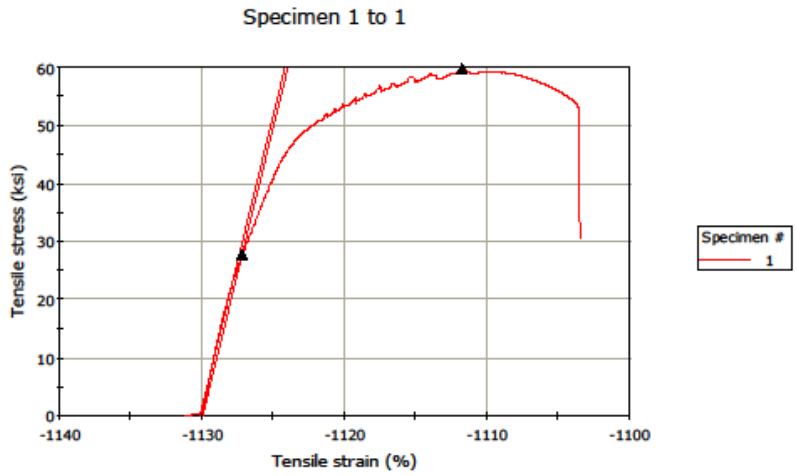


Results Table 1

| | Maximum Load (lbf) | Maximum Stress (ksi) | Load at Break (Standard) (lbf) | Tensile stress at Break (Standard) (ksi) | Elongation at Break (%) |
|---|---|---|---|---|---|
| 1 | 3,516.58 | 59.64 | 3,099.84 | 52.6 | -1,103.6 |

| | Diameter (in) |
|---|---|
| 1 | 0.274 |

9/5/2013 2:36:54 PM PARENT 2_1.is_tens

## Southern Nuclear
### Dedication and Test Facility

Graph 1

Specimen 1 to 1

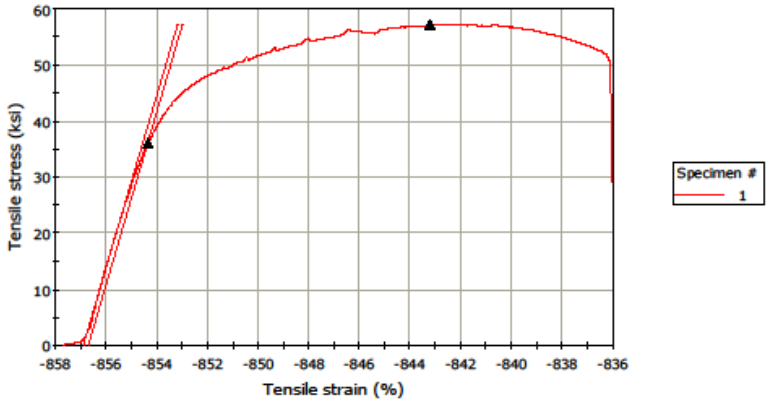


Results Table 1

| | Maximum Load (lbf) | Maximum Stress (ksi) | Load at Break (Standard) (lbf) | Tensile stress at Break (Standard) (ksi) | Elongation at Break (%) |
|---|---|---|---|---|---|
| 1 | 3,444.94 | 57.17 | 3,035.02 | 50.4 | -836.1 |

| | Diameter (in) |
|---|---|
| 1 | 0.277 |

9/5/2013 2:58:32 PM PARENT 2_3.is_tens

## Southern Nuclear
### Dedication and Test Facility

Graph 1

Specimen 1 to 2

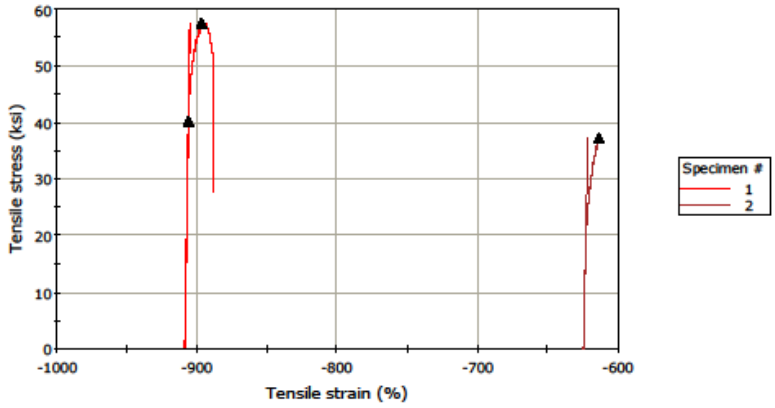


Results Table 1

| | Maximum Load (lbf) | Maximum Stress (ksi) | Load at Break (Standard) (lbf) | Tensile stress at Break (Standard) (ksi) | Elongation at Break (%) |
|---|---|---|---|---|---|
| 1 | 3,391.60 | 57.52 | 2,964.96 | 50.3 | -888.3 |
| 2 | 2,919.28 | 37.34 | 2,919.28 | 37.3 | -615.3 |

| | Diameter (in) |
|---|---|
| 1 | 0.274 |

7/17/2014 3:01:48 PM Parent.is_tens

## Southern Nuclear
### Dedication and Test Facility

Graph 1

Specimen 1 to 1

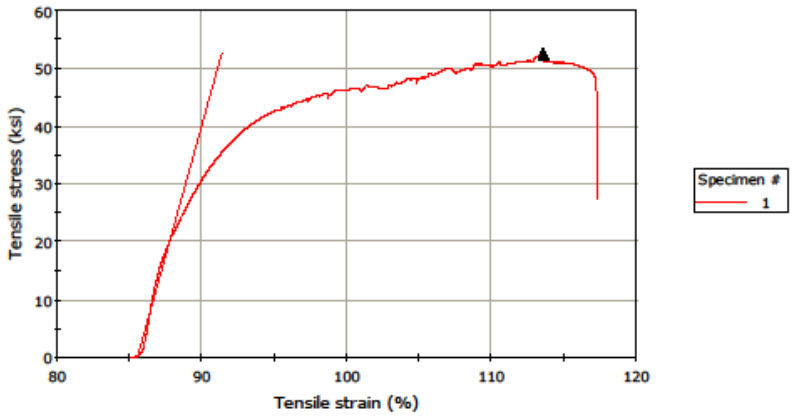


Results Table 1

| | Maximum Load (lbf) | Maximum Stress (ksi) | Load at Break (Standard) (lbf) | Tensile stress at Break (Standard) (ksi) | Elongation at Break (%) |
|---|---|---|---|---|---|
| 1 | 3,604.21 | 52.45 | 3,304.29 | 48.1 | 117.2 |

| | Diameter (in) |
|---|---|
| 1 | 0.296 |

7/17/2014 3:11:10 PM Parent_2.is_tens

## Southern Nuclear
### Dedication and Test Facility

Graph 1

Specimen 1 to 1

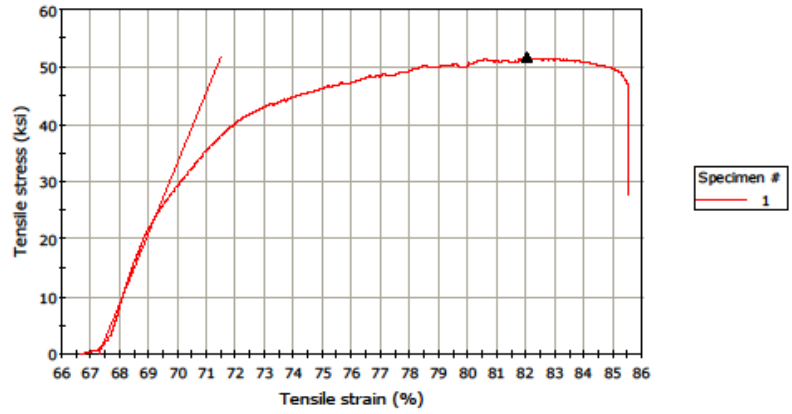


Results Table 1

| | Maximum Load (lbf) | Maximum Stress (ksi) | Load at Break (Standard) (lbf) | Tensile stress at Break (Standard) (ksi) | Elongation at Break (%) |
|---|---|---|---|---|---|
| 1 | 3,543.37 | 51.56 | 3,237.04 | 47.1 | 85.5 |

| | Diameter (in) |
|---|---|
| 1 | 0.296 |

9/26/2014 10:38:33 AM Parent2.is_tens

**Southern Nuclear**
**Dedication and Test Facility**

Graph 1

Specimen 1 to 1

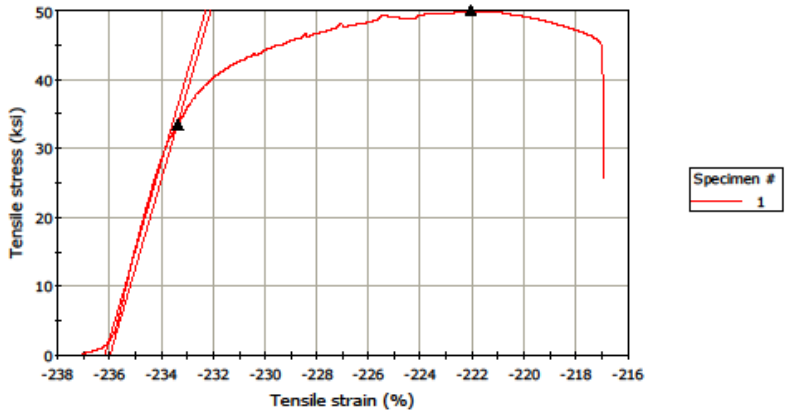


Results Table 1

| | Maximum Load (lbf) | Maximum Stress (ksi) | Load at Break (Standard) (lbf) | Tensile stress at Break (Standard) (ksi) | Elongation at Break (%) |
|---|---|---|---|---|---|
| 1 | 3,433.27 | 49.96 | 3,077.93 | 44.8 | -217.1 |

| | Diameter (in) |
|---|---|
| 1 | 0.296 |

9/26/2014 10:40:49 AM Parent2_2.is_tens

**Southern Nuclear**
**Dedication and Test Facility**

Graph 1

Specimen 1 to 1

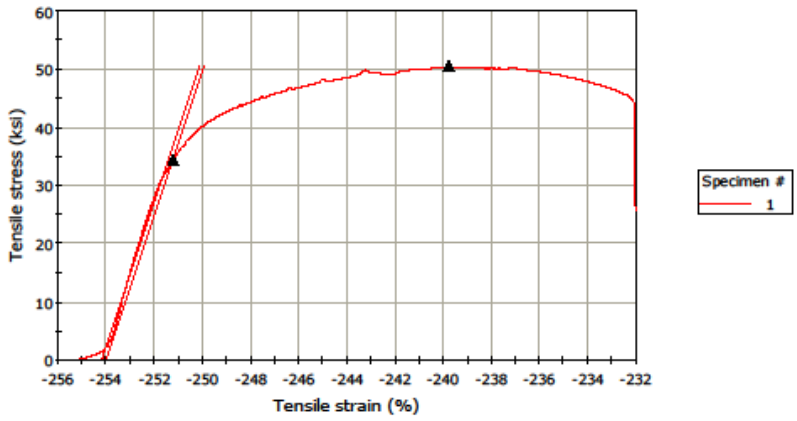


Results Table 1

| | Maximum Load (lbf) | Maximum Stress (ksi) | Load at Break (Standard) (lbf) | Tensile stress at Break (Standard) (ksi) | Elongation at Break (%) |
|---|---|---|---|---|---|
| 1 | 3,470.07 | 50.50 | 3,024.71 | 44.0 | -232.1 |

| | Diameter (in) |
|---|---|
| 1 | 0.296 |

9/26/2014 10:42:46 AM Parent2_3.is_tens

## Southern Nuclear
### Dedication and Test Facility

Graph 1

Specimen 1 to 1

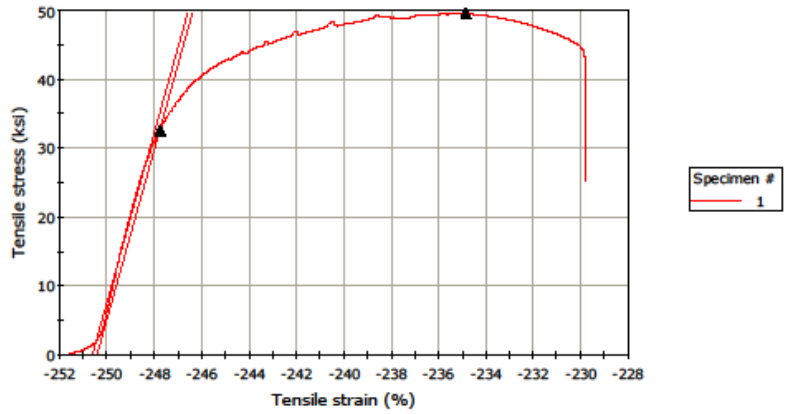


Results Table 1

| | Maximum Load (lbf) | Maximum Stress (ksi) | Load at Break (Standard) (lbf) | Tensile stress at Break (Standard) (ksi) | Elongation at Break (%) |
|---|---|---|---|---|---|
| 1 | 3,407.46 | 49.58 | 3,024.56 | 44.0 | -229.9 |

| | Diameter (in) |
|---|---|
| 1 | 0.296 |

9/26/2014 10:44:36 AM Parent2_4.is_tens

## Southern Nuclear
### Dedication and Test Facility

Graph 1

Specimen 1 to 1

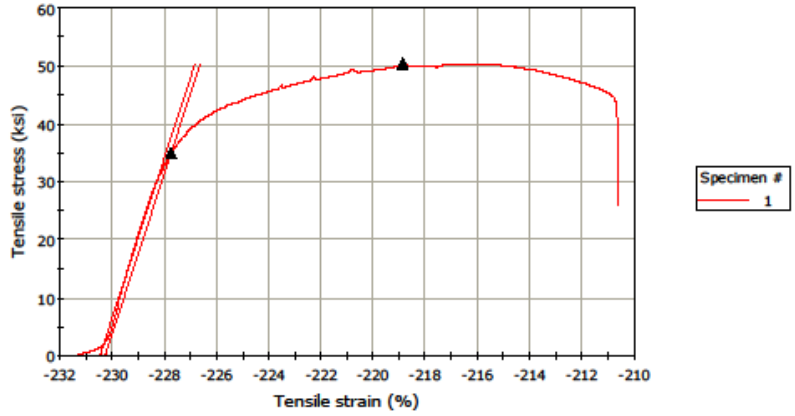


Results Table 1

| | Maximum Load (lbf) | Maximum Stress (ksi) | Load at Break (Standard) (lbf) | Tensile stress at Break (Standard) (ksi) | Elongation at Break (%) |
|---|---|---|---|---|---|
| 1 | 3,461.70 | 50.37 | 3,012.66 | 43.8 | -210.7 |

| | Diameter (in) |
|---|---|
| 1 | 0.296 |

**Southern Nuclear**
**Dedication and Test Facility**

Graph 1

Specimen 1 to 1

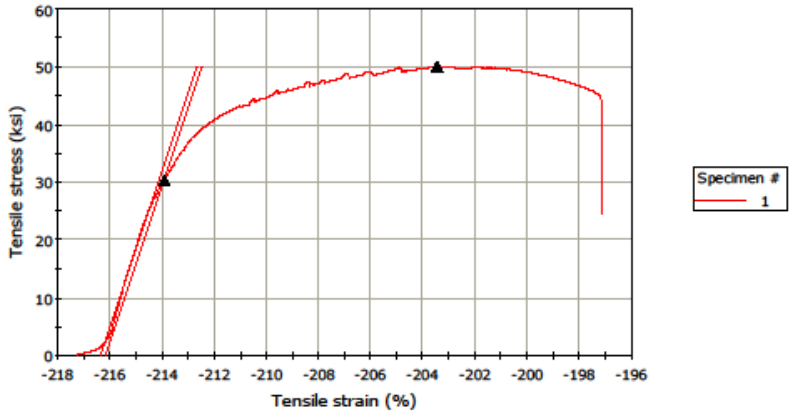


Results Table 1

| | Maximum Load (lbf) | Maximum Stress (ksi) | Load at Break (Standard) (lbf) | Tensile stress at Break (Standard) (ksi) | Elongation at Break (%) |
|---|---|---|---|---|---|
| 1 | 3,439.75 | 50.05 | 3,088.19 | 44.9 | -197.2 |

| | Diameter (in) |
|---|---|
| 1 | 0.296 |

9/26/2014 11:02:09 AM 420SS_4_675_13.is_tens

**Southern Nuclear**
**Dedication and Test Facility**

Graph 1

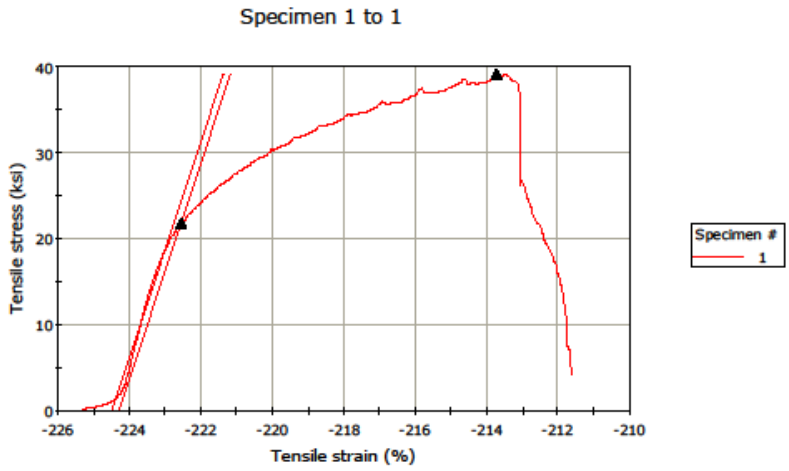


Results Table 1

| | Maximum Load (lbf) | Maximum Stress (ksi) | Load at Break (Standard) (lbf) | Tensile stress at Break (Standard) (ksi) | Elongation at Break (%) |
|---|---|---|---|---|---|
| 1 | 2,687.92 | 39.11 | 494.11 | 7.2 | -211.7 |

| | Diameter (in) |
|---|---|
| 1 | 0.296 |

7/25/2014 1:31:49 PM 420SS_4_675_2.is_tens

# Southern Nuclear
## Dedication and Test Facility

Graph 1

Specimen 1 to 1

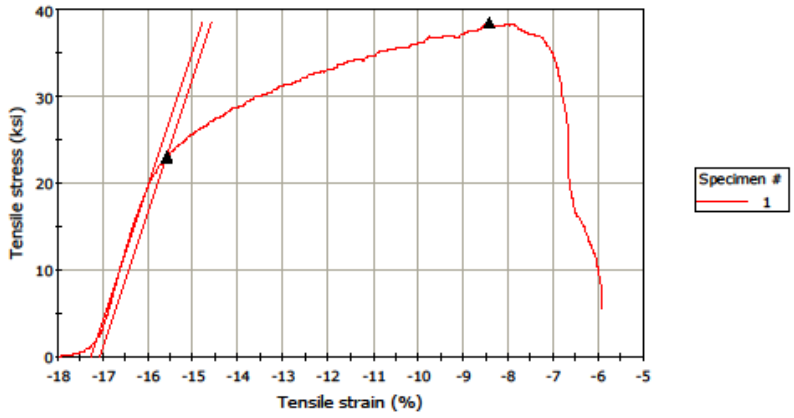


Results Table 1

| | Maximum Load (lbf) | Maximum Stress (ksi) | Load at Break (Standard) (lbf) | Tensile stress at Break (Standard) (ksi) | Elongation at Break (%) |
|---|---|---|---|---|---|
| 1 | 2,641.06 | 38.43 | 651.68 | 9.5 | -6.0 |

| | Diameter (in) |
|---|---|
| 1 | 0.296 |

7/25/2014 1:37:02 PM 420SS_4_675_4.is_tens

# Southern Nuclear
## Dedication and Test Facility

Graph 1

Specimen 1 to 1

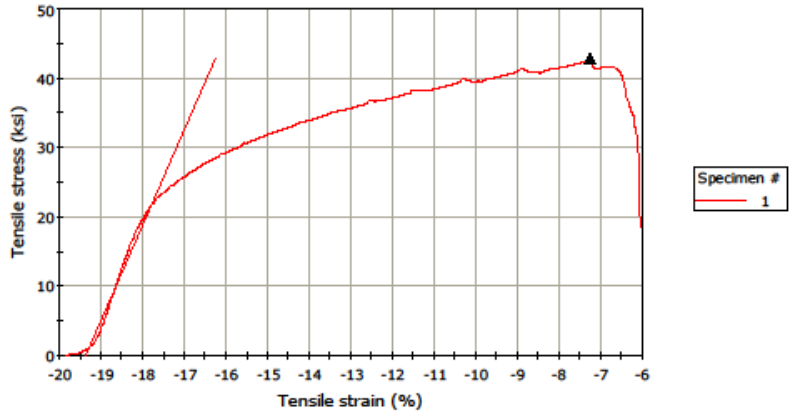


Results Table 1

| | Maximum Load (lbf) | Maximum Stress (ksi) | Load at Break (Standard) (lbf) | Tensile stress at Break (Standard) (ksi) | Elongation at Break (%) |
|---|---|---|---|---|---|
| 1 | 2,945.62 | 42.86 | 2,144.62 | 31.2 | -6.1 |

| | Diameter (in) |
|---|---|
| 1 | 0.296 |

7/25/2014 1:39:03 PM 420SS_4_675_5.is_tens

## Southern Nuclear
### Dedication and Test Facility

Graph 1

Specimen 1 to 1

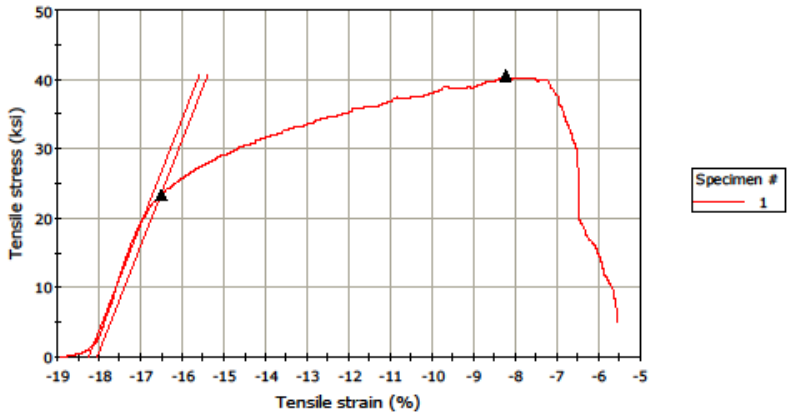


Results Table 1

| | Maximum Load (lbf) | Maximum Stress (ksi) | Load at Break (Standard) (lbf) | Tensile stress at Break (Standard) (ksi) | Elongation at Break (%) |
|---|---|---|---|---|---|
| 1 | 2,788.09 | 40.57 | 592.74 | 8.6 | -5.6 |

| | Diameter (in) |
|---|---|
| 1 | 0.296 |

7/25/2014 1:41:05 PM 420SS_4_675_6.is_tens

## Southern Nuclear
### Dedication and Test Facility

Graph 1

Specimen 1 to 1

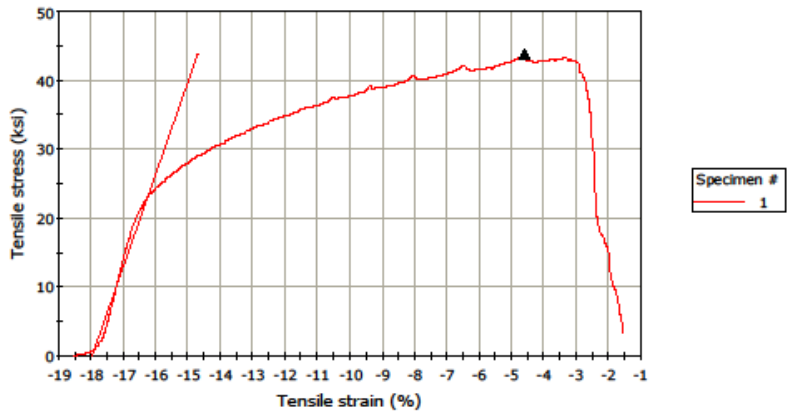


Results Table 1

| | Maximum Load (lbf) | Maximum Stress (ksi) | Load at Break (Standard) (lbf) | Tensile stress at Break (Standard) (ksi) | Elongation at Break (%) |
|---|---|---|---|---|---|
| 1 | 3,006.17 | 43.74 | 382.81 | 5.6 | -1.6 |

| | Diameter (in) |
|---|---|
| 1 | 0.296 |

9/26/2014 9:52:58 AM 420SS_4_675_7.is_tens

## Southern Nuclear
### Dedication and Test Facility

Graph 1

Specimen 1 to 1

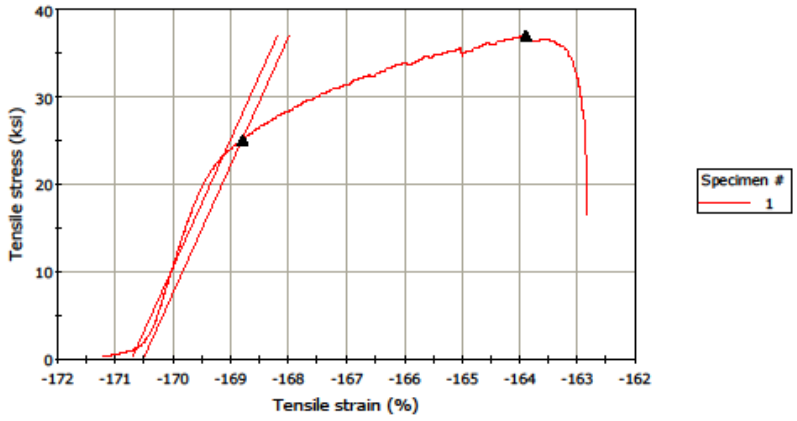


Results Table 1

| | Maximum Load (lbf) | Maximum Stress (ksi) | Load at Break (Standard) (lbf) | Tensile stress at Break (Standard) (ksi) | Elongation at Break (%) |
|---|---|---|---|---|---|
| 1 | 2,544.52 | 37.03 | 1,906.19 | 27.7 | -162.9 |

| | Diameter (in) |
|---|---|
| 1 | 0.296 |

9/26/2014 10:00:25 AM 420SS_4_675_9.is_tens

## Southern Nuclear
### Dedication and Test Facility

Graph 1

Specimen 1 to 1

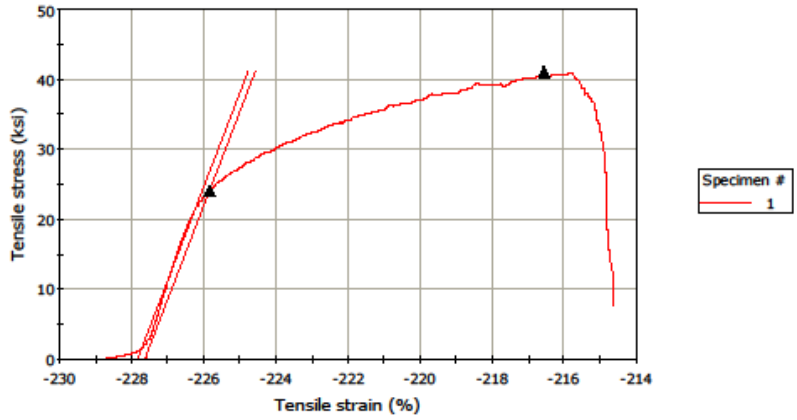


Results Table 1

| | Maximum Load (lbf) | Maximum Stress (ksi) | Load at Break (Standard) (lbf) | Tensile stress at Break (Standard) (ksi) | Elongation at Break (%) |
|---|---|---|---|---|---|
| 1 | 2,821.60 | 41.06 | 903.73 | 13.2 | -214.7 |

| | Diameter (in) |
|---|---|
| 1 | 0.296 |

## Southern Nuclear
### Dedication and Test Facility

Graph 1

Specimen 1 to 1

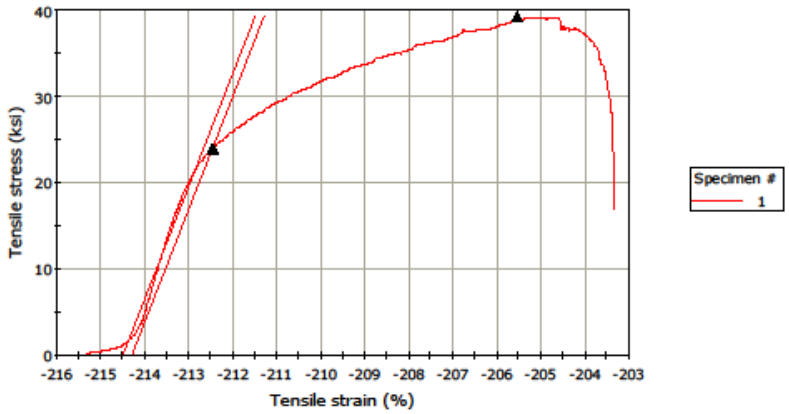


Results Table 1

| | Maximum Load (lbf) | Maximum Stress (ksi) | Load at Break (Standard) (lbf) | Tensile stress at Break (Standard) (ksi) | Elongation at Break (%) |
|---|---|---|---|---|---|
| 1 | 2,696.27 | 39.24 | 1,961.49 | 28.5 | -203.4 |

| | Diameter (in) |
|---|---|
| 1 | 0.296 |



## Southern Nuclear
### Dedication and Test Facility

Graph 1

Specimen 1 to 1

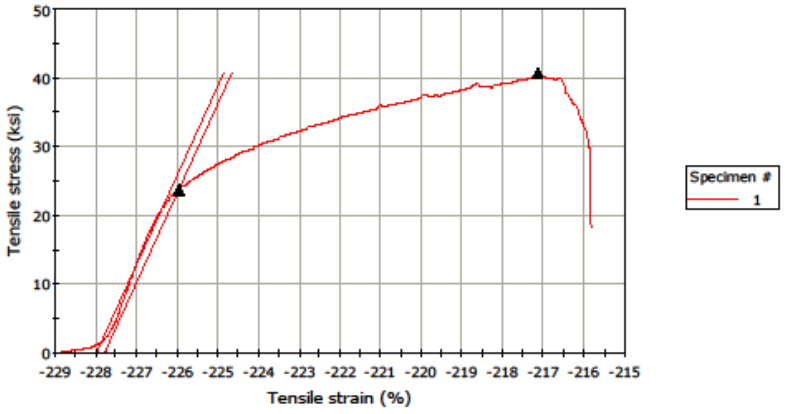


Results Table 1

| | Maximum Load (lbf) | Maximum Stress (ksi) | Load at Break (Standard) (lbf) | Tensile stress at Break (Standard) (ksi) | Elongation at Break (%) |
|---|---|---|---|---|---|
| 1 | 2,794.40 | 40.66 | 2,114.06 | 30.8 | -215.9 |

| | Diameter (in) |
|---|---|
| 1 | 0.296 |

# Southern Nuclear
## Dedication and Test Facility

Graph 1

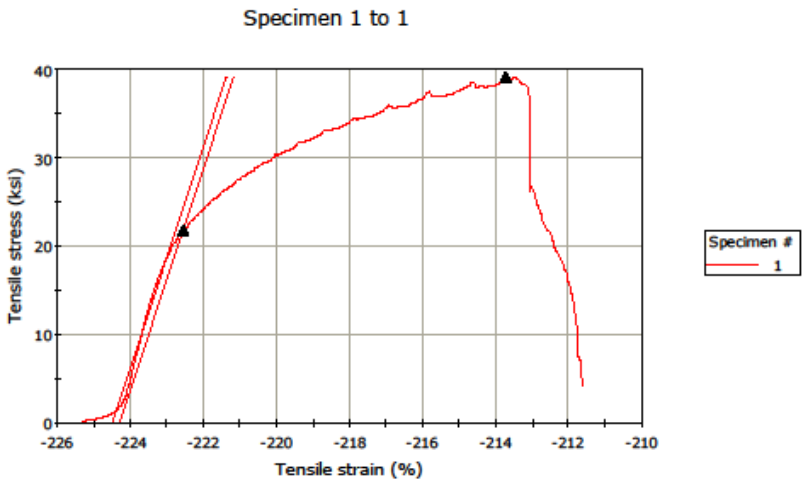


Results Table 1

| | Maximum Load (lbf) | Maximum Stress (ksi) | Load at Break (Standard) (lbf) | Tensile stress at Break (Standard) (ksi) | Elongation at Break (%) |
|---|---|---|---|---|---|
| 1 | 2,687.92 | 39.11 | 494.11 | 7.2 | -211.7 |

| | Diameter (in) |
|---|---|
| 1 | 0.296 |

7/17/2014 3:25:24 PM H13_35_500_2.is_tens

**Southern Nuclear**
**Dedication and Test Facility**

Graph 1

Specimen 1 to 1

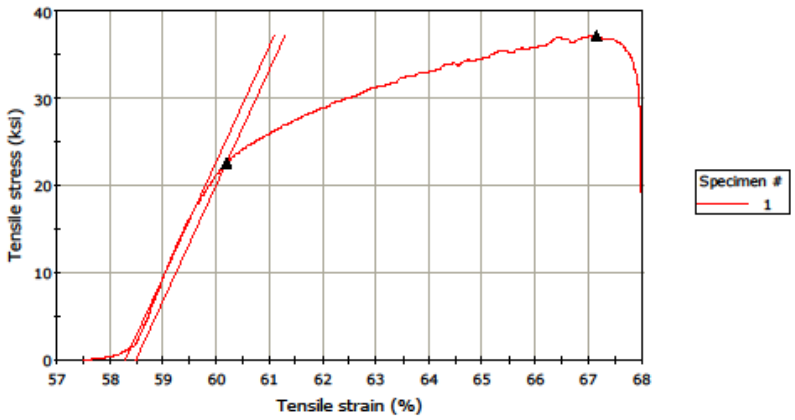


Results Table 1

| | Maximum Load (lbf) | Maximum Stress (ksi) | Load at Break (Standard) (lbf) | Tensile stress at Break (Standard) (ksi) | Elongation at Break (%) |
|---|---|---|---|---|---|
| 1 | 2,551.44 | 37.13 | 2,200.45 | 32.0 | 67.9 |

| | Diameter (in) |
|---|---|
| 1 | 0.296 |

7/17/2014 3:35:08 PM H13_35_500_4.is_tens

**Southern Nuclear**
**Dedication and Test Facility**

Graph 1

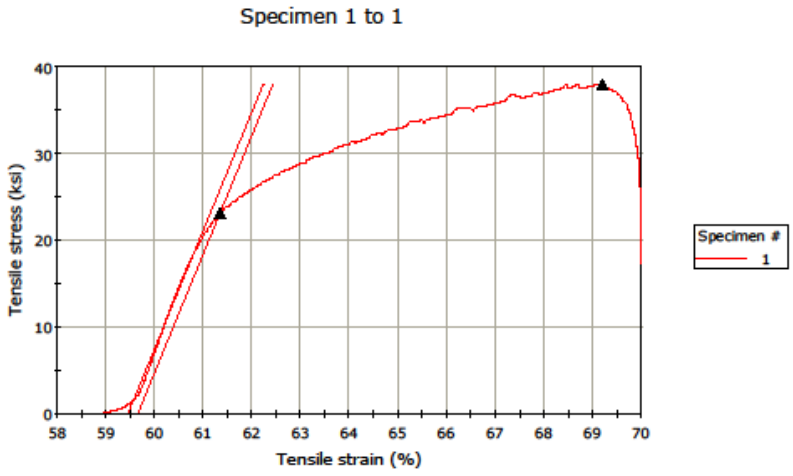


Results Table 1

| | Maximum Load (lbf) | Maximum Stress (ksi) | Load at Break (Standard) (lbf) | Tensile stress at Break (Standard) (ksi) | Elongation at Break (%) |
|---|---|---|---|---|---|
| 1 | 2,610.83 | 37.99 | 2,053.98 | 29.9 | 69.9 |

| | Diameter (in) |
|---|---|
| 1 | 0.296 |

7/17/2014 3:41:09 PM H13_35_500_5.is_tens

**Southern Nuclear**
**Dedication and Test Facility**

Graph 1

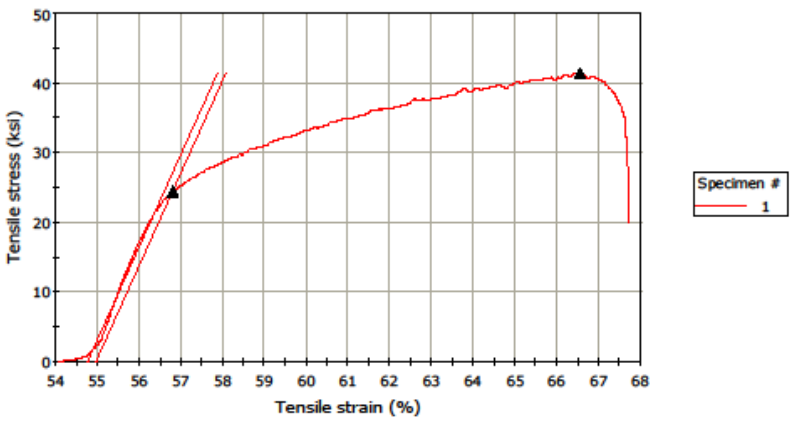


Results Table 1

| | Maximum Load (lbf) | Maximum Stress (ksi) | Load at Break (Standard) (lbf) | Tensile stress at Break (Standard) (ksi) | Elongation at Break (%) |
|---|---|---|---|---|---|
| 1 | 2,846.40 | 41.42 | 2,347.41 | 34.2 | 67.6 |

| | Diameter (in) |
|---|---|
| 1 | 0.296 |

7/17/2014 3:44:53 PM H13_35_500_6.is_tens

# Southern Nuclear
## Dedication and Test Facility

Graph 1

Specimen 1 to 1

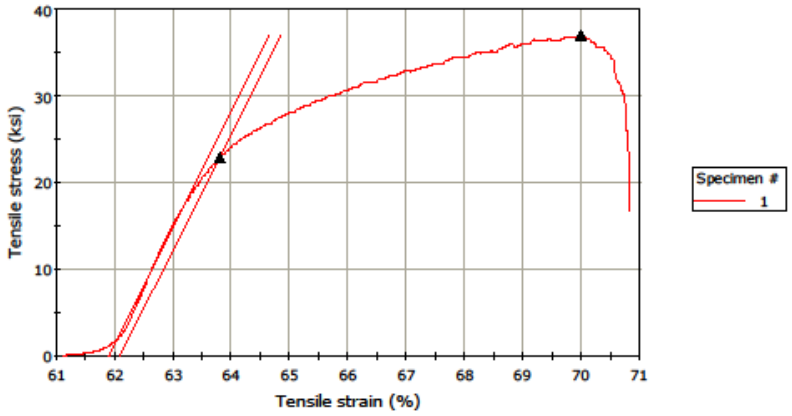


Results Table 1

| | Maximum Load (lbf) | Maximum Stress (ksi) | Load at Break (Standard) (lbf) | Tensile stress at Break (Standard) (ksi) | Elongation at Break (%) |
|---|---|---|---|---|---|
| 1 | 2,535.72 | 36.90 | 1,949.19 | 28.4 | 70.8 |

| | Diameter (in) |
|---|---|
| 1 | 0.296 |

7/17/2014 3:49:58 PM H13_35_500_7.is_tens

# Southern Nuclear
## Dedication and Test Facility

Graph 1

Specimen 1 to 1

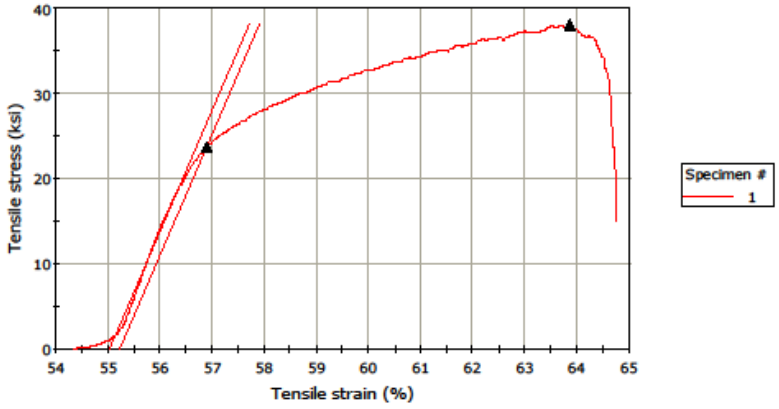


Results Table 1

| | Maximum Load (lbf) | Maximum Stress (ksi) | Load at Break (Standard) (lbf) | Tensile stress at Break (Standard) (ksi) | Elongation at Break (%) |
|---|---|---|---|---|---|
| 1 | 2,613.05 | 38.02 | 1,701.33 | 24.8 | 64.7 |

| | Diameter (in) |
|---|---|
| 1 | 0.296 |

7/17/2014 3:51:50 PM H13_35_500_8.is_tens

## Southern Nuclear
### Dedication and Test Facility

Graph 1

Specimen 1 to 1

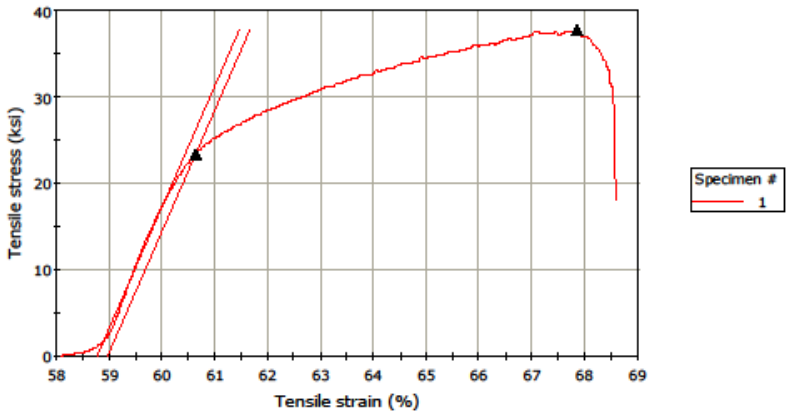


Results Table 1

| | Maximum Load (lbf) | Maximum Stress (ksi) | Load at Break (Standard) (lbf) | Tensile stress at Break (Standard) (ksi) | Elongation at Break (%) |
|---|---|---|---|---|---|
| 1 | 2,589.83 | 37.69 | 2,141.71 | 31.2 | 68.5 |

| | Diameter (in) |
|---|---|
| 1 | 0.296 |

9/26/2014 10:12:56 AM H13_35_500_22.is_tens

## Southern Nuclear
### Dedication and Test Facility

Graph 1

Specimen 1 to 1

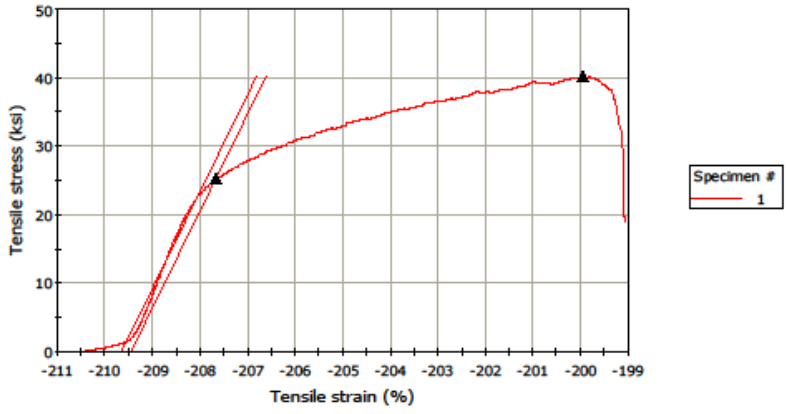


Results Table 1

| | Maximum Load (lbf) | Maximum Stress (ksi) | Load at Break (Standard) (lbf) | Tensile stress at Break (Standard) (ksi) | Elongation at Break (%) |
|---|---|---|---|---|---|
| 1 | 2,757.02 | 40.12 | 2,199.96 | 32.0 | -199.2 |

| | Diameter (in) |
|---|---|
| 1 | 0.296 |

**Southern Nuclear**
**Dedication and Test Facility**

Graph 1

Specimen 1 to 1

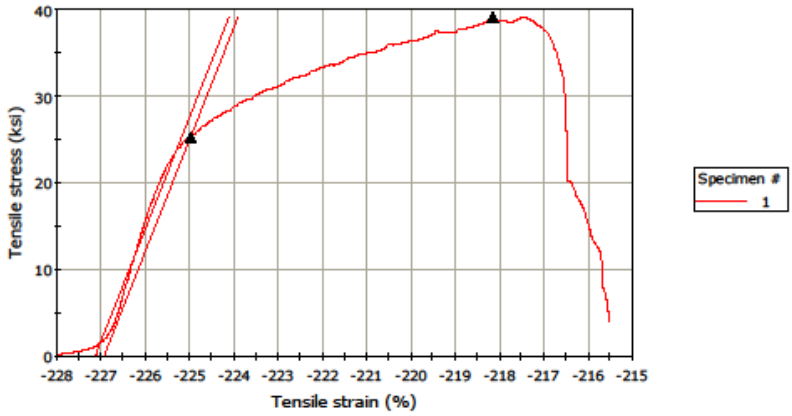


Results Table 1

| | Maximum Load (lbf) | Maximum Stress (ksi) | Load at Break (Standard) (lbf) | Tensile stress at Break (Standard) (ksi) | Elongation at Break (%) |
|---|---|---|---|---|---|
| 1 | 2,684.77 | 39.07 | 488.80 | 7.1 | -215.6 |

| | Diameter (in) |
|---|---|
| 1 | 0.296 |

9/26/2014 10:18:30 AM H13_35_500_25.is_tens

**Southern Nuclear**
**Dedication and Test Facility**

Graph 1

Specimen 1 to 1

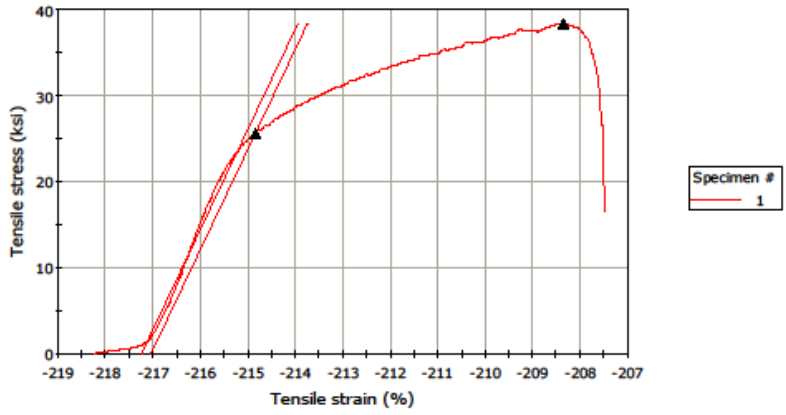


Results Table 1

| | Maximum Load (lbf) | Maximum Stress (ksi) | Load at Break (Standard) (lbf) | Tensile stress at Break (Standard) (ksi) | Elongation at Break (%) |
|---|---|---|---|---|---|
| 1 | 2,631.70 | 38.30 | 1,915.08 | 27.9 | -207.6 |

| | Diameter (in) |
|---|---|
| 1 | 0.296 |

# Southern Nuclear
## Dedication and Test Facility

Graph 1

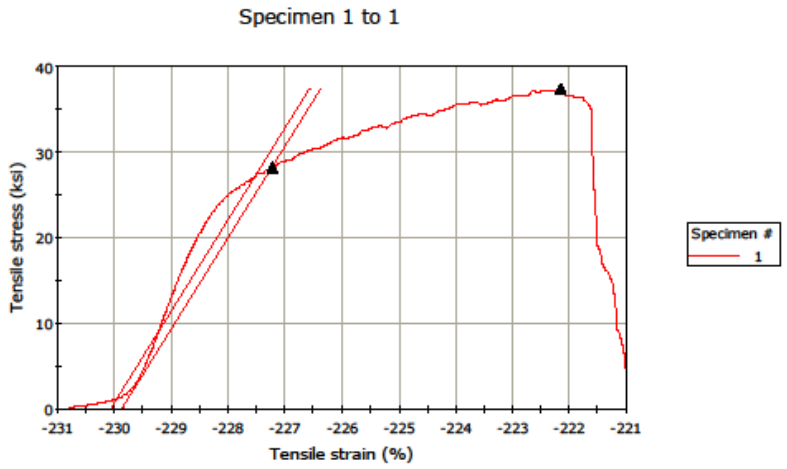


Results Table 1

| | Maximum Load (lbf) | Maximum Stress (ksi) | Load at Break (Standard) (lbf) | Tensile stress at Break (Standard) (ksi) | Elongation at Break (%) |
|---|---|---|---|---|---|
| 1 | 2,569.61 | 37.39 | 546.80 | 8.0 | -221.1 |

| | Diameter (in) |
|---|---|
| 1 | 0.296 |

7/17/2014 4:21:55 PM Tig5.is_tens

**Southern Nuclear**
**Dedication and Test Facility**

Graph 1

Specimen 1 to 1

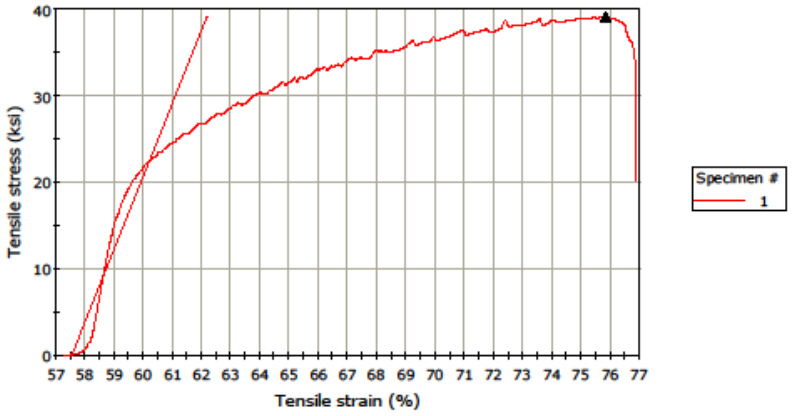


Results Table 1

| | Maximum Load (lbf) | Maximum Stress (ksi) | Load at Break (Standard) (lbf) | Tensile stress at Break (Standard) (ksi) | Elongation at Break (%) |
|---|---|---|---|---|---|
| 1 | 2,683.28 | 39.05 | 2,367.90 | 34.5 | 76.8 |

| | Diameter (in) |
|---|---|
| 1 | 0.296 |

7/17/2014 4:24:37 PM Tig6.is_tens

## Southern Nuclear
### Dedication and Test Facility

Graph 1

Specimen 1 to 1

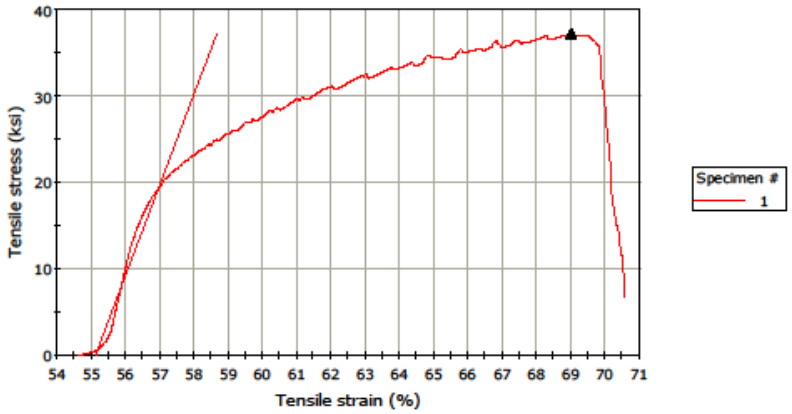


Results Table 1

| | Maximum Load (lbf) | Maximum Stress (ksi) | Load at Break (Standard) (lbf) | Tensile stress at Break (Standard) (ksi) | Elongation at Break (%) |
|---|---|---|---|---|---|
| 1 | 2,557.19 | 37.21 | 766.51 | 11.2 | 70.5 |

| | Diameter (in) |
|---|---|
| 1 | 0.296 |

9/26/2014 10:23:33 AM Tig7.is_tens

## Southern Nuclear
### Dedication and Test Facility

Graph 1

Specimen 1 to 1

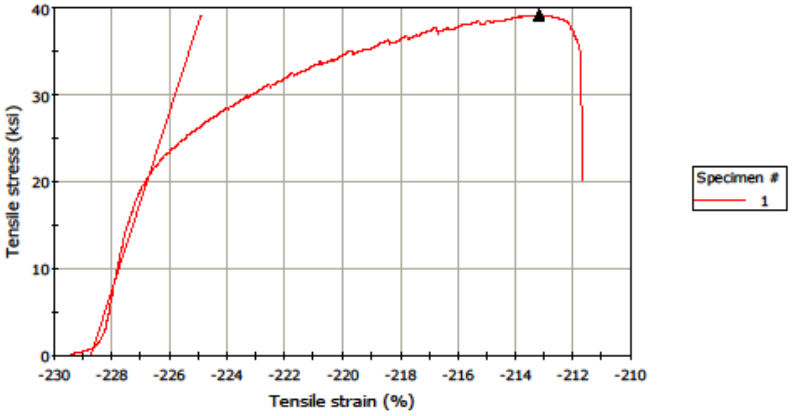


Results Table 1

| | Maximum Load (lbf) | Maximum Stress (ksi) | Load at Break (Standard) (lbf) | Tensile stress at Break (Standard) (ksi) | Elongation at Break (%) |
|---|---|---|---|---|---|
| 1 | 2,690.38 | 39.15 | 2,416.97 | 35.2 | -211.8 |

| | Diameter (in) |
|---|---|
| 1 | 0.296 |

9/26/2014 10:28:03 AM Tig9.is_tens

## Southern Nuclear
### Dedication and Test Facility

Graph 1

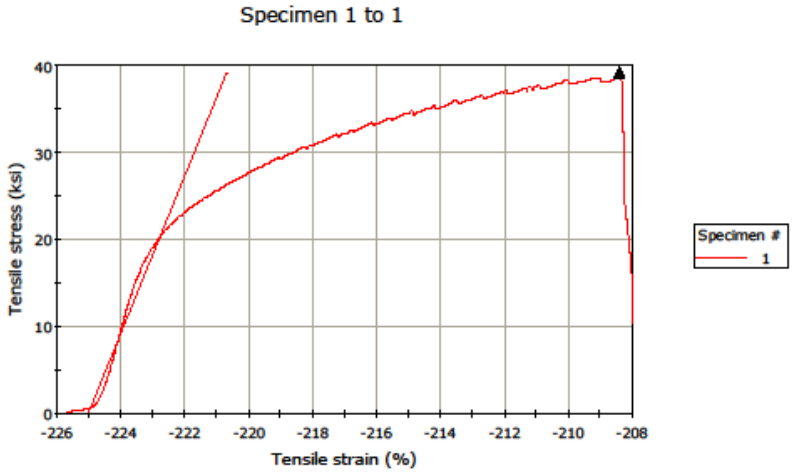


Results Table 1

| | Maximum Load (lbf) | Maximum Stress (ksi) | Load at Break (Standard) (lbf) | Tensile stress at Break (Standard) (ksi) | Elongation at Break (%) |
|---|---|---|---|---|---|
| 1 | 2,690.10 | 39.15 | 1,208.58 | 17.6 | -208.1 |

| | Diameter (in) |
|---|---|
| 1 | 0.296 |

9/26/2014 10:29:42 AM Tig10.is_tens

## Southern Nuclear
### Dedication and Test Facility

Graph 1

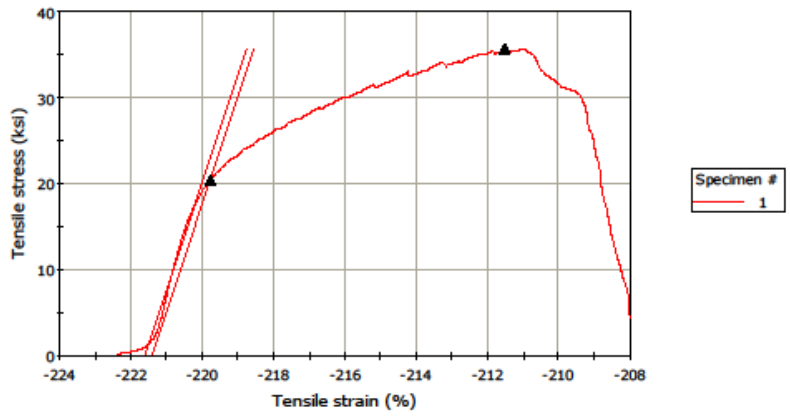


Results Table 1

| | Maximum Load (lbf) | Maximum Stress (ksi) | Load at Break (Standard) (lbf) | Tensile stress at Break (Standard) (ksi) | Elongation at Break (%) |
|---|---|---|---|---|---|
| 1 | 2,450.90 | 35.66 | 508.88 | 7.4 | -208.1 |

| | Diameter (in) |
|---|---|
| 1 | 0.296 |

9/26/2014 10:31:48 AM Tig11.is_tens

## Southern Nuclear
### Dedication and Test Facility

Graph 1

Specimen 1 to 1

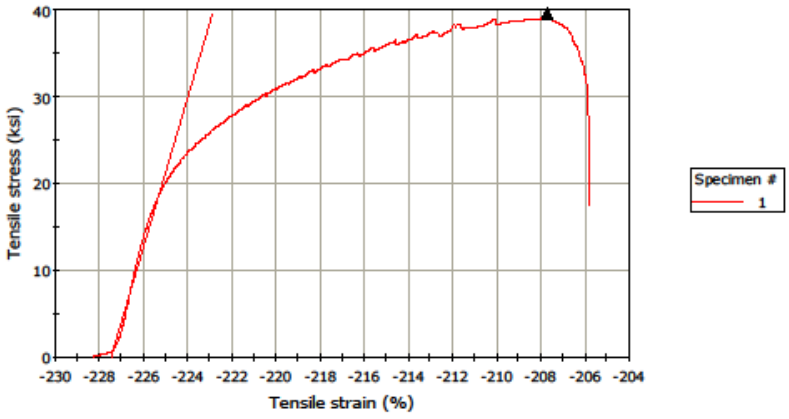


Results Table 1

| | Maximum Load (lbf) | Maximum Stress (ksi) | Load at Break (Standard) (lbf) | Tensile stress at Break (Standard) (ksi) | Elongation at Break (%) |
|---|---|---|---|---|---|
| 1 | 2,717.07 | 39.54 | 2,026.36 | 29.5 | -205.9 |

| | Diameter (in) |
|---|---|
| 1 | 0.296 |

9/26/2014 10:33:30 AM Tig12.is_tens

## Southern Nuclear
### Dedication and Test Facility

Graph 1

Specimen 1 to 1

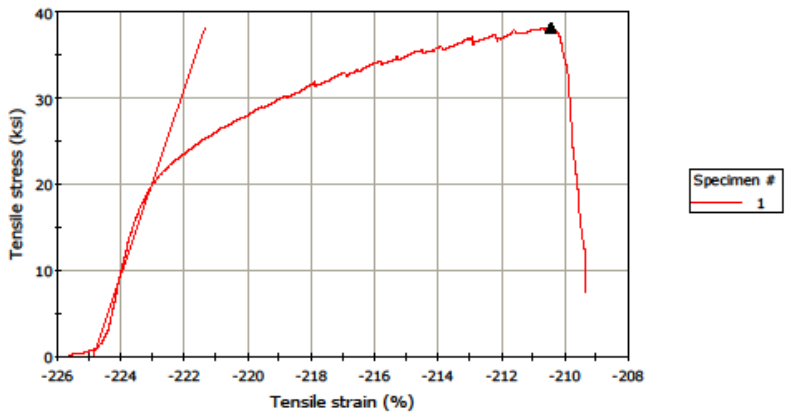


Results Table 1

| | Maximum Load (lbf) | Maximum Stress (ksi) | Load at Break (Standard) (lbf) | Tensile stress at Break (Standard) (ksi) | Elongation at Break (%) |
|---|---|---|---|---|---|
| 1 | 2,623.00 | 38.17 | 886.40 | 12.9 | -209.4 |

| | Diameter (in) |
|---|---|
| 1 | 0.296 |

# Southern Nuclear
## Dedication and Test Facility

Graph 1

Specimen 1 to 1

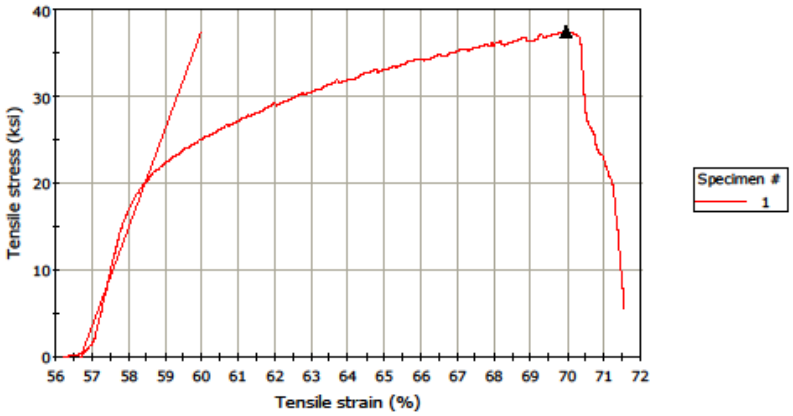


Results Table 1

| | Maximum Load (lbf) | Maximum Stress (ksi) | Load at Break (Standard) (lbf) | Tensile stress at Break (Standard) (ksi) | Elongation at Break (%) |
|---|---|---|---|---|---|
| 1 | 2,572.84 | 37.44 | 638.43 | 9.3 | 71.5 |

| | Diameter (in) |
|---|---|
| 1 | 0.296 |



# Southern Nuclear
## Dedication and Test Facility

Graph 1

Specimen 1 to 1

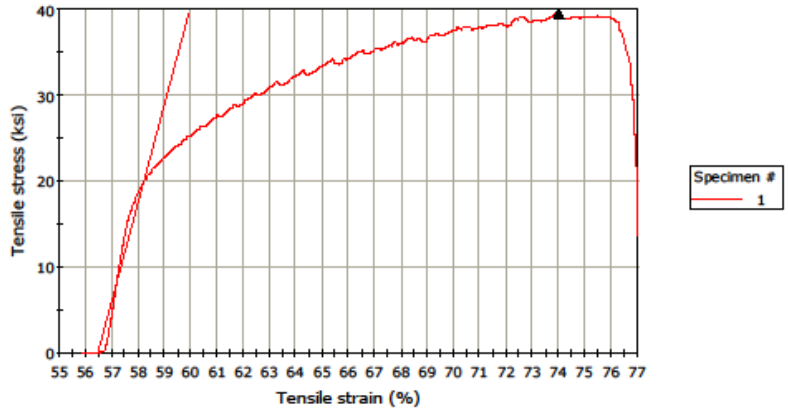


Results Table 1

| | Maximum Load (lbf) | Maximum Stress (ksi) | Load at Break (Standard) (lbf) | Tensile stress at Break (Standard) (ksi) | Elongation at Break (%) |
|---|---|---|---|---|---|
| 1 | 2,709.52 | 39.43 | 1,570.83 | 22.9 | 76.9 |

| | Diameter (in) |
|---|---|
| 1 | 0.296 |

# Southern Nuclear
## Dedication and Test Facility

Graph 1

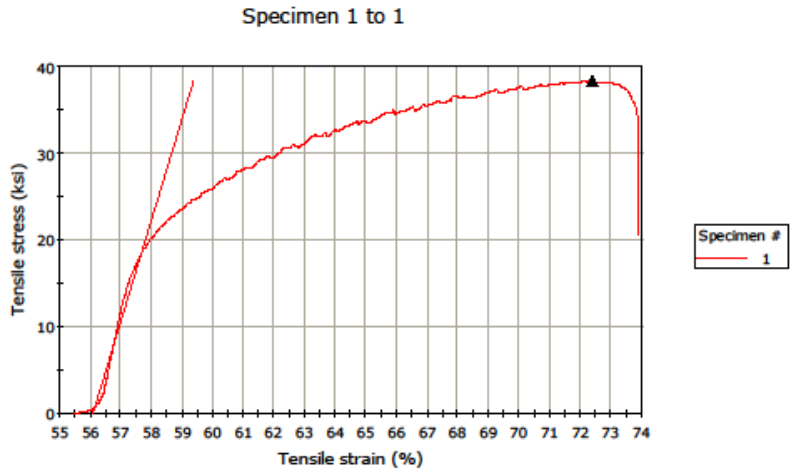


Results Table 1

| | Maximum Load (lbf) | Maximum Stress (ksi) | Load at Break (Standard) (lbf) | Tensile stress at Break (Standard) (ksi) | Elongation at Break (%) |
|---|---|---|---|---|---|
| 1 | 2,628.80 | 38.25 | 2,373.33 | 34.5 | 73.8 |

| | Diameter (in) |
|---|---|
| 1 | 0.296 |

# A2 Tool Weld Tensile Testing

11/5/2014 4:17:05 PM A2_35_500.is_tens

**Southern Nuclear**
**Dedication and Test Facility**

Graph 1

Specimen 1 to 1

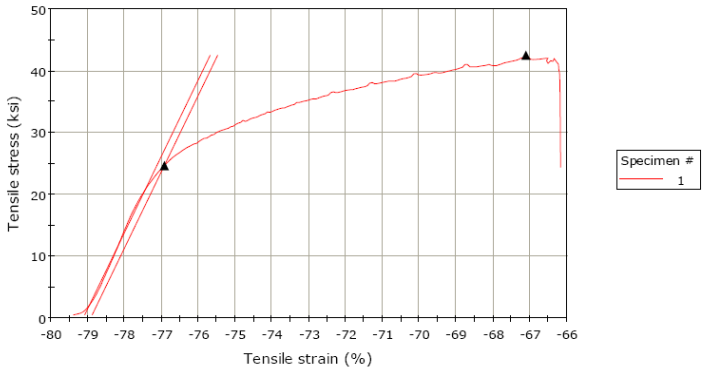


Results Table 1

| | Maximum Load (lbf) | Maximum Stress (ksi) | Load at Break (Standard) (lbf) | Tensile stress at Break (Standard) (ksi) | Elongation at Break (%) |
|---|---|---|---|---|---|
| 1 | 2,920.93 | 42.50 | 2,823.45 | 41.1 | -66.2 |

| | Diameter (in) |
|---|---|
| 1 | 0.296 |

11/5/2014 4:18:59 PM A2_35_500_2.is_tens

**Southern Nuclear**
**Dedication and Test Facility**

Graph 1

Specimen 1 to 1

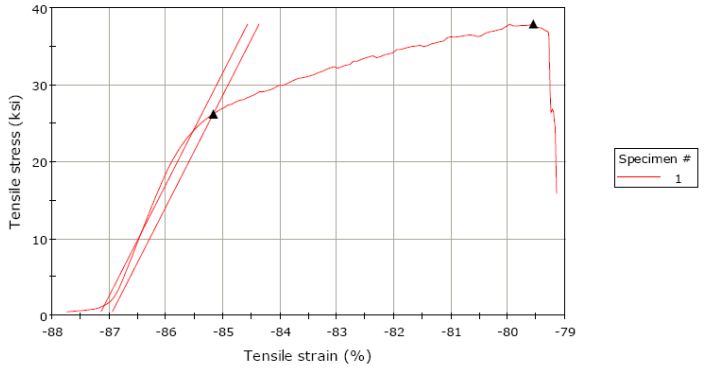


Results Table 1

| | Maximum Load (lbf) | Maximum Stress (ksi) | Load at Break (Standard) (lbf) | Tensile stress at Break (Standard) (ksi) | Elongation at Break (%) |
|---|---|---|---|---|---|
| 1 | 2,604.72 | 37.90 | 1,844.30 | 26.8 | -79.2 |

| | Diameter (in) |
|---|---|
| 1 | 0.296 |

## Southern Nuclear
### Dedication and Test Facility

Graph 1

Specimen 1 to 2

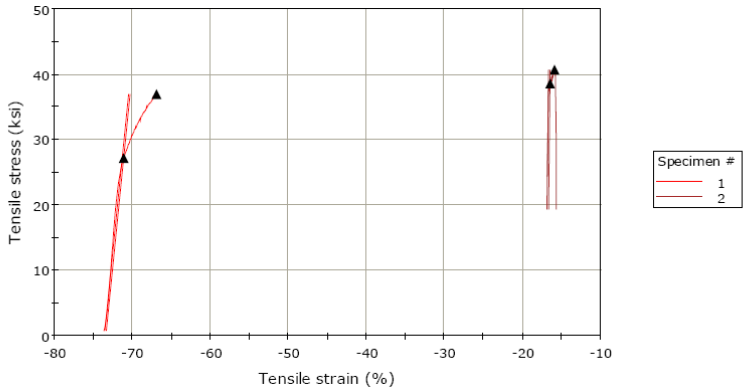


Results Table 1

| | Maximum Load (lbf) | Maximum Stress (ksi) | Load at Break (Standard) (lbf) | Tensile stress at Break (Standard) (ksi) | Elongation at Break (%) |
|---|---|---|---|---|---|
| 1 | 2,541.63 | 36.99 | 2,541.63 | 37.0 | -66.9 |
| 2 | 2,797.26 | 40.70 | 2,219.10 | 32.3 | -16.1 |

| | Diameter (in) |
|---|---|
| 1 | 0.296 |

9/26/2014 9:57:44 AM A2_35_500_4.is_tens

## Southern Nuclear
### Dedication and Test Facility

Graph 1

Specimen 1 to 1

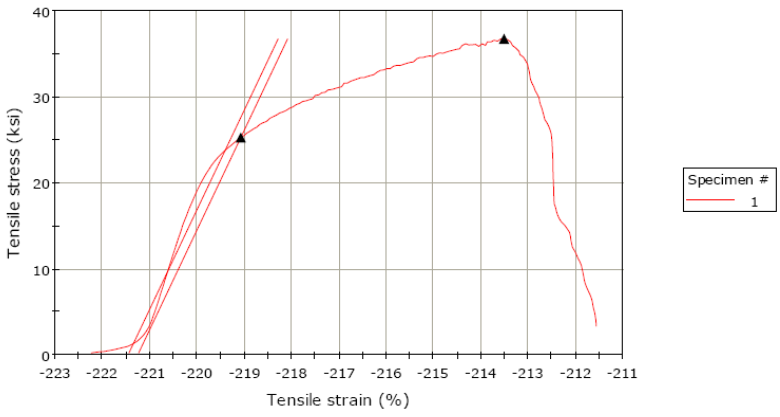


Results Table 1

| | Maximum Load (lbf) | Maximum Stress (ksi) | Load at Break (Standard) (lbf) | Tensile stress at Break (Standard) (ksi) | Elongation at Break (%) |
|---|---|---|---|---|---|
| 1 | 2,524.67 | 36.74 | 399.34 | 5.8 | -211.6 |

| | Diameter (in) |
|---|---|
| 1 | 0.296 |

7/17/2014 3:31:46 PM A2_35_500_5.is_tens

## Southern Nuclear
### Dedication and Test Facility

Graph 1

Specimen 1 to 1

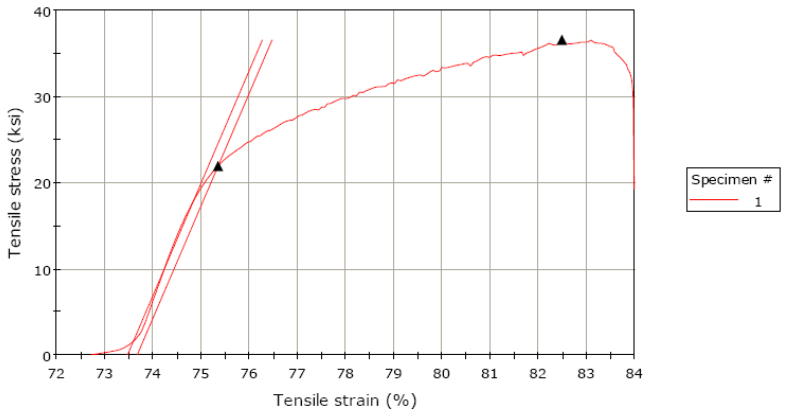


Results Table 1

| | Maximum Load (lbf) | Maximum Stress (ksi) | Load at Break (Standard) (lbf) | Tensile stress at Break (Standard) (ksi) | Elongation at Break (%) |
|---|---|---|---|---|---|
| 1 | 2,513.50 | 36.58 | 2,222.84 | 32.3 | 83.9 |

| | Diameter (in) |
|---|---|
| 1 | 0.296 |

7/17/2014 3:17:15 PM A2_35_500_6.is_tens

## Southern Nuclear
### Dedication and Test Facility

Graph 1

Specimen 1 to 1

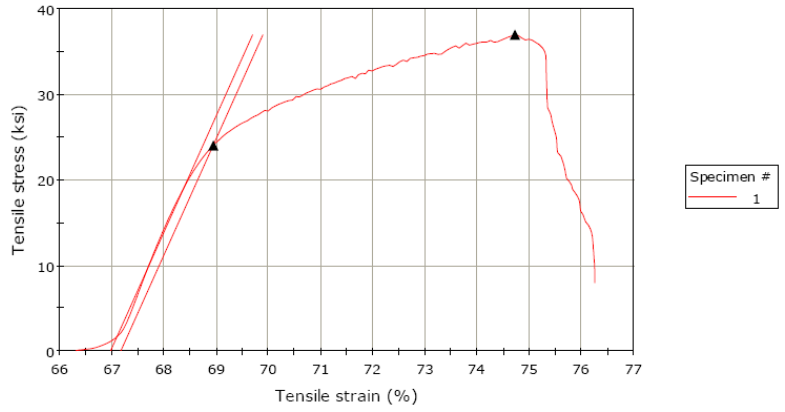


Results Table 1

| | Maximum Load (lbf) | Maximum Stress (ksi) | Load at Break (Standard) (lbf) | Tensile stress at Break (Standard) (ksi) | Elongation at Break (%) |
|---|---|---|---|---|---|
| 1 | 2,540.88 | 36.97 | 954.48 | 13.9 | 76.2 |

| | Diameter (in) |
|---|---|
| 1 | 0.296 |

11/14/2014 1:31:33 PM A2_35_500_7.is_tens

## Southern Nuclear
### Dedication and Test Facility

Graph 1

Specimen 1 to 1

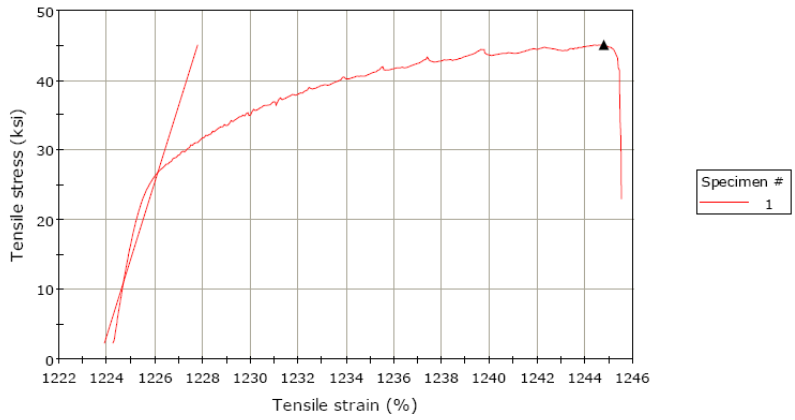


Results Table 1

| | Maximum Load (lbf) | Maximum Stress (ksi) | Load at Break (Standard) (lbf) | Tensile stress at Break (Standard) (ksi) | Elongation at Break (%) |
|---|---|---|---|---|---|
| 1 | 3,098.84 | 45.09 | 2,646.37 | 38.5 | 1,245.4 |

| | Diameter (in) |
|---|---|
| 1 | 0.296 |

7/17/2014 4:09:00 PM A2_35_500_8.is_tens

## Southern Nuclear
### Dedication and Test Facility

Graph 1

Specimen 1 to 1

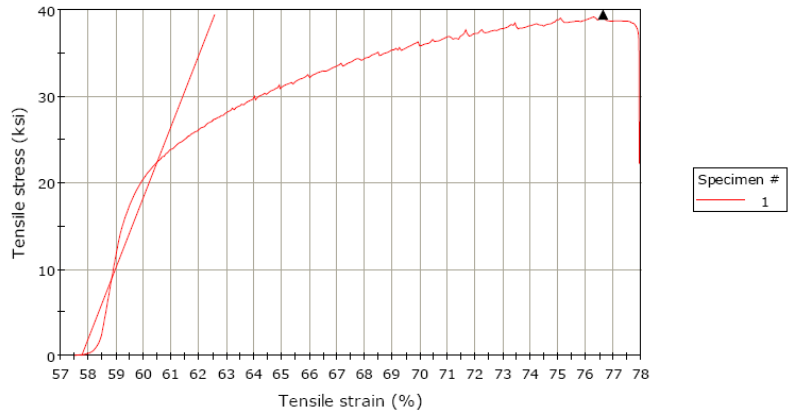


Results Table 1

| | Maximum Load (lbf) | Maximum Stress (ksi) | Load at Break (Standard) (lbf) | Tensile stress at Break (Standard) (ksi) | Elongation at Break (%) |
|---|---|---|---|---|---|
| 1 | 2,711.19 | 39.45 | 2,598.15 | 37.8 | 77.8 |

| | Diameter (in) |
|---|---|
| 1 | 0.296 |

**Southern Nuclear**
**Dedication and Test Facility**

Graph 1

Specimen 1 to 1

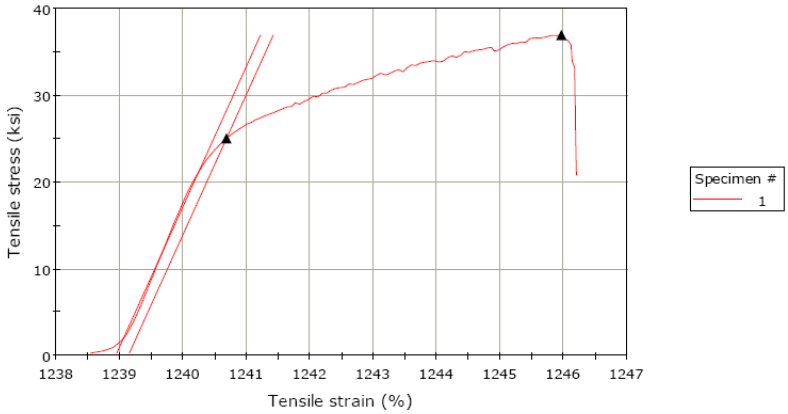


Results Table 1

| | Maximum Load (lbf) | Maximum Stress (ksi) | Load at Break (Standard) (lbf) | Tensile stress at Break (Standard) (ksi) | Elongation at Break (%) |
|---|---|---|---|---|---|
| 1 | 2,538.69 | 36.94 | 2,387.53 | 34.7 | 1,246.1 |

| | Diameter (in) |
|---|---|
| 1 | 0.296 |



**Southern Nuclear**
**Dedication and Test Facility**

Graph 1

Specimen 1 to 1

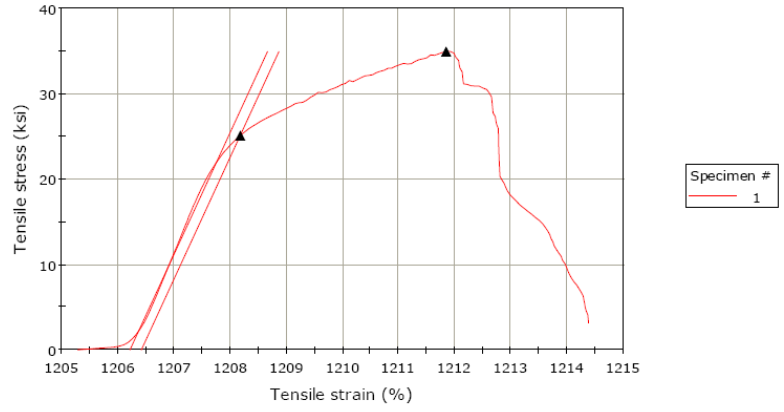


Results Table 1

| | Maximum Load (lbf) | Maximum Stress (ksi) | Load at Break (Standard) (lbf) | Tensile stress at Break (Standard) (ksi) | Elongation at Break (%) |
|---|---|---|---|---|---|
| 1 | 2,401.22 | 34.94 | 345.82 | 5.0 | 1,214.3 |

| | Diameter (in) |
|---|---|
| 1 | 0.296 |

Statistical Data

F-Test Two-Sample for Variances

| *Tensile Tests* | *H13 Welds* | *420SS Welds* |
|---|---|---|
| Mean | 2639.035 | 2794.739 |
| Variance | 9568.895 | 25232.9623 |
| Observations | 10 | 10 |
| df | 9 | 9 |
| F | 0.379222 | |
| P(F<=f) one-tail | 0.082399 | |
| F Critical one-tail | 0.314575 | |

t-Test: Two-Sample Assuming Equal Variances

| *Tensile Tests* | *H13 Welds* | *420SS Welds* |
|---|---|---|
| Mean | 2639.035 | 2794.739 |
| Variance | 9568.895 | 25232.9623 |
| Observations | 10 | 10 |
| Pooled Variance | 17400.93 | |
| Hypothesized Mean Difference | 0 | |
| df | 18 | |
| t Stat | -2.63936 | |
| P(T<=t) one-tail | 0.00833 | |
| t Critical one-tail | 1.734064 | |
| P(T<=t) two-tail | 0.016659 | |
| t Critical two-tail | 2.100922 | |

F-Test Two-Sample for Variances

| *Tensile Tests* | *A2 Welds* | *H13 Welds* |
|---|---|---|
| Mean | 2665.19 | 2639.035 |
| Variance | 46729.05 | 9568.89501 |
| Observations | 10 | 10 |
| df | 9 | 9 |
| F | 4.883433 | |
| P(F<=f) one-tail | 0.013546 | |
| F Critical one-tail | 3.178893 | |

t-Test: Two-Sample Assuming Unequal Variances

| *Tensile Tests* | *A2 Welds* | *H13 Welds* |
|---|---|---|
| Mean | 2665.19 | 2639.035 |
| Variance | 46729.05 | 9568.89501 |
| Observations | 10 | 10 |
| Hypothesized Mean Difference | 0 | |
| df | 13 | |
| t Stat | 0.348585 | |
| P(T<=t) one-tail | 0.366491 | |
| t Critical one-tail | 1.770933 | |
| P(T<=t) two-tail | 0.732982 | |
| t Critical two-tail | 2.160369 | |

F-Test Two-Sample for Variances

| *Tensile Tests* | *A2 Welds* | *420SS Welds* |
|---|---|---|
| Mean | 2665.19 | 2794.739 |
| Variance | 46729.05 | 25232.9623 |
| Observations | 10 | 10 |
| df | 9 | 9 |
| F | 1.851905 | |
| P(F<=f) one-tail | 0.186119 | |
| F Critical one-tail | 3.178893 | |

t-Test: Two-Sample Assuming Equal Variances

| *Tensile Tests* | *A2 Welds* | *420SS Welds* |
|---|---|---|
| Mean | 2665.19 | 2794.739 |
| Variance | 46729.05 | 25232.9623 |
| Observations | 10 | 10 |
| Pooled Variance | 35981.01 | |
| Hypothesized Mean Difference | 0 | |
| df | 18 | |
| t Stat | -1.527152 | |
| P(T<=t) one-tail | 0.072052 | |
| t Critical one-tail | 1.734064 | |
| P(T<=t) two-tail | 0.144104 | |
| t Critical two-tail | 2.100922 | |

F-Test Two-Sample for Variances

| *Tensile Tests* | *H13 Welds* | *Mig Welds* |
|---|---|---|
| Mean | 2639.035 | 2632.301 |
| Variance | 9568.895 | 7181.3121 |
| Observations | 10 | 10 |
| df | 9 | 9 |
| F | 1.332472 | |
| P(F<=f) one-tail | 0.337942 | |
| F Critical one-tail | 3.178893 | |

t-Test: Two-Sample Assuming Equal Variances

| *Tensile Tests* | *H13 Welds* | *Mig Welds* |
|---|---|---|
| Mean | 2639.035 | 2632.301 |
| Variance | 9568.895 | 7181.3121 |
| Observations | 10 | 10 |
| Pooled Variance | 8375.104 | |
| Hypothesized Mean Difference | 0 | |
| df | 18 | |
| t Stat | 0.164537 | |
| P(T<=t) one-tail | 0.435571 | |
| t Critical one-tail | 1.734064 | |
| P(T<=t) two-tail | 0.871142 | |
| t Critical two-tail | 2.100922 | |

F-Test Two-Sample for Variances

| *Tensile Tests* | *H13 Welds* | *Parent* |
|---|---|---|
| Mean | 2639.035 | 3471.295 |
| Variance | 9568.895 | 4285.25252 |
| Observations | 10 | 10 |
| df | 9 | 9 |
| F | 2.232983 | |
| P(F<=f) one-tail | 0.123576 | |
| F Critical one-tail | 3.178893 | |

t-Test: Two-Sample Assuming Equal Variances

| *Tensile Tests* | *H13 Welds* | *Parent* |
|---|---|---|
| Mean | 2639.035 | 3471.295 |
| Variance | 9568.895 | 4285.25252 |
| Observations | 10 | 10 |
| Pooled Variance | 6927.074 | |
| Hypothesized Mean Difference | 0 | |
| df | 18 | |
| t Stat | -22.35986 | |
| P(T<=t) one-tail | 6.96E-15 | |
| t Critical one-tail | 1.734064 | |
| P(T<=t) two-tail | 1.39E-14 | |
| t Critical two-tail | 2.100922 | |

F-Test Two-Sample for Variances

| *Tensile Tests* | *A2 Welds* | *Mig Welds* |
|---|---|---|
| Mean | 2665.19 | 2632.301 |
| Variance | 46729.05 | 7181.3121 |
| Observations | 10 | 10 |
| df | 9 | 9 |
| F | 6.507036 | |
| P(F<=f) one-tail | 0.005093 | |
| F Critical one-tail | 3.178893 | |

t-Test: Two-Sample Assuming Unequal Variances

| *Tensile Tests* | *A2 Welds* | *Mig Welds* |
|---|---|---|
| Mean | 2665.19 | 2632.301 |
| Variance | 46729.05 | 7181.3121 |
| Observations | 10 | 10 |
| Hypothesized Mean Difference | 0 | |
| df | 12 | |
| t Stat | 0.447935 | |
| P(T<=t) one-tail | 0.33109 | |
| t Critical one-tail | 1.782288 | |
| P(T<=t) two-tail | 0.66218 | |
| t Critical two-tail | 2.178813 | |

F-Test Two-Sample for Variances

| *Tensile Tests* | *A2 Welds* | *Parent* |
|---|---|---|
| Mean | 2665.19 | 3471.295 |
| Variance | 46729.05 | 4285.25252 |
| Observations | 10 | 10 |
| df | 9 | 9 |
| F | 10.90462 | |
| P(F<=f) one-tail | 0.000745 | |
| F Critical one-tail | 3.178893 | |

t-Test: Two-Sample Assuming Unequal Variances

| *Tensile Tests* | *A2 Welds* | *Parent* |
|---|---|---|
| Mean | 2665.19 | 3471.295 |
| Variance | 46729.05 | 4285.25252 |
| Observations | 10 | 10 |
| Hypothesized Mean Difference | 0 | |
| df | 11 | |
| t Stat | -11.28614 | |
| P(T<=t) one-tail | 1.09E-07 | |
| t Critical one-tail | 1.795885 | |
| P(T<=t) two-tail | 2.18E-07 | |
| t Critical two-tail | 2.200985 | |

F-Test Two-Sample for Variances

| *Tensile Tests* | *420SS Welds* | *Mig Welds* |
|---|---|---|
| Mean | 2794.739 | 2632.301 |
| Variance | 25232.96 | 7181.3121 |
| Observations | 10 | 10 |
| df | 9 | 9 |
| F | 3.513698 | |
| P(F<=f) one-tail | 0.037572 | |
| F Critical one-tail | 3.178893 | |

t-Test: Two-Sample Assuming Unequal Variances

| *Tensile Tests* | *420SS Welds* | *Mig Welds* |
|---|---|---|
| Mean | 2794.739 | 2632.301 |
| Variance | 25232.96 | 7181.3121 |
| Observations | 10 | 10 |
| Hypothesized Mean Difference | 0 | |
| df | 14 | |
| t Stat | 2.853116 | |
| P(T<=t) one-tail | 0.006386 | |
| t Critical one-tail | 1.76131 | |
| P(T<=t) two-tail | 0.012771 | |
| t Critical two-tail | 2.144787 | |

F-Test Two-Sample for Variances

| *Tensile Tests* | *420SS Welds* | *Parent* |
|---|---|---|
| Mean | 2794.739 | 3471.295 |
| Variance | 25232.96 | 4285.25252 |
| Observations | 10 | 10 |
| df | 9 | 9 |
| F | 5.888326 | |
| P(F<=f) one-tail | 0.007219 | |
| F Critical one-tail | 3.178893 | |

t-Test: Two-Sample Assuming Unequal Variances

| *Tensile Tests* | *420SS Welds* | *Parent* |
|---|---|---|
| Mean | 2794.739 | 3471.295 |
| Variance | 25232.96 | 4285.25252 |
| Observations | 10 | 10 |
| Hypothesized Mean Difference | 0 | |
| df | 12 | |
| t Stat | -12.45256 | |
| P(T<=t) one-tail | 1.6E-08 | |
| t Critical one-tail | 1.782288 | |
| P(T<=t) two-tail | 3.2E-08 | |
| t Critical two-tail | 2.178813 | |

Appendix 5

Hardness Test Results

| **Hardness Testing** | | | | | |
|---|---|---|---|---|---|
| **Position** | 1 | 2 | 3 | 4 | 5 |
| **Sample #** | **Mig Weld Sample Hardness** | | | | |
| 1 | 18.5 | 19.4 | 18.5 | 21.4 | 29 |
| 2 | 11.8 | 15.1 | 14.8 | 16.4 | 27.3 |
| 3 | 17.7 | 15.6 | 14.2 | 14.4 | 30.2 |
| 4 | 18.1 | 13.1 | 13 | 16 | 16.8 |
| 5 | 17.4 | 19.3 | 17 | 16.4 | 26.5 |
| 6 | 17.9 | 12.9 | 15.8 | 17.5 | 18.4 |
| 7 | 19.7 | 20.9 | 22.1 | 23.3 | 25.4 |
| 8 | 18.9 | 11.8 | 12.9 | 12.1 | 16.1 |
| 9 | 15.4 | 17 | 12.5 | 14.2 | 23 |
| 10 | 18.8 | 13.3 | 13.1 | 12.3 | 27.4 |
| **Mean** | 17.42 | 15.84 | 15.39 | 16.4 | 24.01 |
| **Sample #** | **H13 Weld Sample Hardness (**3.5 ipm @ 500 rpm**)** | | | | |
| 1 | 27.2 | 32.8 | 33.6 | 36 | 29.6 |
| 2 | 30.4 | 36 | 35.7 | 35.1 | 29.8 |
| 3 | 25.8 | 29.1 | 29.3 | 28 | 22.5 |
| 4 | 25.5 | 31.5 | 31.5 | 29.3 | 23.1 |
| 5 | 25.5 | 29.3 | 29.7 | 31 | 23.3 |
| 6 | 23.8 | 30 | 33.1 | 31.9 | 22.9 |
| 7 | 25.5 | 30.2 | 36.7 | 35.8 | 32.5 |
| 8 | 31.7 | 36.9 | 38.4 | 35.7 | 34.6 |
| 9 | 30.3 | 28.2 | 29 | 28.1 | 29 |
| 10 | 24 | 28 | 29.3 | 28.7 | 24 |
| **Mean** | 26.97 | 31.2 | 32.63 | 31.96 | 27.13 |
| **Sample #** | **420SS Weld Sample Hardness (**4 ipm @ 675 rpm**)** | | | | |
| 1 | 23.2 | 28.9 | 29 | 28.2 | 25.5 |
| 2 | 35.3 | 36.2 | 38.5 | 37.5 | 38.5 |
| 3 | 32.8 | 29.9 | 32.7 | 31.3 | 33 |
| 4 | 27.1 | 33.1 | 36.6 | 35 | 33 |
| 5 | 30.8 | 31.6 | 35 | 33.1 | 36.6 |
| 6 | 32.9 | 31.9 | 36.4 | 35.6 | 36.6 |
| 7 | 24.5 | 19.9 | 29 | 27.9 | 23.9 |
| 8 | 21.1 | 25.2 | 30 | 29.1 | 28.8 |
| 9 | 29.6 | 34.8 | 32.3 | 30 | 27.6 |
| 10 | 23.5 | 24 | 29.6 | 28.5 | 26.8 |
| **Mean** | 28.08 | 29.55 | 32.91 | 31.62 | 31.03 |

| **Sample #** | **A2 Weld Sample Hardness** (3.5 ipm @ 500 rpm) | | | | |
|---|---|---|---|---|---|
| 1 | 25.7 | 29 | 34.7 | 32.8 | 28.6 |
| 2 | 28.9 | 31.9 | 34.2 | 34.3 | 29.3 |
| 3 | 22.9 | 37.4 | 40.4 | 36.1 | 37.1 |
| 4 | 20 | 20.8 | 29.7 | 31.7 | 27.7 |
| 5 | 31.7 | 37.5 | 35.9 | 31.9 | 27.7 |
| 6 | 22.2 | 31.5 | 35.3 | 33.8 | 30.2 |
| 7 | 30.1 | 38.5 | 38.1 | 33.9 | 31.2 |
| 8 | 23.2 | 31.4 | 37.4 | 32.3 | 28.2 |
| 9 | 30.9 | 37.5 | 35 | 35.1 | 26.6 |
| 10 | 29.7 | 33.5 | 36.1 | 34.5 | 26.3 |
| **Mean** | 26.53 | 32.9 | 35.68 | 33.64 | 29.29 |

| Parent Material |
|---|
| 37.4 |
| 42.9 |
| 52.6 |
| 50.1 |
| 46.8 |
| 52.4 |
| 49.6 |
| 45.6 |
| 47.3 |
| 50.8 |
| 52.9 |
| Mean: 48.036 |

Line graphs of hardness across the weld profile

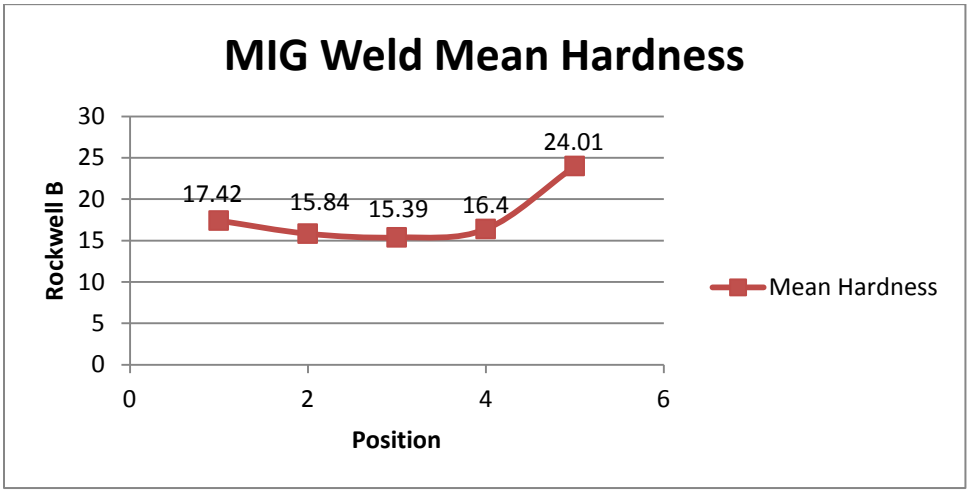


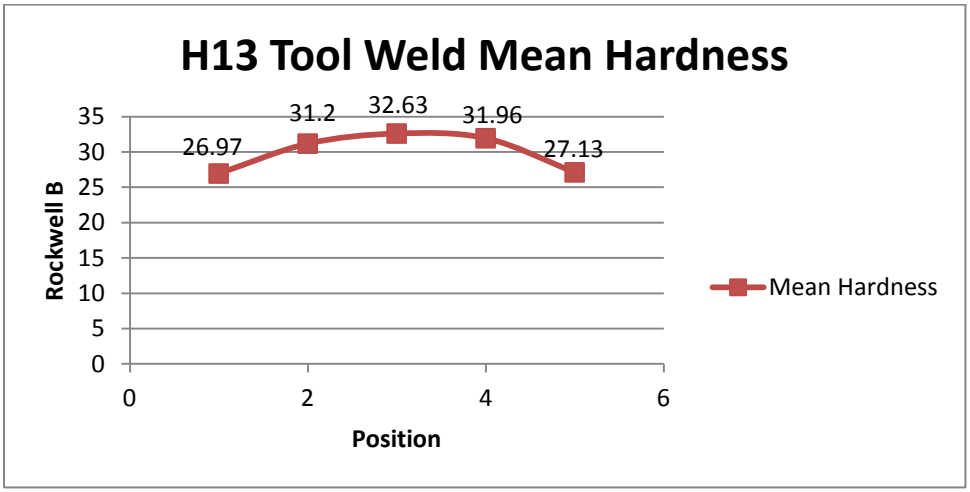

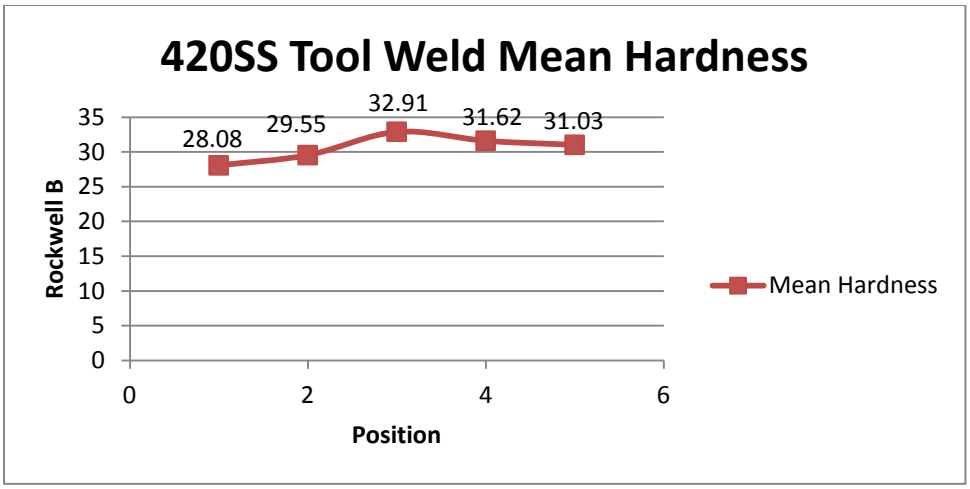
420SS Tool Weld Mean Hardness
Rockwell B
35
30
25
20
15
10
5
0
0
2
4
6
Position
28.08
29.55
32.91
31.62
31.03
Mean Hardness

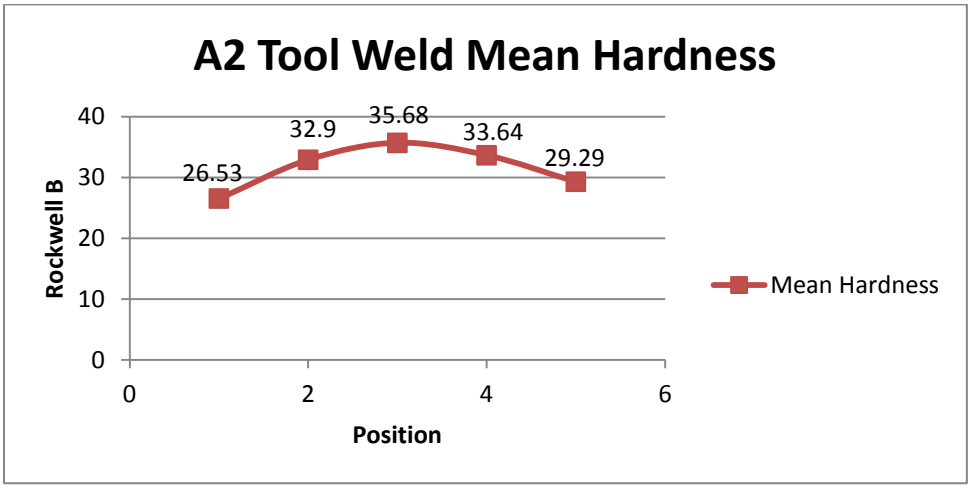
A2 Tool Weld Mean Hardness
Rockwell B
40
30
20
10
0
0
2
4
6
Position
26.53
32.9
35.68
33.64
29.29
Mean Hardness

Statistical comparison of mean hardness values between the groups

Anova: Two-Factor Without Replication

Hardness Tests

| *SUMMARY* | *Count* | *Sum* | *Average* | *Variance* |
|---|---|---|---|---|
| Position 1 | 3 | 81.58 | 27.19333 | 0.638033 |
| Position 2 | 3 | 93.65 | 31.21667 | 2.805833 |
| Position 3 | 3 | 101.22 | 33.74 | 2.8423 |
| Position 4 | 3 | 97.22 | 32.40667 | 1.169733 |
| Position 5 | 3 | 87.45 | 29.15 | 3.8172 |
| H13 TS | 5 | 149.89 | 29.978 | 7.40347 |
| 420 SS | 5 | 153.19 | 30.638 | 3.50177 |
| A2 TS | 5 | 158.04 | 31.608 | 13.38467 |

ANOVA

| *Source of Variation* | *SS* | *df* | *MS* | *F* | *P-value* | *F crit* |
|---|---|---|---|---|---|---|
| Position | 81.33577 | 4 | 20.33394 | 10.28014 | 0.0030595 | 3.837853 |
| Material | 6.722333 | 2 | 3.361167 | 1.69929 | 0.242637006 | 4.45897 |
| Error | 15.82387 | 8 | 1.977983 | | | |
| Total | 103.882 | 14 | | | | |

Anova: Two-Factor Without Replication

Hardness Tests

| *SUMMARY* | *Count* | *Sum* | *Average* | *Variance* |
|---|---|---|---|---|
| Position 1 | 4 | 99 | 24.75 | 24.30487 |
| Position 2 | 4 | 109.49 | 27.3725 | 60.98102 |
| Position 3 | 4 | 116.61 | 29.1525 | 86.07549 |
| Position 4 | 4 | 113.62 | 28.405 | 64.83317 |
| Position 5 | 4 | 111.46 | 27.865 | 9.1497 |
| MIG | 5 | 89.06 | 17.812 | 12.57937 |
| H13 TS | 5 | 149.89 | 29.978 | 7.40347 |
| 420 SS | 5 | 153.19 | 30.638 | 3.50177 |
| A2 TS | 5 | 158.04 | 31.608 | 13.38467 |

ANOVA

| *Source of Variation* | *SS* | *df* | *MS* | *F* | *P-value* | *F crit* |
|---|---|---|---|---|---|---|
| Position | 45.04543 | 4 | 11.26136 | 1.319282 | 0.31801649 | 3.259167 |
| Material | 633.6011 | 3 | 211.2004 | 24.74238 | 1.99929E-05 | 3.490295 |
| Error | 102.4317 | 12 | 8.535974 | | | |
| Total | 781.0782 | 19 | | | | |

Anova: Two-Factor Without Replication

Hardness Tests

| *SUMMARY* | *Count* | *Sum* | *Average* | *Variance* |
|---|---|---|---|---|
| Position 1 | 4 | 129.58 | 32.395 | 108.6547 |
| Position 2 | 4 | 141.65 | 35.4125 | 72.29062 |
| Position 3 | 4 | 149.22 | 37.305 | 52.73177 |
| Position 4 | 4 | 145.22 | 36.305 | 61.56783 |
| Position 5 | 4 | 135.45 | 33.8625 | 91.37543 |
| Parent | 5 | 240 | 48 | 0 |
| H13 TS | 5 | 149.89 | 29.978 | 7.40347 |
| 420 SS | 5 | 153.19 | 30.638 | 3.50177 |
| A2 TS | 5 | 158.04 | 31.608 | 13.38467 |

ANOVA

| *Source of Variation* | *SS* | *df* | *MS* | *F* | *P-value* | *F crit* |
|---|---|---|---|---|---|---|
| Position | 61.00183 | 4 | 15.25046 | 5.061299 | 0.012663462 | 3.259167 |
| Material | 1123.703 | 3 | 374.5677 | 124.311 | 2.65552E-09 | 3.490295 |
| Error | 36.15781 | 12 | 3.013151 | | | |
| Total | 1220.863 | 19 | | | | |

Appendix 6

Visual examination samples of welds with optimum process parameters

420 Stainless Steel Welds

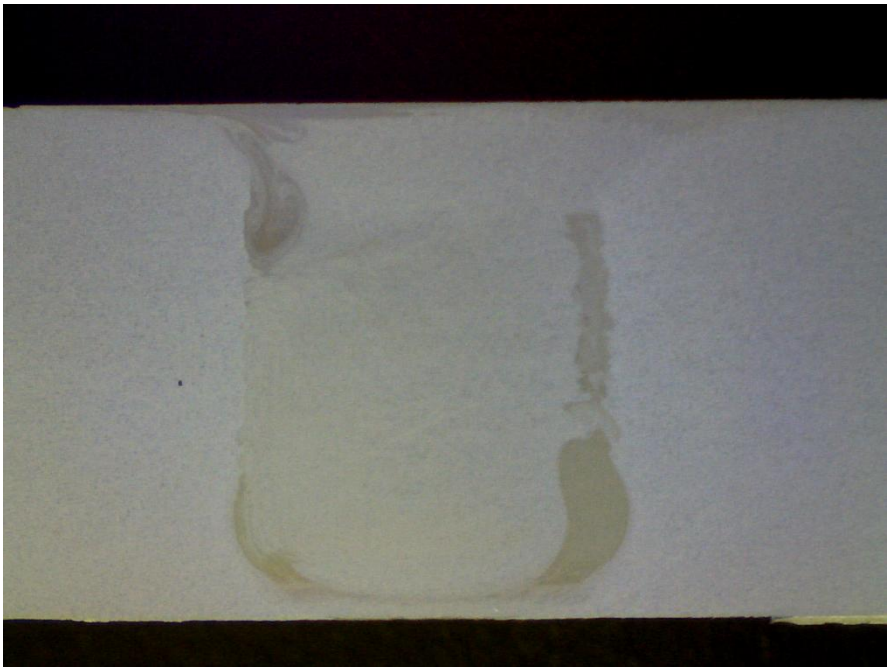

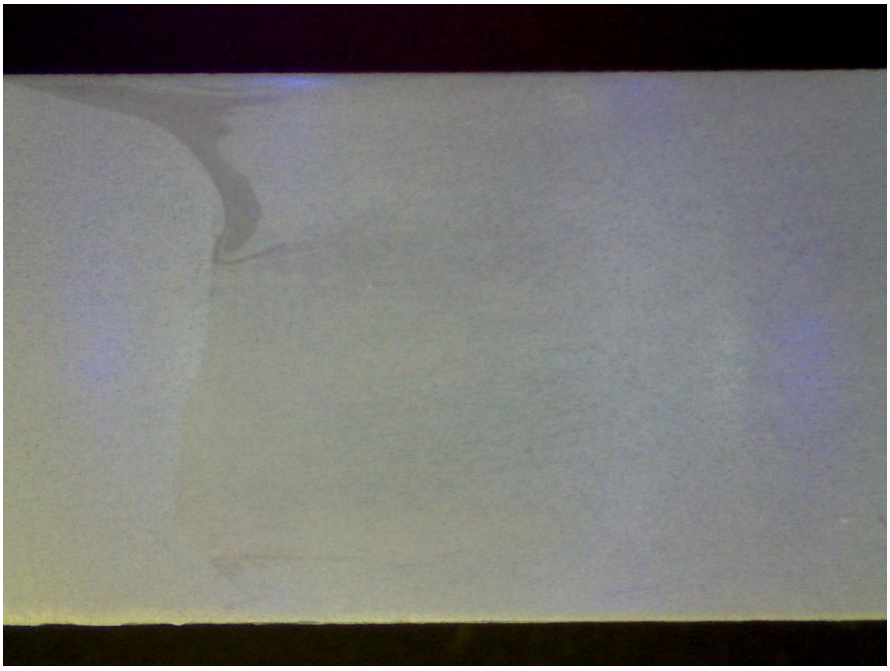

H13 Tool Steel Welds

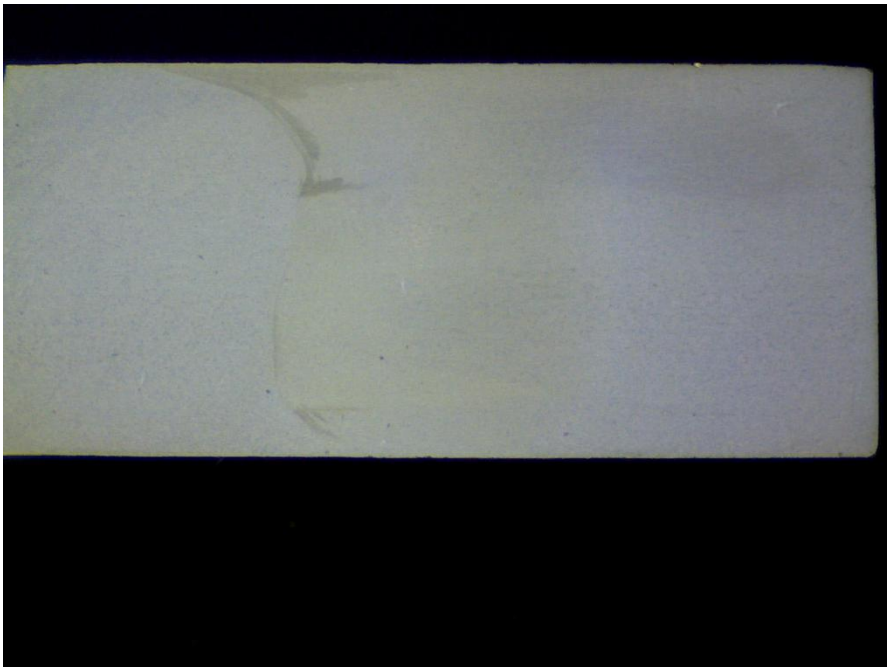

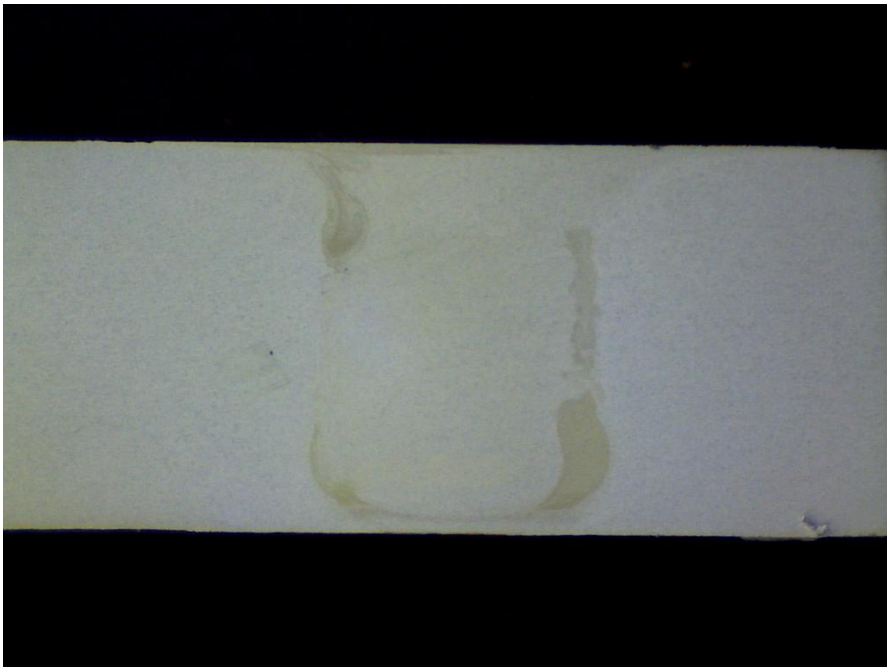

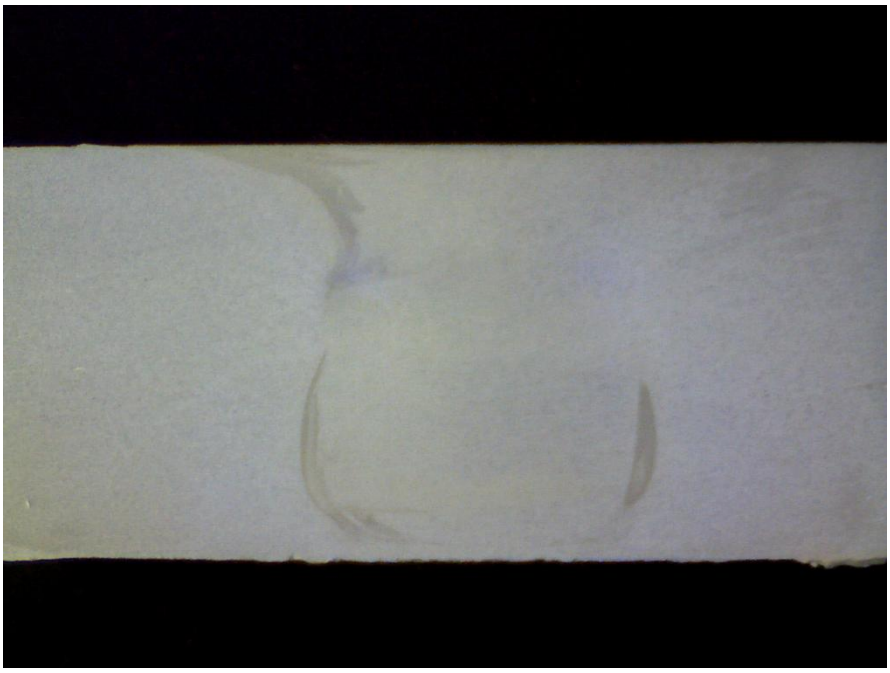

A2 Welds

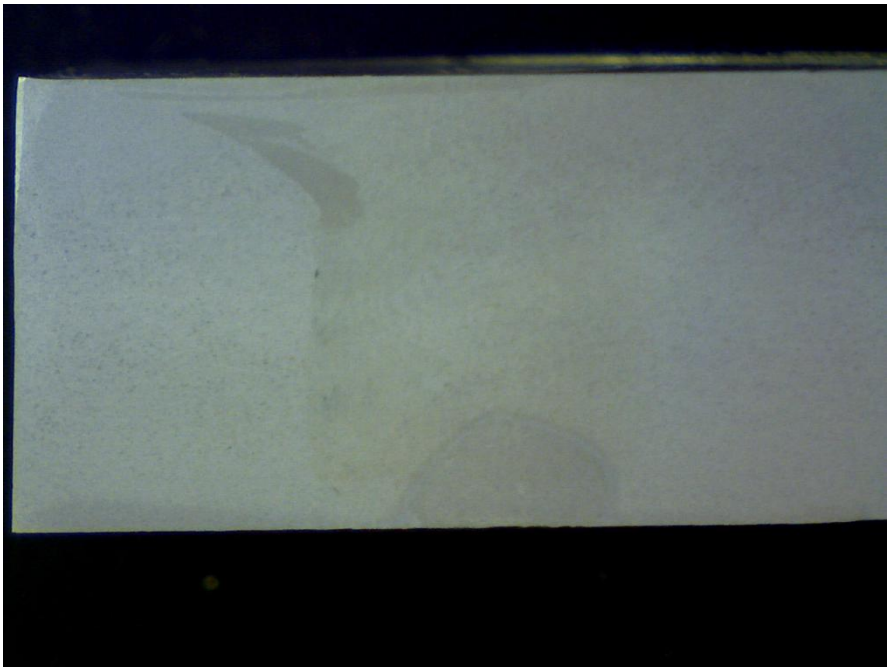

MIG Welds

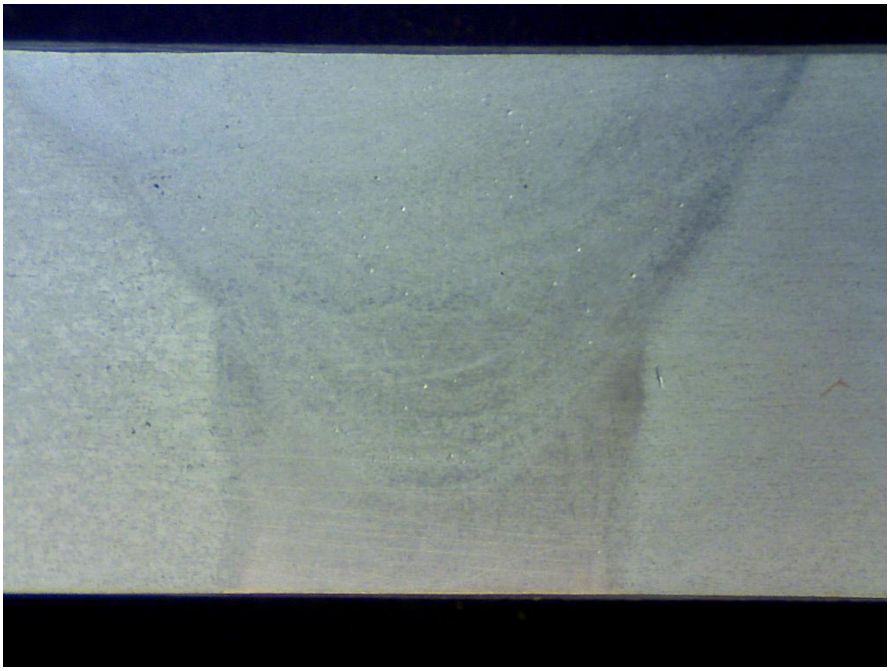

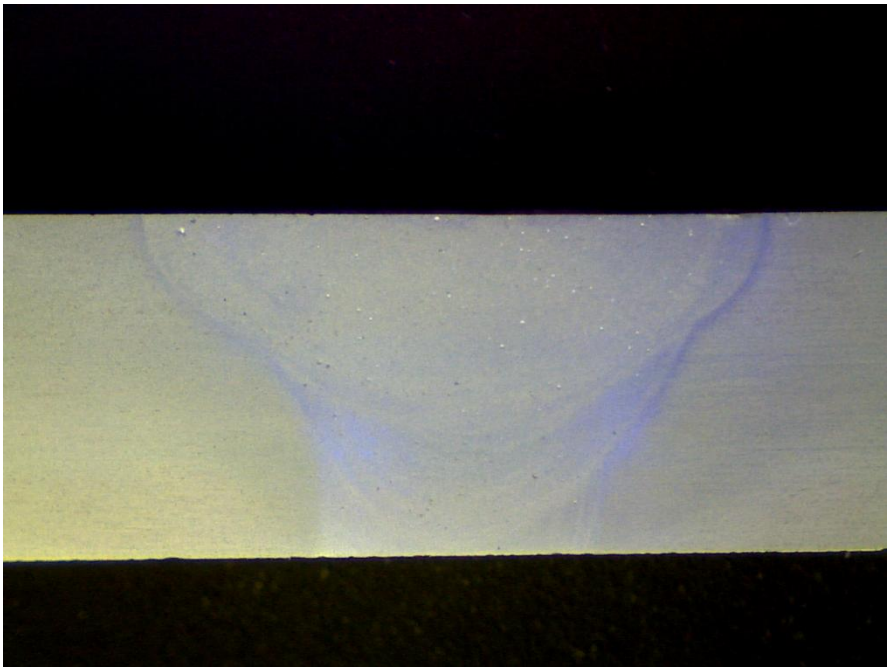

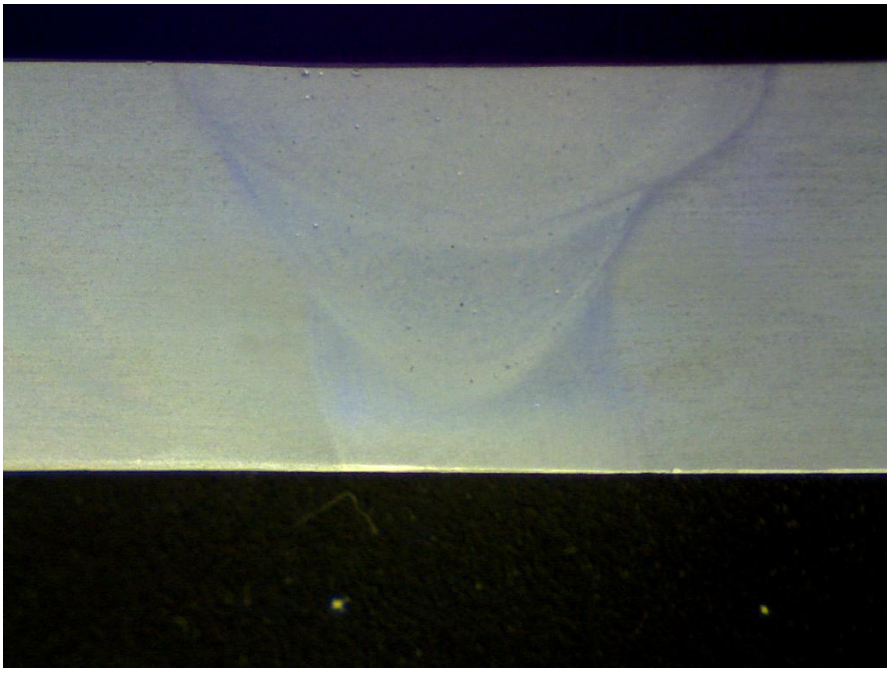

Appendix 7

Procedural Weld Results

A2 Weld Bend and Tensile results

| Material | Parent | Mig Welds | A2 Welds 3.5ipm @ 500 rpm | Parent | Mig Welds | A2 Welds 3.5 ipm @ 500 rpm |
|---|---|---|---|---|---|---|
| Sample # | Bend Testing | | | Tensile Testing | | |
| 1 | 821.2 | 547.3 | 770.5 | 3391.6 | 2450.9 | 2401.22 |
| 2 | 839.3 | 562.4 | 792.1 | 3407.46 | 2557.19 | 2513.5 |
| 3 | 842.2 | 576 | 788.7 | 3433.27 | 2572.84 | 2524.67 |
| 4 | 901.2 | 580 | 798.4 | 3439.75 | 2623 | 2538.69 |
| 5 | 903.4 | 598.8 | 799.2 | 3444.94 | 2628.8 | 2540.88 |
| 6 | 922.9 | 632.5 | 796.4 | 3461.7 | 2683.28 | 2604.72 |
| 7 | 942.9 | 635.2 | 797.9 | 3470.07 | 2690.1 | 2711.19 |
| 8 | 946.8 | 636.1 | 789.7 | 3516.58 | 2690.38 | 2797.26 |
| 9 | 977.3 | 646.3 | 794.5 | 3543.37 | 2709.52 | 2920.93 |
| 10 | 980.6 | 652.3 | 793 | 3604.21 | 2717 | 3098.84 |
| Mean: | 907.78 | 606.69 | 792.04 | 3471.30 | 2632.30 | 2665.19 |
| Std Dev: | 57.41583 | 38.2947763 | 8.384138 | 65.46184 | 84.74262 | 216.169 |
| Kurtosis: | 1.714397 | 1.33272699 | 8.434076 | 3.460092 | 3.923209 | 3.281745 |
| Skewness: | -0.3113 | -0.3015645 | -2.14921 | 0.96228 | -1.14443 | 0.987917 |

A2 Weld Hardness Results

| Sample # | A2 Weld Sample Hardness (3.5 ipm @ 500 rpm) | | | | |
|---|---|---|---|---|---|
| 1 | 25.7 | 29 | 34.7 | 32.8 | 28.6 |
| 2 | 28.9 | 31.9 | 34.2 | 34.3 | 29.3 |
| 3 | 22.9 | 37.4 | 40.4 | 36.1 | 37.1 |
| 4 | 20 | 20.8 | 29.7 | 31.7 | 27.7 |
| 5 | 31.7 | 37.5 | 35.9 | 31.9 | 27.7 |
| 6 | 22.2 | 31.5 | 35.3 | 33.8 | 30.2 |
| 7 | 30.1 | 38.5 | 38.1 | 33.9 | 31.2 |
| 8 | 23.2 | 31.4 | 37.4 | 32.3 | 28.2 |
| 9 | 30.9 | 37.5 | 35 | 35.1 | 26.6 |
| 10 | 29.7 | 33.5 | 36.1 | 34.5 | 26.3 |
| **Mean** | 26.53 | 32.9 | 35.68 | 33.64 | 29.29 |

A2 Welds and associated pictures

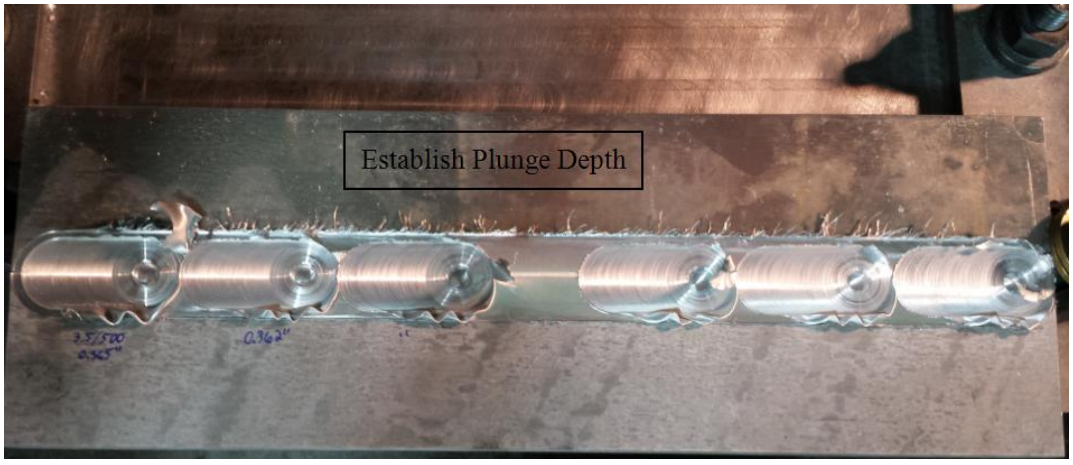


Corresponding Microscopy

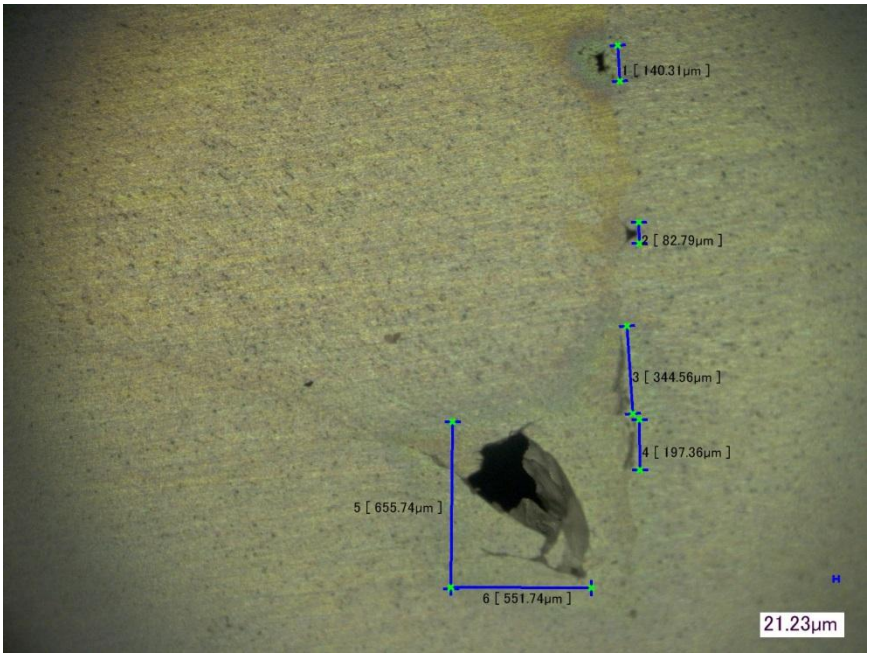


Sample 1

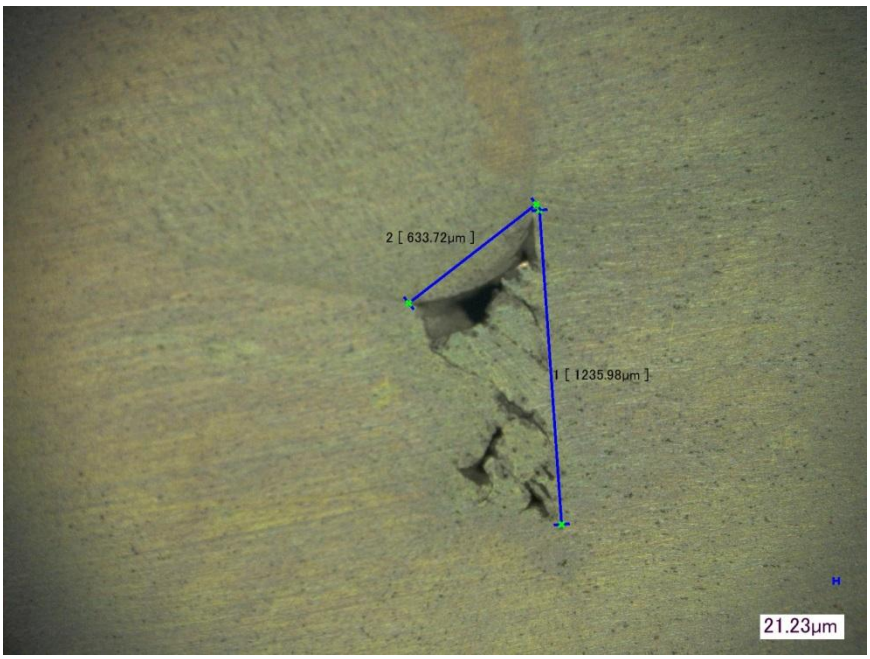


Sample 2

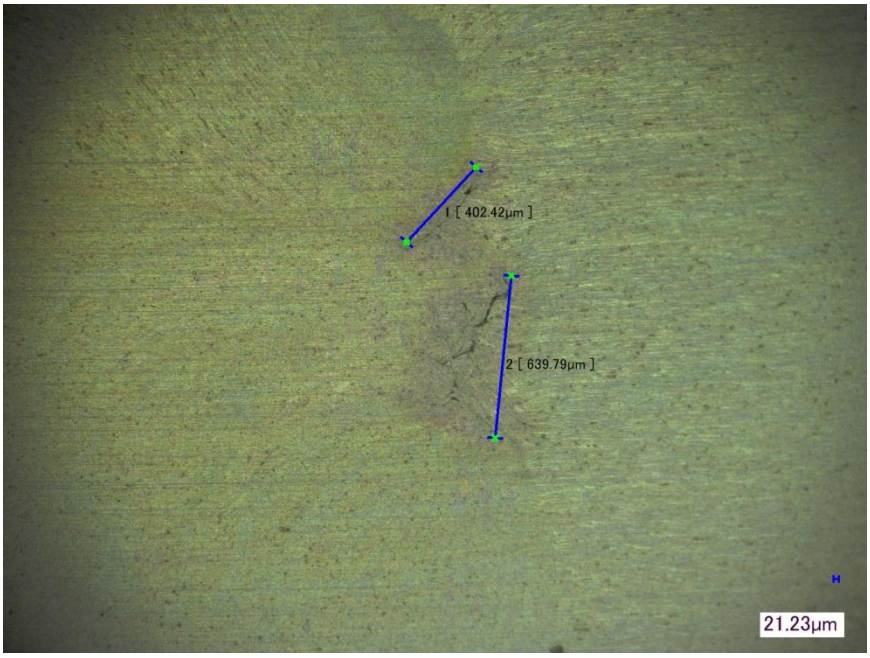


Sample 3

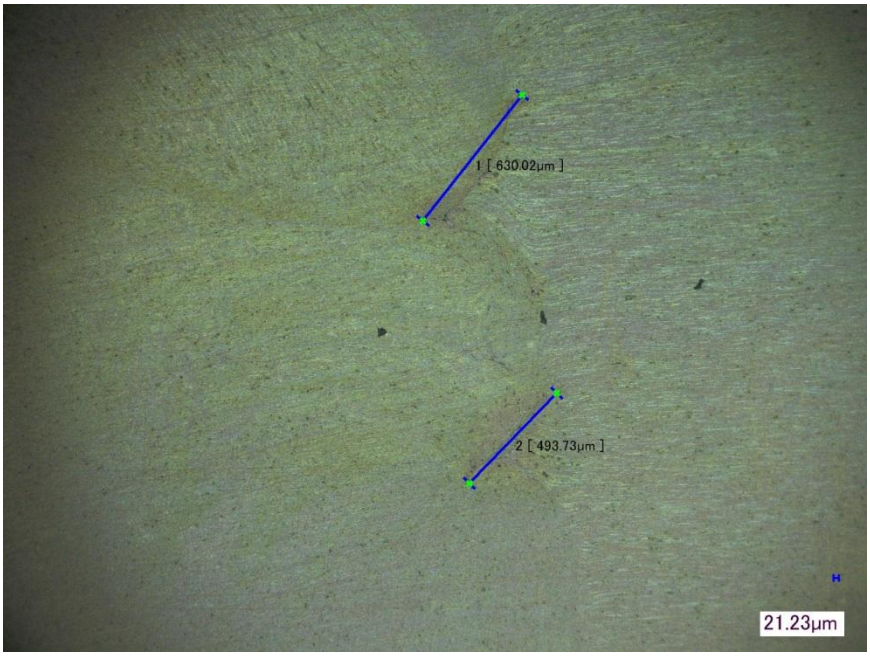


Sample 4

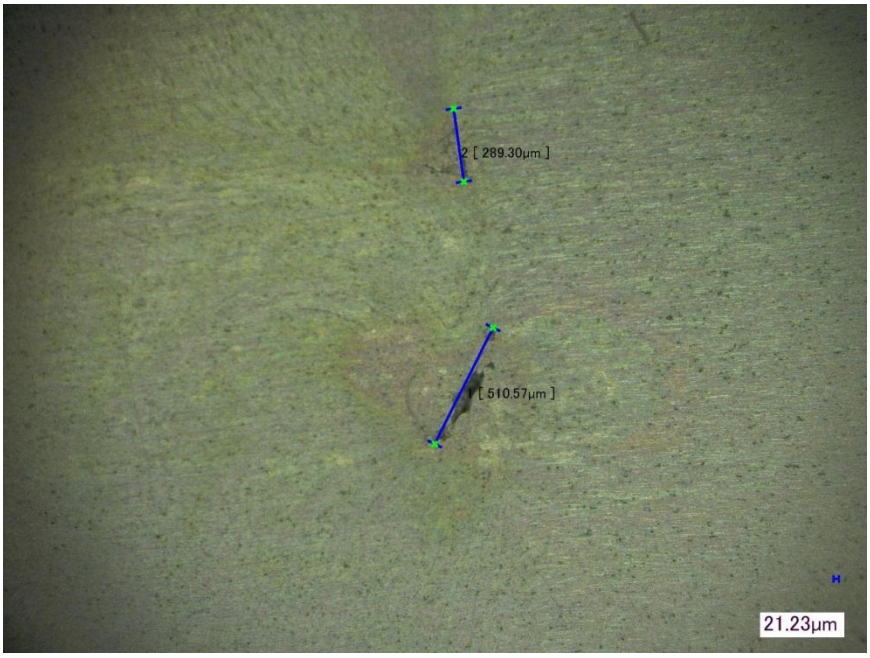


Sample 5

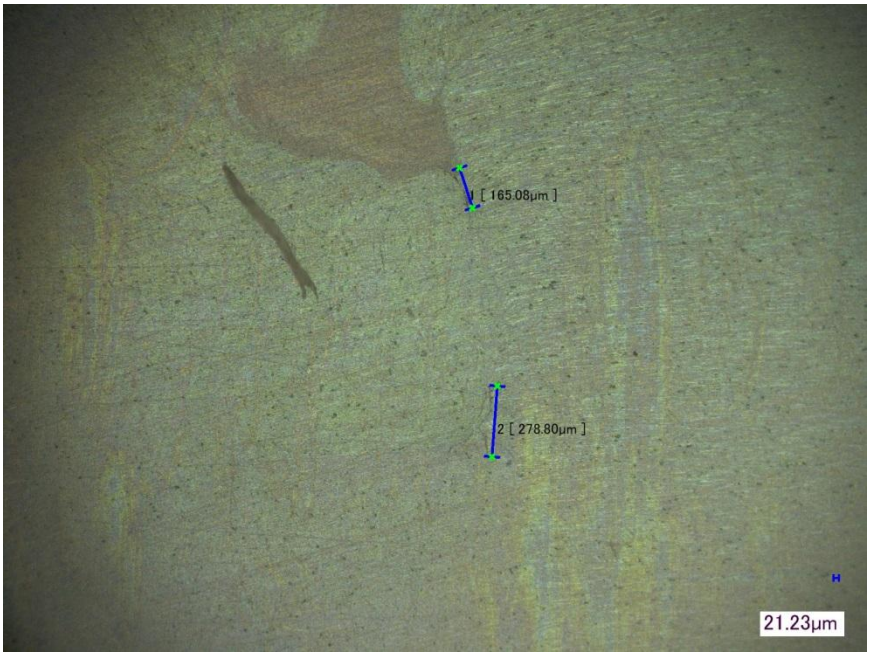


Sample 6

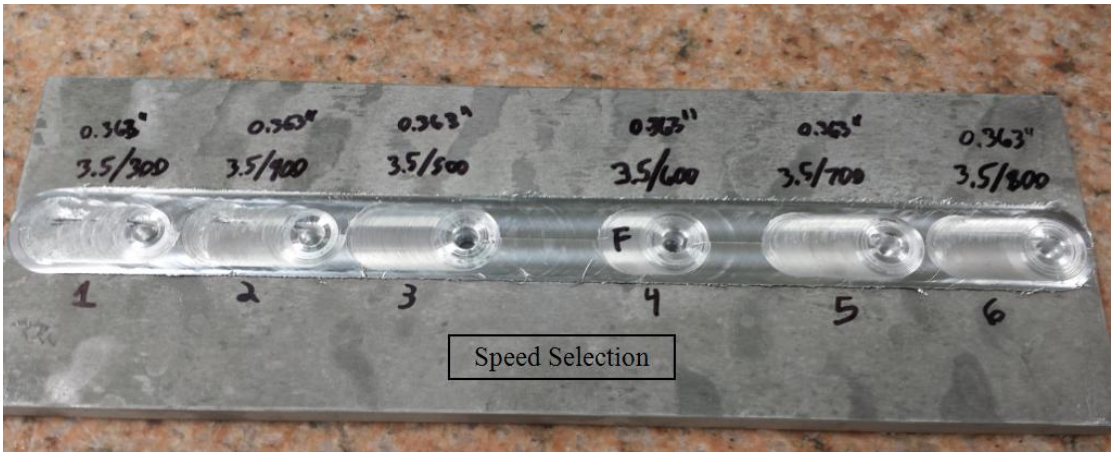


Corresponding Microscopy

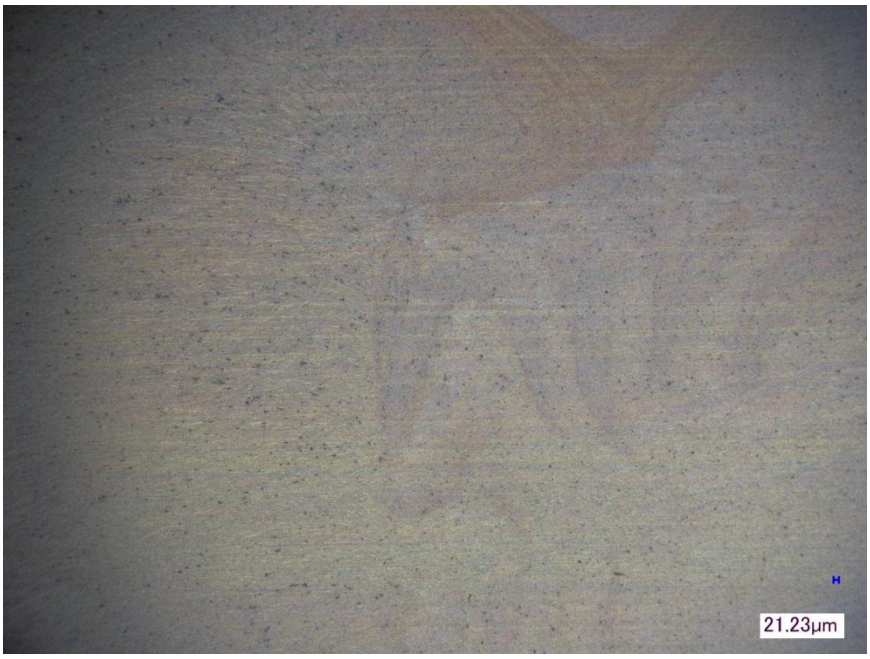


Sample 3

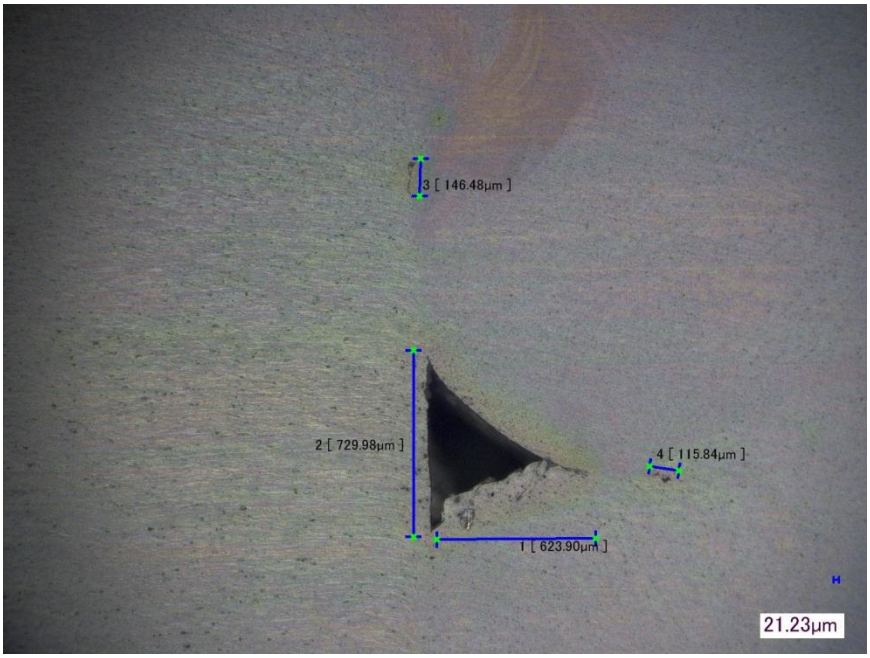


Sample 5

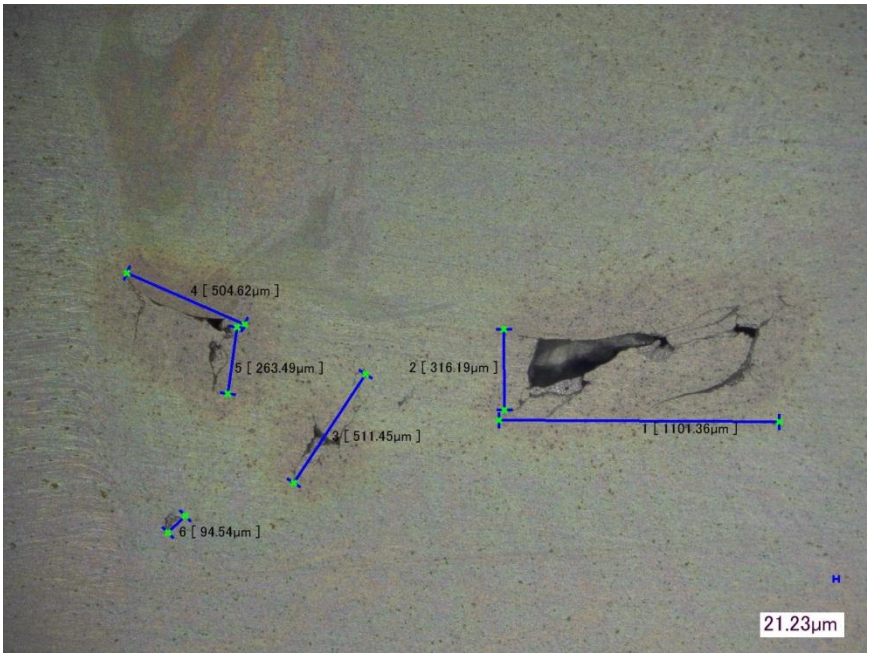


Sample 6

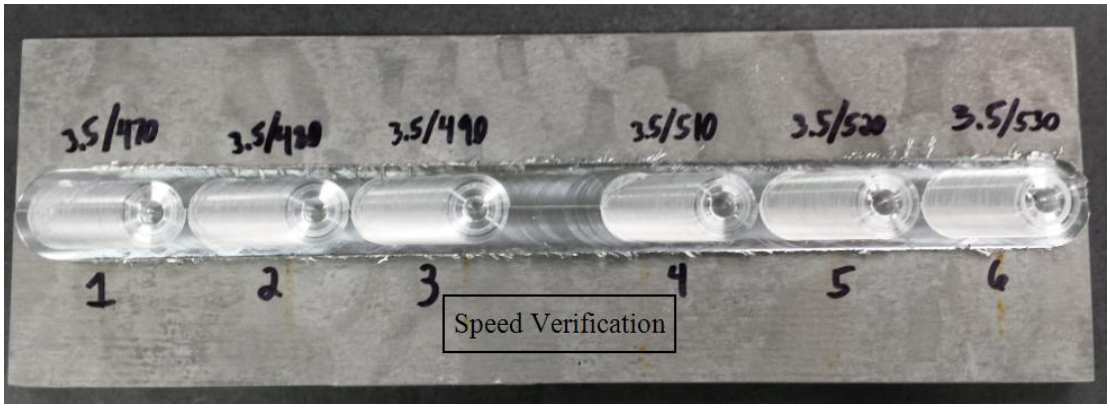


Corresponding Microscopy

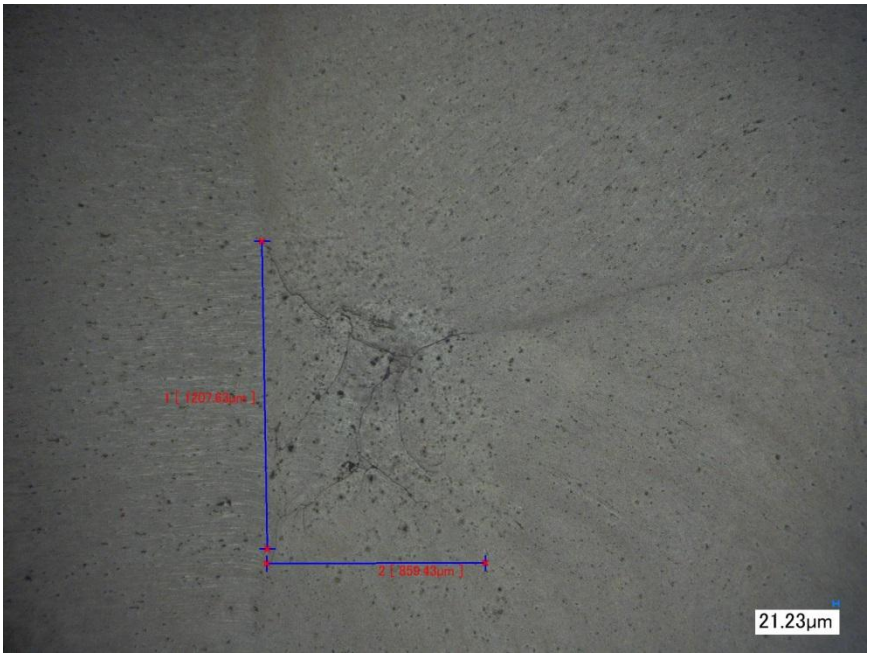


Sample 1

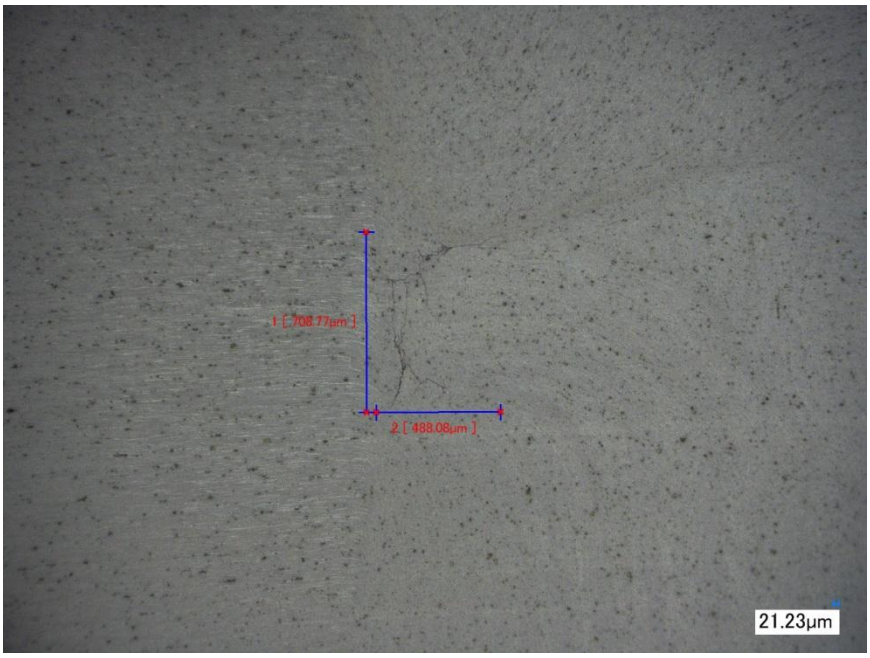


Sample 2

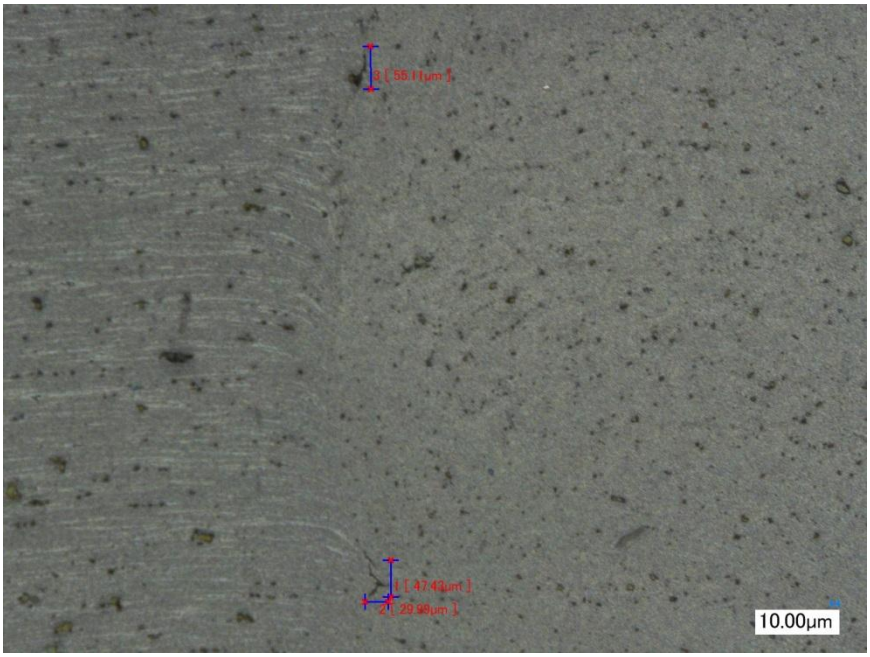


Sample 3

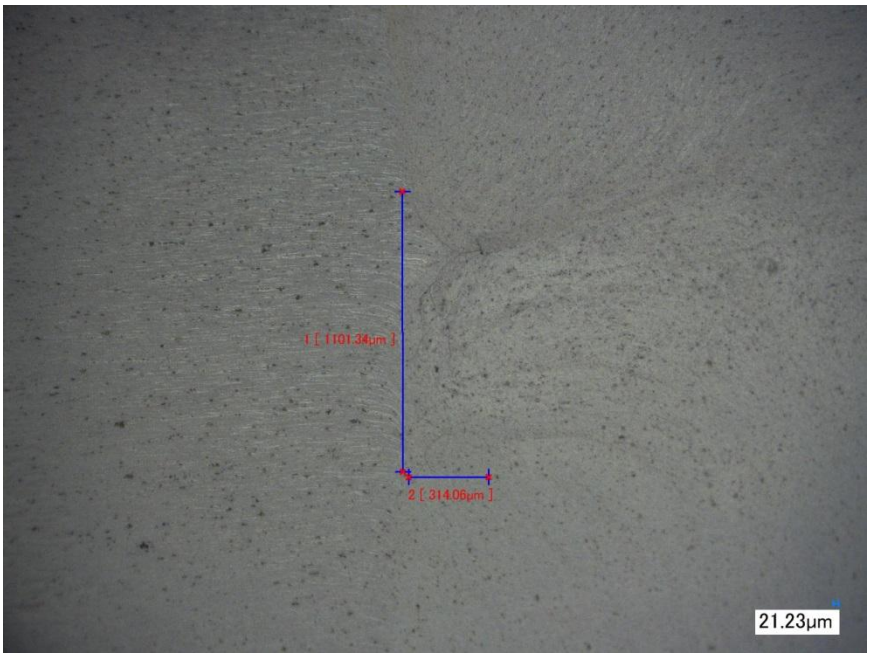


Sample 4

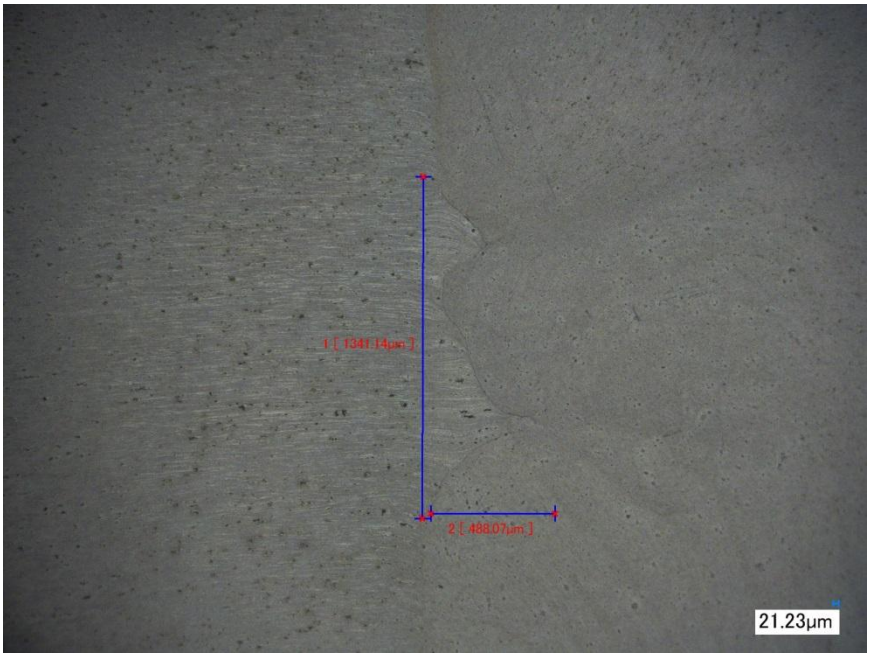


Sample 5

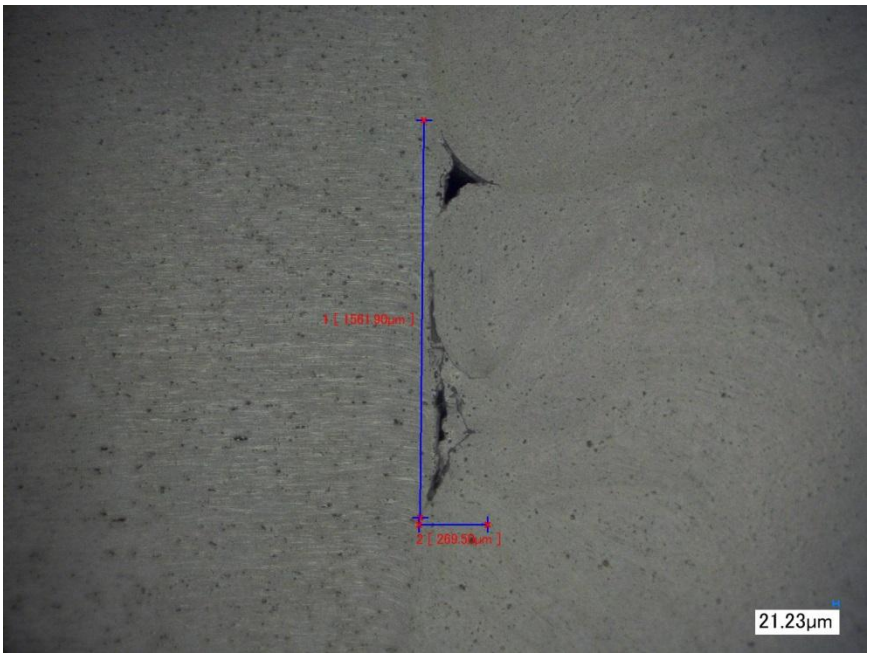


Sample 6

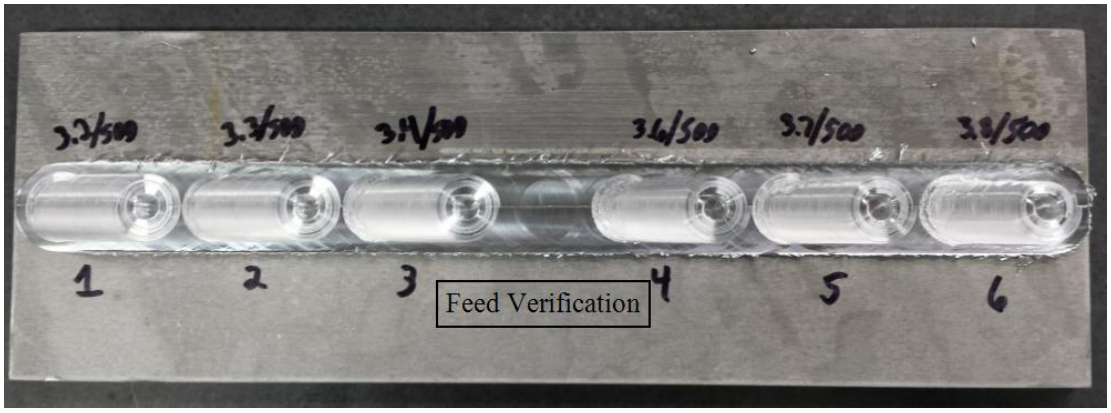


Corresponding Microscopy

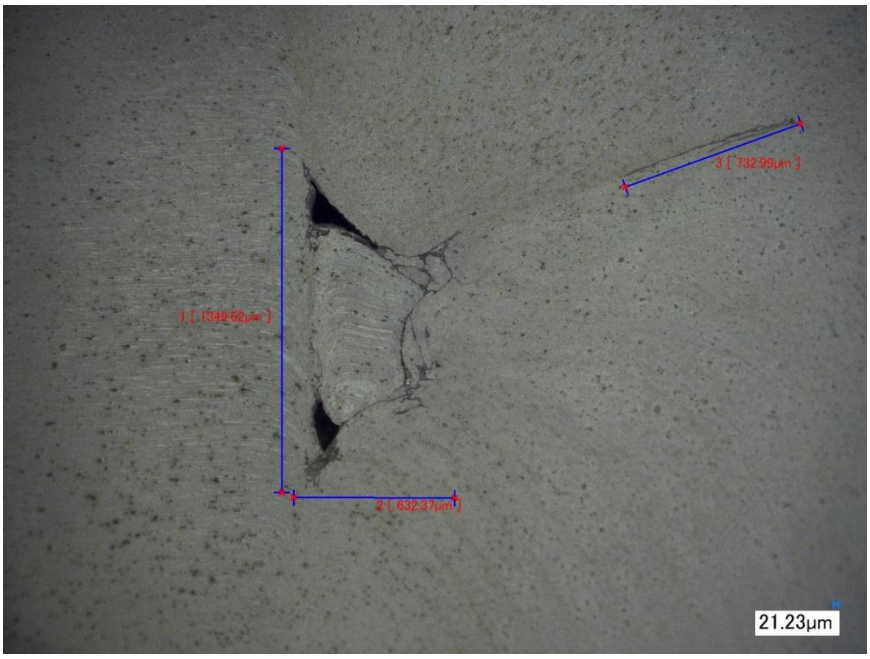


Sample 1

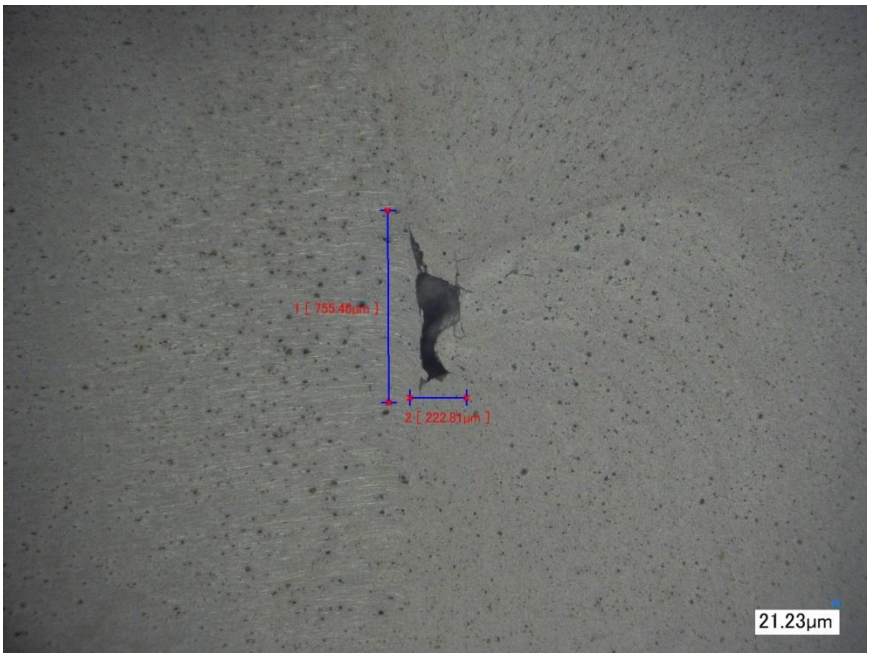


Sample 2

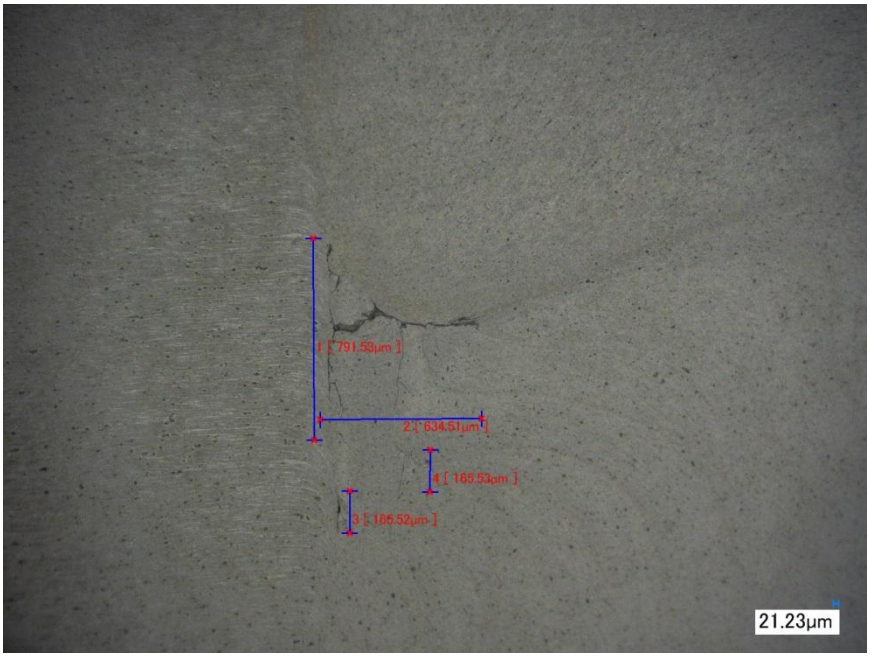


Sample 3

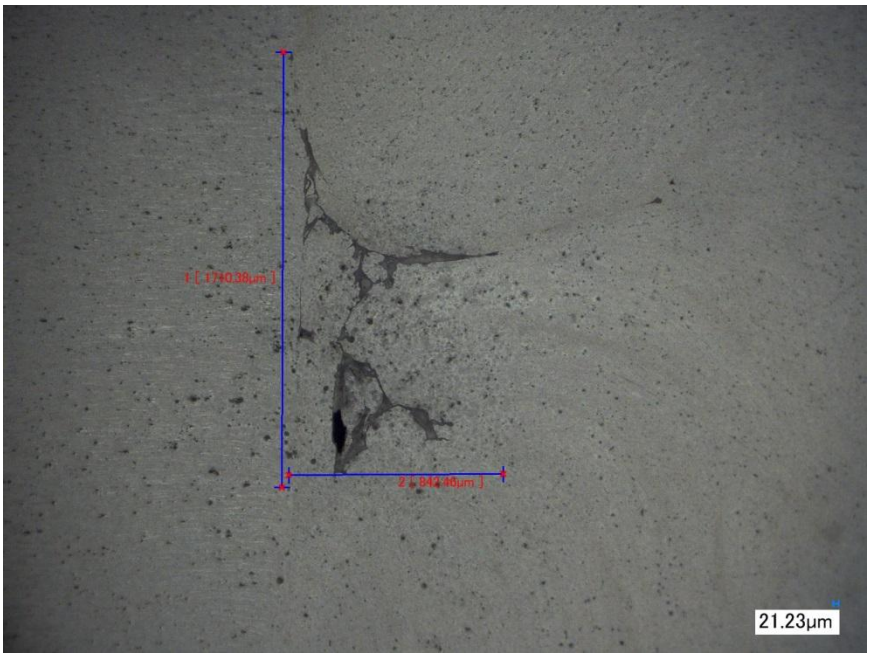


Sample 4

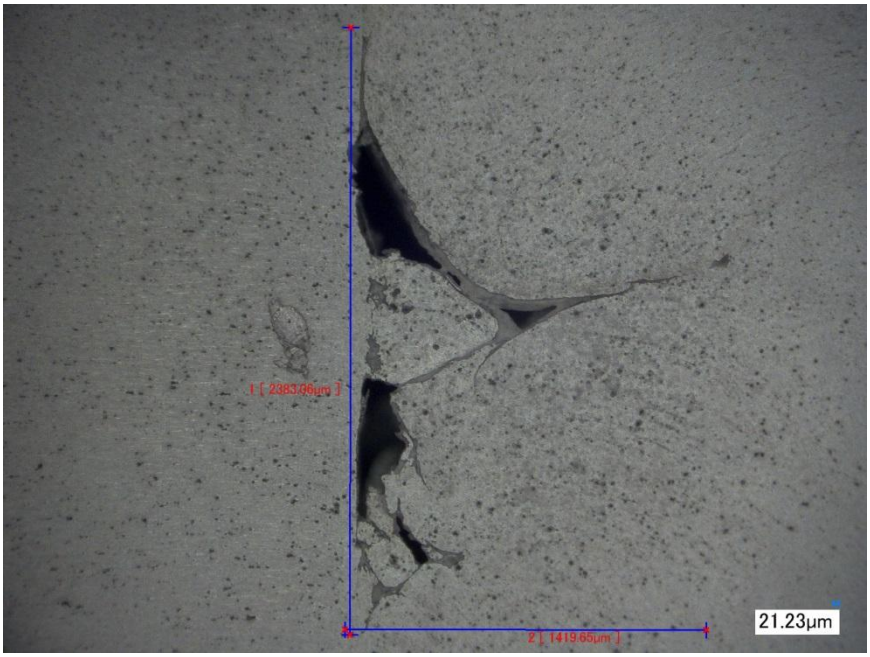


Sample 5

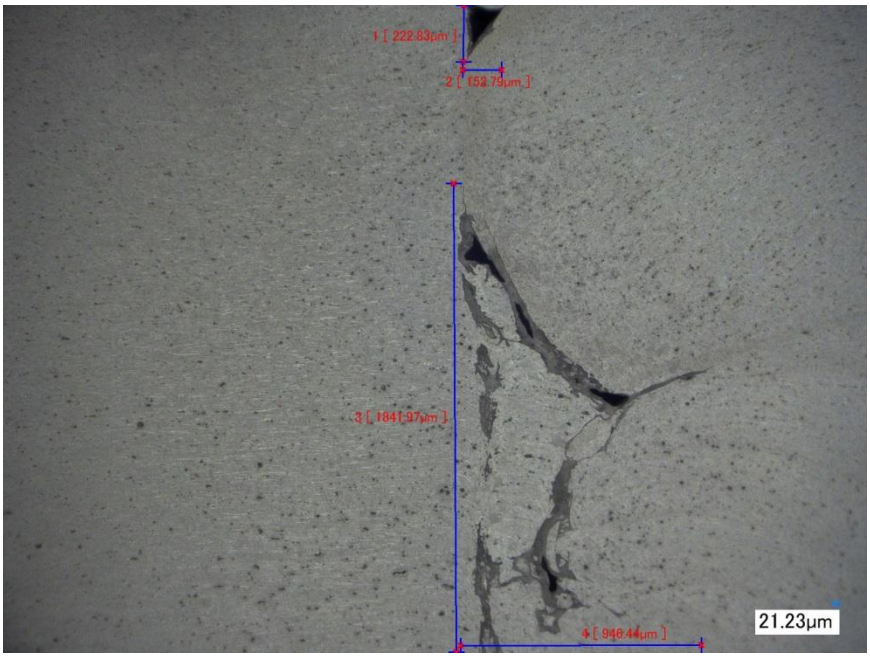


Sample 6